A ROLE FOR METHYL-CpG BINDING DOMAIN PROTEIN 2 IN OLFACTORY NEURONAL DEVELOPMENT

by

JENNY S CHENG

B.Sc., The University of British Columbia, 1999

A THESIS SUBMITTED IN PARTIAL FULFILLMENT OF
THE REQUIREMENTS FOR THE DEGREE OF

MASTER OF SCIENCE

in

THE FACULTY OF GRADUATE STUDIES

(Department of Psychiatry, Graduate Program in Neuroscience)

We accept this thesis as conforming
to the required standard

THE UNIVERSITY OF BRITISH COLUMBIA

June 2001

In presenting this thesis in partial fulfilment of the requirements for an advanced degree at the University of British Columbia, I agree that the Library shall make it freely available for reference and study. I further agree that permission for extensive copying of this thesis for scholarly purposes may be granted by the head of my department or by his or her representatives. It is understood that copying or publication of this thesis for financial gain shall not be allowed without my written permission.

Department of Psychiatry, Neuroscience Program

The University of British Columbia
Vancouver, Canada

Date June 28/2001

Abstract

Methylation of DNA is a common modification of CpG di-nucleotides and is associated with transcriptional repression. This mechanism of gene silencing can be mediated by methyl-CpG binding domain (MBD) proteins, which form repressor complexes that are important in linking DNA methylation and transcriptional repression by altering chromatin structure. We have identified MBD2 as a gene that is highly up-regulated following bulbectomy in mouse. MBD2 has been shown to bind methylated DNA and belongs to the MeCP1 repressor complex, which includes the histone deacetylases HDAC1 and HDAC2 and the histone binding proteins RbAp46 and RbAp48 (Hendrich and Bird, 1998; Bird and Wolffe, 1999). The bulbectomy paradigm recapitulates ORN developmental events and suggests that MBD2 is important in regulating gene expression during ORN development. This study sought to determine if MBD2 is involved in ORN development by silencing genes that are no longer needed for ORNs to achieve a mature phenotype. MBD2 was found to be dynamically expressed by ORNs at different stages of maturation during development. In the absence of MBD2 there are abnormalities in the primary neuraxis. MBD2-/- neonates have more ORNs, more axon bundles and significantly larger axon bundles and glomeruli, when compared to MBD2+/+ controls for OMP and NCAM staining. We have also generated an *in vitro* model of ORN development to help us understand ORN developmental events and in particular, MBD2 function. Conditionally immortalized temperature sensitive cell lines were generated from the embryonic mouse olfactory placode. Two of these, OP6 and OP27 were chosen for further characterization and confirmed to be olfactory neuron-like in nature. Both OP6 and OP27 express general neuronal and ORN markers, neurotrophin

receptors and after differentiation, express OMP. Both express endogenous ORs and respond to odorant stimulation. OP6 and OP27 also express MBD2 and MBD3 in a differentiation dependent manner consistent with observations *in vivo*. Both OP6 and OP27 also express MeCP2, mSin3A, HDAC1 and HDAC2, all potential protein interactors of MBD2. The *in vivo* and *in vitro* data demonstrate that MBD2 is important in regulating gene expression during olfactory neuronal development.

Table of Contents

List of Tables

List of Figures

List of Abbreviations

5'AZA-CdR	5-AZA-2'-deoxycytidine
ACIII	adenylate cyclase III
BDNF	brain derived neurotrophic factor
CNS	central nervous system
DIV	days in vitro
DNMT	DNA methyl transferase
E	embryonic day
ES	embryonic stem cells
FOB	front of olfactory bulb region
GAP	growth associated protein
GBC	globose basal cell
Golf	olfactory G protein
HBC	horizontal basal cell
HDAC	histone deacetylase
INP	immediate neuronal precursor
IRN	immature receptor neuron
kb	kilobase
kD	kilodalton
LP	lamina propria
M1	Mash-1 expressing cell
MAP	microtubule associated protein
MBD	methyl-CpG binding domain
MeCP	methyl-CpG
MOB	middle of olfactory protein region
MOE	middle of olfactory epithelium region
mORN	mature olfactory receptor neuron
mRNA	messenger RNA
NCAM	neural cell adhesion molecule
NGF	nerve growth factor
NST	neuron specific tubulin
NT-3	neutrophin-3
OB	olfactory bulb
OE	olfactory epithelium
OEG	olfactory ensheathing glia
OMP	olfactory marker protein
ONL	olfactory nerve layer
OP	olfactory placode
OR	odorant receptor
ORN	olfactory receptor neuron
P	postnatal day
PBS	phosphate buffered saline
PFA	paraformaldehyde
PLC-γ2	phospholipase C-γ2

RA	all trans retinoic acid
RAR	retinoic acid receptor
RT-PCR	reverse transcription polymerase chain reaction
RTT	Rett syndrome
RXR	retinoid X receptor
TRD	transcriptional repression domain
Trk	tyrosine kinase receptor
TSA	trichostatin A
VNO	vomeronasal organ

Acknowledgements

I would like to acknowledge my fiancé Arek Siwoski and my family for their encouragement, support and optimism. And Arek again for constantly making me laugh. I would like to thank my supervisor Dr. Jane Roskams for her ideas, scientific enthusiasm and guidance and members of my laboratory: Kathryn Clark, Joellen Fung, Lisa Garcia, and Murray Gilbert for technical assistance. I would also like to acknowledge Dr. Adrian Bird for providing us with the MBD2-/- mice and Dr. James Eubanks and Dr. Frank Margolis for MBD3 and OMP antisera, respectively. Lastly I would like to acknowledge NSERC for awarding me a NSERC PGS A studentship.

Chapter 1: Introduction

The Olfactory System-Neuronal cell death in mammalian systems occurs throughout development and following trauma or disease. Unlike other regenerating tissues such as the liver, muscle and blood, vertebrates do not have the ability to regenerate lost neurons in the central nervous system (CNS), making the death of neurons a permanent event. Several factors contribute to inhibiting axonal outgrowth and functional reconnection in the CNS including astroglial scarring and CNS myelin, which act as a physical barrier to regenerating axons. One exception to the norm can be found in the vertebrate olfactory epithelium (OE) (Graziadei, 1973; Graziadei and Monti Graziadei, 1978). The OE lines the nasal cavity and contains only one neuronal cell type-the olfactory receptor neuron (ORN), which is responsible for our sense of smell (Buck, 2000). Unlike other CNS neurons, ORNs undergo a continuous cycle of cell death, neurogenesis, axon outgrowth and functional reconnection in response to environmental insult, infection and trauma (Graziadei, 1973; Graziadei and Monti Graziadei, 1978). [^{3}H]thymidine labeling of ORNs *in vivo* has indicated that the turnover time is approximately 4 weeks (Murray and Calof, 1999). The fact that ORNs are continually replaced suggests that the adult OE contains a stem cell population that has the ability to differentiate into mature ORNs (Graziadei, 1973; Graziadei and Monti Graziadei, 1978; Margolis *et al.*, 1991; Huard *et al.*, 1998).

The regenerative properties of ORNs make the olfactory system make it an ideal model in which to study the processes of neuronal differentiation, regeneration, plasticity and neuronal development and the mechanisms that control them (Margolis *et al.*, 1991).

At any given time during development and even in the adult, the OE contains ORNs at various stages of maturation, with the most mature olfactory receptor neurons (mORNs) located apically and immature olfactory receptor neurons (IRNs) located basally (Fig 1). In addition, the OE is peripherally located allowing it to be studied in the living animal and in cell culture. It has been studied extensively and much is known about the cellular interactions and molecular factors that regulate neurogenesis (Murray and Calof, 1999). Although the OE is similar to germinal epithelia both morphologically and functionally, it is much easier to study because the OE contains only one neuronal cell type. Understanding the processes of neuronal development, differentiation and regulatory approaches, as well as plasticity in the olfactory system will further our understanding of more complex neuronal systems.

Three main experimental paradigms have been used to take advantage of the unique properties of the olfactory system to study neuronal cell death and neurogenesis. A commonly used experimental paradigm is axotomy, which involves severing ORN axons, or bulbectomy, which involves surgical removal of the ORN target organ, the olfactory bulb (OB). Axotomy causes ORN degeneration and regeneration from progenitor cells in the basal cell population. This is a technically difficult procedure making the bulbectomy paradigm more common. Following unilateral bulbectomy, IRNs and ORNs on the ipsilateral side die by apoptosis. Apoptosis is maximal at approximately 48 hours post-bulbectomy and is complete within 3 days. Replacement of these cells by progenitors peaks at approximately 6 days post-bulbectomy; however, newborn neurons seldom mature without the OB and only have a lifespan of less than 2 weeks. ORN proliferation is permanently up-regulated on the ipsilateral side following

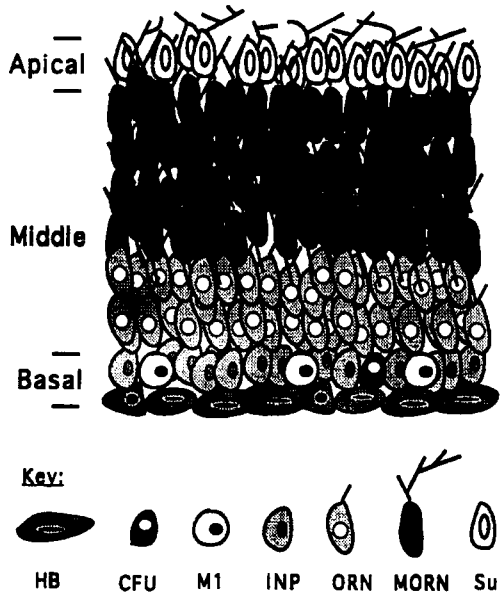

Figure 1: The three major compartments of the olfactory epithelium. The OE contains three major compartments: the apical, middle and basal compartments. The apical region contains sustentacular cells (Su), the middle region contains immature ORNs (ORN) and mature ORNs (MORN) and the basal region contains horizontal (HB) and globose basal cells. Globose basal cells can be further subdivided into putative neuronal stem cells or neuronal colony-forming cells (CFU), Mash-1 expressing cells (M1) and immediate neuronal precursors (INP) (Calof *et al.*, 1998).

bulbectomy suggesting that the number of dying neurons or mature neurons in the environment regulates the differentiation of precursors into neurons. *In vitro* experiments have supported this hypothesis.

A second experimental paradigm involves physically damaging the OE with chemical solutions or corrosive gases such as methyl bromide, Triton-X-100 and zinc sulfate. In this model, the capacity to regenerate cells from the neuronal lineage is limited by the strength of damage. Most ORNs die within a day of treatment and depending on the severity of the lesion, complete regeneration occurs within 6 weeks to more than 150 days post-lesion.

A third experimental paradigm is naris occlusion, which involves closing one nostril in a neonate mouse to reduce the airflow and input to ORNs. This procedure does not affect the number of mORNs but results in a 10-15% reduction in the thickness of the OE. The cause of this reduction is unclear but it is thought to be due to a decrease in ORN death or a decrease in the number of immature ORNs. The OE can return to normal thickness in 6-10 days following re-opening of the occluded naris and is likely due to the proliferation of progenitor cells (Brunjes and Borror, 1983; Murray and Calof, 1999).

Physically, the OE can be divided into three major compartments: the apical, middle and basal compartments (Fig 1). The apical compartment contains a single layer of sustentacular or supporting cells that do not belong to the neuronal lineage (Hempstead and Morgan, 1983; Farbman, 1992, Calof *et al.*, 1998; Murray and Calof, 1999). Sustentacular cells apically terminate with microvilli at the epithelial surface and basally terminate at the basement membrane close to acinar cells of Bowman's gland or capillaries in connective tissue. Sustentacular cells are thought to regulate the passage of

substances between connective tissue and the OE to maintain the ionic composition of the overlying mucosa (Farbman, 1992).

The middle compartment of the OE contains ORNs (Calof *et al.*, 1998), which generate nerve impulses in response to chemical stimuli (Farbman, 1992). Mature ORNs send an apical dendritic process that terminates with cilia in the overlying mucosa at the epithelial surface. The cilia are directly exposed to chemical odorants in the nasal cavity. The cell bodies of ORNs lie in the middle to lower one-third of the OE and often contact each other. ORN axons form axon bundles that exit the OE into the lamina propria (LP), project across the cribiform plate before synapsing with secondary afferents in the OB, the primary target organ of ORNs (Fig 2) (Farbman, 1992; Calof *et al.*, 1998; Murray and Calof, 1999). The LP is a connective tissue layer underlying the OE containing thin collagen, elastic fibers and components of connective tissue including fibroblasts, macrophages, mast cells and leukocytes (Farbman, 1992). The glial cell of the olfactory system, olfactory ensheathing glia (OEG), ensheath axon bundles as they exit the LP and enter the CNS in the olfactory nerve layer (ONL) of the OB (Doucette, 1990; Doucette, 1991; Astic *et al.*, 1998).

The basal compartment of the OE is believed to contain putative neural stem cells. This compartment contains two cell types, horizontal (HBC) and globose basal cells (GBC), (Graziadei and Monti Graziadei, 1978, Calof and Chikaraishi, 1989; Calof *et al.*, 1998) that differ in morphology. HBCs form a layer adjacent to the basal lamina with GBCs lying apically next to HBCs. It is currently unclear which cell type is the putative neural stem cell. The GBC population is thought to contain three distinct cell types: putative neuronal stem cells or neural colony-forming cells (CFUs), Mash-1 (M1)

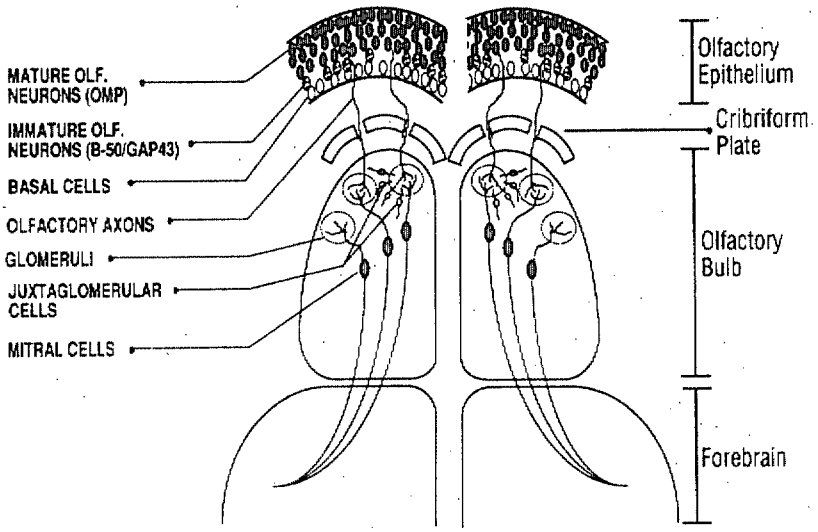

Figure 2: Schematic of the primary olfactory pathway. Olfactory receptor neurons (ORNs) located in the olfactory epithelium (OE) send axonal projections through the cribriform plate to synapse on target cells in glomeruli of the OB (Margolis *et al.*, 1991).

expressing cells and immediate neuronal precursors (INPs) (Fig 1) (Murray and Calof, 1999).

ORNs can be further subdivided based on their maturity, the molecular markers they express and their relative location in the OE. Mature ORNs are located apically and express neural cell adhesion molecule (NCAM) and olfactory marker protein (OMP), a protein that appears to be expressed exclusively in mORNs (Farbman and Margolis, 1980; Calof and Chikaraishi, 1989). Immature ORNs are located basally, underneath mORNs, and express the growth associated protein GAP-43 and NCAM, but not OMP (Calof and Chikaraishi, 1989; Verhaagen *et al.*, 1989; Murray and Calof, 1999). In order to mature and survive, IRNs require contact with the OB (Schwob *et al.*, 1992; Murray and Calof, 1999).

As previously mentioned, ORNs generate nerve impulses in response to chemical stimuli and thus, are responsible for our sense of smell. They express the odorant receptors (ORs) that provide it with the ability to distinguish between thousands of odorant ligands. Odorants are small organic molecules less than 400 Da in size and differ from each other based on size, shape, functional groups and charge. They consist of a diverse combination of aliphatic acids, alcohol, ketone, and ester groups and aromatic, alicyclic, polycyclic and heterocyclic ring structures. The perceived odor can change with extremely small changes in odorant structure as well as odorant concentration. In addition, sensitivity to odorants and the perceived odor varies among individuals (Malnic *et al.*, 1999; Mombaerts, 1999).

The olfactory system has the amazing ability to distinguish between each odorant and this ability is due to a multigene family of an estimated 500-1000 different ORs. OR

genes encode for seven transmembrane G protein coupled receptors, which share similar motifs but vary widely in sequence, suggesting that they have the ability to recognize diverse odorant ligands (Buck and Axel, 1991; Ebrahimi and Chess, 1998; Buck, 2000).

OR genes are the largest gene family in the genome, comprising approximately 1% of all genes (Sosinsky *et al.*, 2000). ORs are organized in clusters that are randomly distributed throughout the genome. In mouse, OR clusters have been mapped to 11 loci on 7 different chromosomes. Each ORN only expresses a single allele of a single OR gene or a single allele of a small number of highly related OR genes (Chess *et al.*, 1994). Furthermore, the axons of ORNs expressing the same or a highly related OR converge at a few defined loci called glomeruli, out of the approximately 2000 glomeruli in the OB (Ressler *et al.*, 1994).

ORs are expressed in 4 distinct spatial zones along the anterior-posterior and dorsal-ventral axes of the OE (Fig 3). ORNs that express the same OR are found within the same spatial zone but are randomly interspersed with ORNs expressing other ORs in that zone. The zonal distribution of ORs is thought to initially sort olfactory information; further organization into a sensory map occurs in the glomeruli of the OB. These sensory maps are the same between individuals. The mechanism controlling selective OR expression by ORNs and the selective expression within a given zone is currently not known. The clustering of OR genes appears to be important in how they are regulated. In the majority of cases, ORs within a gene cluster are preferentially expressed within the same zone of the OE (Strotmann *et al.*, 1994; Strotmann *et al.*, 1994). For example the P2 receptor is restricted to zone 3 of the OE (Wang *et al.*, 1999). It has been suggested that when an ORN chooses to express a given OR, it may be limited to a given OR cluster

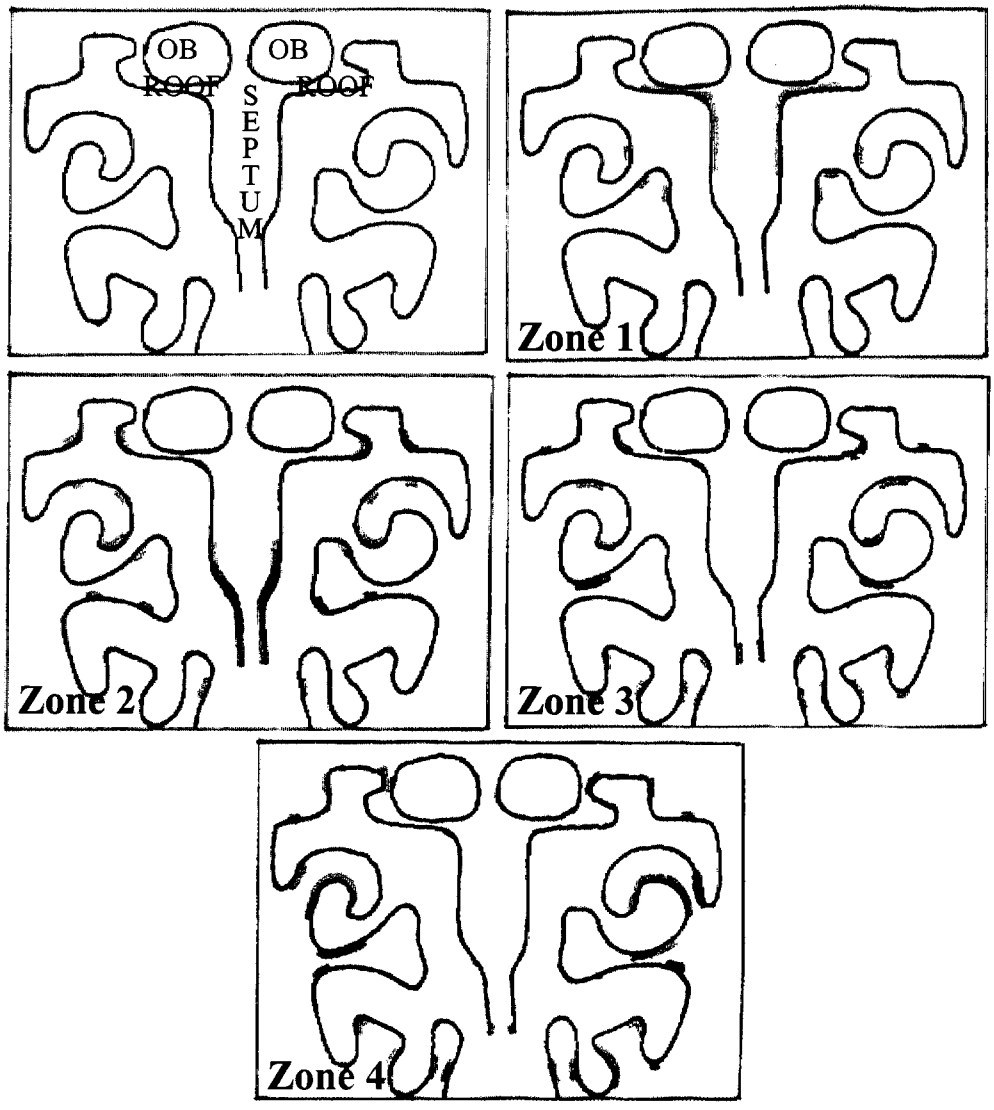

Figure 3: Odorant receptor expression zones. Four OR expression zones are present in the OE. The regions of OR expression within each zone is indicated in red. The zonality is present in the anterior-posterior and dorsal-ventral axes of the OE.

but selection from that cluster is stochastic (Chess *et al.*, 1994; Sullivan *et al.*, 1996; Malnic *et al.*, 1999; Mombaerts, 1999; Strotmann *et al.*, 1999; Buck, 2000).

Although ORs vary in sequence and odorant specificity, all ORs initiate the same signal transduction cascade upon binding odorant ligands. Odorants enter the nasal cavity and are detected by ORNs lining the OE. The signal transduction cascade begins with the activation of G_{olf}, a $G_s\alpha$-like G protein, leading to the activation of adenylate cyclase III, which raises intracellular cAMP levels. Increased intracellular cAMP results in the opening of a cyclic nucleotide gated channel and the subsequent influx of cations generates an action potential. The action potential generated in the activated ORN travels along the axon to the OB where it converges with axons from other ORNs that express similar ORs in glomeruli, which are thought to organize ORN axons. The brain can determine which OR has been activated by spatial pattern of activity in the OB (Ebrahimi and Chess, 1998; Xu *et al.*, 2000). Nerve impulses from the OB are relayed to the primary olfactory cortex and limbic system, and then to higher cortical regions (Malnic *et al.*, 1999; Buck, 2000).

Olfactory Development-Development of the olfactory system is first noted by the formation of the olfactory placodes at E9.5, which appear as paired oval-shaped epithelial tissue at the anterolateral region of the head. As development proceeds the surrounding mesenchyme grows, resulting in an invagination called the olfactory pit, which forms olfactory tissue; by E11.5 the nasal cavity is formed. In mammals, the surface area of the epithelium lining the nasal cavity is increased by the presence of folds or turbinates. In mouse and humans there are three turbinates: superior (ectoturbinates A, B, C), middle

(endoturbinates I, II) and inferior (endoturbinates III, IV); however other mammals such as rabbits and pigs have more. The vomeronasal organ (VNO), an accessory olfactory organ thought to be responsible for detection of pheromones and social behavior, develops from an invagination of the nasal septum and is lined with nasal epithelium (Farbman, 1991; Farbman, 1992).

Early in the development of the olfactory system, presumptive sensory cells are mitotically active. Mitotic activity decreases significantly in the mouse at E12, when the OE first becomes apparent. At this stage, the OE has one layer of sensory cells located basally, with a layer of sustentacular cells adjacent apically. The decrease in mitotic activity is thought to be a result of cells leaving the cell cycle and differentiating into neurons. From this stage onward, the OE thickens as cells proliferate and differentiate into ORNs. By E12 GAP-43 positive IRNs begin to display multiple cilia, which roughly coincides with the time that axons make contact with the developing OB. As axon outgrowth occurs, GAP-43 expression levels increase. Synapses in the OB are not observed until E14 (Hinds and Hinds, 1976; Farbman 1986; Farbman, 1991).

Neuronal markers are expressed early in olfactory development. As previously mentioned, GAP-43 is expressed at E12. Weak NCAM expression is detected as early as E9 (Farbman, 1991). As olfactory neuronal development proceeds, GAP-43 expression increases and by post-natal day P1, GAP-43 positive ORNs are present throughout the OE. At the same time, OMP is only expressed in a small population of neurons located in a single cell layer superficially in the OE. OMP expression increases with age and by P9, expression is 3-4 cell layers thick. A shift in GAP-43 and OMP expression is seen with

increasing age. When ORNs mature, GAP-43 expression becomes limited and is seen as a single cell layer next to the basal region of the OE (Margolis *et al.*, 1991).

Behavioral, electrophysiological and morphological studies support the idea that the olfactory system is functional in utero. Electrophysiological experiments using single cell patch clamp have demonstrated that at E16 in rat (equivalent to E13 in mouse), ORNs generate action potential in response to stimulation by all classes of odorant ligands. At this point, ORNs are not selective but a few days later, ORNs can discriminate between odorants. These observations suggest that the olfactory system is functional in utero and that selective odorant recognition does not occur until approximately E18 to E19 (equivalent to E16 in mouse) (Farbman, 1991).

The OB and accessory olfactory bulb develop as an out pocketing of the rostral end of the cerebral vesicles. In mice OB development begins at E12, just as IRN axons reach this region. At this developmental stage, the OB is only two layers thick consisting of a ventricular layer, where neurogenesis occurs, and a marginal layer. A mitral cell layer is visible in the OB at E15, with a subventricular layer between it and the ventricular layer. The subventricular layer later generates the granule and periglomerular cells of the OB. Whereas the OB is the target organ of ORNs from the OE, the accessory OB is the target organ of ORNs from the vomeronasal organ (Farbman, 1991; Farbman, 1992).

At the time of birth there are few glomeruli in the OB; the majority of glomerular formation occurs postnatally and is dependent on cell activity. However at birth there are a few distinct glomeruli that are formed located near the caudal boundary with the accessory OB. These glomeruli are referred to as the modified glomerular complex and

are thought to be important in the recognition of odorants associated with suckling in neonates. The majority of growth and maturation of the OB occurs postnatally, particularly within the first two weeks of birth. This is thought to be due to a ten-fold increase in the number of ORNs, a thicker ONL and increased numbers of interneurons, glomeruli and mitral cells in the OB. These factors contribute to the formation of the laminar structure of the OB (Farbman,1991; Farbman, 1992).

As seen in other systems, interactions between tissues are important in development. Studies have demonstrated that the ORNs in the OE influence OB development and vice versa. The former has been shown in amphibians by ablation of the olfactory placode, which causes the OB to be much smaller. The converse experiment is also true, transplantation of additional olfactory placodal tissue results in cell proliferation. The observation that ORNs influence the OB is seen not only during development, but in adult animals as well. The latter has been shown in explant cultures. In the absence of OB tissue, OE explants undergo differentiation but fail to completely mature. The effect of OB on ORN maturation is thought to be due to physical contact between ORN axons and OB tissue as opposed to diffusion of factors (Farbman,1991; Farbman, 1992).

Gene regulation in Olfactory Neurogenesis-Neurogenesis is a complex process under strict control not only during development, but also in the normal regenerating olfactory epithelium. Stringent regulatory processes are necessary to ensure that: 1) the correct number of neurons are made at the right time and place, 2) they achieve the same terminally differentiated state as their predecessor, and 3) they make the proper functional

connections. In the initial stages of neuronal development in the nervous system, progenitor cells proliferate rapidly but slow down as maturity is reached; in most regions of the nervous system proliferation ceases completely at the end of development (Calof *et al.*, 1998). However in the OE, similar regulatory processes required during development are still required in the adult. Understanding the regulatory processes in the relatively simple OE will provide a groundwork for understanding comparable mechanisms in more complex regions of the nervous system that contain diverse populations of cell types, where not much is known about the molecular mechanisms involved in regulating mammalian neurogenesis (Jan and Jan, 1990).

Extrinsic and intrinsic factors are known to regulate the proliferation and differentiation of neural precursors. Culture systems that permit the manipulation of the environment in which precursors proliferate and differentiate have allowed the identification of extrinsic, or environmental factors. The intrinsic, or endogenous factors that regulate neurogenesis have been more difficult to identify (Guillemot, 1995). In eukaryotes, there are two general levels of regulating gene expression intrinsically: firstly, through regulation of transcription factors and secondly, through the modification of chromatin structure (Ashraf and Ip, 1998). The regulation of transcription factors during olfactory neuronal development has been well studied and much of what is known about the control of mammalian, and olfactory neurogenesis in particular, has come from genetic studies of sense organ formation performed in *Drosophila* (Guillemot, 1995); however, the regulation of gene expression through chromatin modification is a relatively novel mechanism that has not been explored in olfactory neurogenesis.

A classification scheme has been developed to group genes that control different aspects of sense organ formation in *Drosophila* that is commonly used in other systems. Six classes have been distinguished based on function, expression and stage of sense organ formation upon which they exert their effects: 1) proneural genes promote neural fate in ectoderm cells, 2) neurogenic genes set apart neural precursors through cell-cell interactions or lateral inhibition, 3) neural precursor genes control neuronal differentiation, 4) neuronal type selector genes specify neuronal type, 5) cell-cycle genes control patterns of cell division, and 6) additional genes control cell fate.

Both proneural and neurogenic genes have been well studied in the olfactory system. Proneural genes are expressed in undifferentiated ectodermal cells or proneural clusters, and the location of their expression specifies where the nervous system will form by providing these cells with the potential of developing into neural precursors (Jan and Jan, 1993). Initially, proneural genes act by inducing the expression of downstream neurogenic genes throughout the proneural cluster and later, their own expression is inhibited (Lewis, 1996).

In the olfactory system, proneural genes have been identified that positively regulate neurogenesis including Mash-1 (mammalian achaete-scute homologue) and Math/neurogenin (mammalian atonal homologue). Mash-1 is required for the early development of olfactory neurons (Guillemot, 1993; Guillemot, 1995; Kageyama *et al.*, 1995). *In vitro* studies using OE explants (Calof *et al.*, 1998) and *in vivo* studies of Mash-1 knockouts, which are post-natal lethal (Guillemot, 1993), have demonstrated that Mash-1 is required for ORN development as opposed to ORN survival and that it is

required to confer the neuronal stem cell of the OE with the capacity to generate neuronal precursors (Calof *et al.*, 1998).

Two Math/neurogenin (ngn) genes have been identified in olfactory development: Math4C/ngn-1/NeuroD3 and Math4A/ngn-2 (Cau *et al.*, 1997). The former is Mash-1 dependent; in Mash-1 knockouts, Math4C expression is absent from E10.5 onwards except in the ventrocaudal domain, which contains Mash-1 independent cells. In contrast, Math4A expression is Mash-1 independent and is expressed in the ventrocaudal domain of the OE (Cau *et al.*, 1997). However, *in vitro* interaction assays have shown that Math4A can homo- and hetero-dimerize and specifically bind to Mash-1 (Gradwohl *et al.*, 1996). Its expression overlaps with the Mash-1 independent Math4C cells (Cau *et al.*, 1997). Although Math4C and Math4A expression have been characterized in the OE, their role in olfactory development has not yet been determined (Cau *et al.*, 1997).

Neurogenic genes are involved in a cell-cell signalling mechanism whereby a cell that has been committed to a neural fate prevents neighbouring cells in a proneural cluster from adopting the same fate. Mutations in neurogenic genes result in a massive over-production of neurons (Lewis, 1996). In the olfactory system, neurogenic genes have been identified that are homologues of *Drosophila* neurogenic genes: Notch1, Notch2, Notch3 and its ligands Delta and Jagged and Hes-1 (*Drosophila* hairy and E(spl) homologue).

The Notch gene encodes for a cell surface receptor that is activated by cell-cell contact with an adjacent ligand expressing cell; there are two classes of Notch ligands: Delta and Serrate. Notch signaling controls when, where and how many progenitor cells differentiate into mature cells; thus it controls cell fate. This signaling system has been

implicated in hematopoiesis, myogenesis and neurogenesis and is conserved across a broad range of species. In mouse, *in situ* hybridization experiments have demonstrated that Notch1, Notch2, Notch 3, Delta1 and Jagged mRNA are differentially expressed in the OE (Lindell *et al.*, 1996). Not much is currently known about Notch signaling in the OE and it is presumed that Notch function is conserved. In *Drosophila* Notch signaling is important in controlling cellular differentiation through lateral inhibition; activation of Notch culminates in alterations in gene expression, including up-regulation of other neurogenic genes (Weinmàster, 1997; Beatus and Lendahl, 1998; Weinmaster, 1998).

Hes-1 is a transcriptional repressor that inhibits neuronal differentiation in the tissue where it is expressed. It acts as a negative regulator, antagonizing and/or decreasing the expression of Mash-1 and other positive regulators of neurogenesis through protein-protein interactions (Kageyama *et al.*, 1995; Kageyama *et al.*, 1997). Hes-1 has been found to associate with Notch proteins (Dattani *et al.*, 1998; Dattani *et al.*, 1999). Although Hes-1 expression has not been characterized in the OE, mouse knockout studies implicate it in olfactory neuronal development. Embryonically, Hes-1 knockouts have hypoplastic olfactory pits and neonates and adults have hypoplastic nasal cavities and OB (Dattani *et al.*, 1998; Dattani *et al.*, 1999). In general, neuronal differentiation proceeds prematurely possibly leading to the depletion of precursor cells. Mash-1 expression is also up-regulated in the absence of Hes-1 (Kageyama *et al.*, 1997). These observations support the idea that Hes-1 is responsible for inhibiting olfactory neurogenesis and maintaining potential neural precursors in an undifferentiated state, possibly by inhibiting Mash-1. *In vitro* transfection experiments have demonstrated that Hes-1 can inhibit Math1 activity (Kageyama *et al.*, 1997).

Currently work is being done to identify and characterize the other gene classes in *Drosophila* as well as in the olfactory system. This work will provide the next level in understanding gene regulation in developmental neurogenesis at the transcription factor level. The expression of transcription factors that appear to be downstream of neurogenic genes have been identified in the OE and include NeuroD, Olf-1, Pax-6 and Neurological Stem Cell Leukemia-1 (NSCL-1) and NSCL-2. NeuroD and Olf-1 may belong to the neural precursor gene class as they appear to control neuronal differentiation.

NeuroD/Beta-2 is a transcription factor that is involved in neuronal differentiation. Mash-1 knockouts fail to develop functional ORNs and the majority of cells in the OE of knockout animals do not express NeuroD, suggesting that NeuroD is downstream of Mash-1. NeuroD is thought to be involved in ORN differentiation (Nibu *et al.*, 1999). The Olf-1 transcription factor binds to a conserved region upstream of several olfactory neuron specific genes and it is thought to be responsible for regulating genes involved in the odorant signal transduction cascade as well as in the continual replacement of ORNs. Olf-1 is expressed in post-mitotic ORNs and in ORN progenitors and is downstream of Mash-1. Studies have shown that Olf-1 expression is turned on in the OE as neuronal precursors leave the cell cycle and differentiate, suggesting that developmentally Olf-1 is responsible for controlling differentiation and in the adult, replacing ORNs. It is thought that Olf-1 may activate transcription of olfactory neuron-specific genes, thereby regulating cell phenotype (Davis and Reed, 1996). Two additional transcription factors have been identified, O/E-2 and O/E-3, that share structural and biochemical similarities and expression patterns to Olf-1 in the OE. Unlike Olf-1, O/E-2 and O/E-3 are expressed only in olfactory tissue. Olf-1 knockout mice have

been generated that show normal olfactory structures suggesting that a level of redundancy may exist (Wang *et al.*, 1997).

Pax-6 is a transcription factor whose expression is limited to non-neuronal structures in the OE; it is expressed in sustentacular cells and in HBCs. *Sey* mice that are homozygous for a mutation in the Pax-6 gene fail to form an olfactory placode suggesting that Pax-6 may be required in early placode formation and later in regulating the expression of non-neuronal, lineage specific genes in the OE (Davis and Reed, 1996). NSCL-1 and NSCL-2 are transcription factors with unknown functions in the OE. *In situ* hybridization experiments have shown that both factors are expressed in the developing mouse OE (Begley, 1992; Lee, 1997). Experiments by Ma *et al.* have suggested that NSCL-1 is downstream of NeuroD (Ma *et al.*, 1998).

DNA Methylation and Gene Silencing-As discussed, the regulation of gene expression through the modulation of transcription factors has been well described in the OE. The recent finding that alterations in chromatin structure, rendering chromatin transcriptionally active/inactive, also plays an important role in regulating gene expression has not been looked at in the OE.

Methylation of DNA is a common modification and occurs most frequently at position 5 of cytosine residues when followed by a guanine (CpG di-nucleotide). Somatic genomes are globally methylated in contrast to CpG islands, small GC-rich regions of DNA that are found throughout the genome. CpG islands on average consist of more than 60% GC, are approximately 1 kb in length and often associated with gene promoters (Hendrich and Bird, 1998, Brock *et al.* 1999). DNA methylation is associated

with transcriptional repression. It is thought that the pattern of methylation is established during embryogenesis, during which developmental genes are silenced. Methylation of CpG islands and the resulting repression of genes has been observed in genes located on the inactive X chromosome, in genes associated with imprinting and tumor suppressor genes in cancer (Brock *et al.* 1999; Hendrich and Bird, 1998; Bird and Wolffe, 1999; Hendrich *et al.*, 2001). DNA methylation patterns are initially established in the gametes. Early in development, there is a global demethylation event followed by the formation of tissue-specific methylation patterns that are necessary for development to proceed normally (Hanel and Wevrick, 2001).

The methylation of DNA and the maintenance of methylation patterns are accomplished by a family of proteins known as DNA methyltransferases (DNMTs): DNMT1, DNMT2, DNMT3a, DNMT3b and DNMT4, that share homology in the methyltransferase (MTase) domain with cytosine DNA methyltransferases. It has been found that mutations in the maintenance DNA methyltransferase DNMT4 and *de novo* DNA methyltransferases DNMT3a and DNMT3b are embryonic lethal; animals fail to complete development (Hendrich *et al.*, 2001). Embryonic stem (ES) cells lacking functional DNMTs grow normally in culture but cannot support embryonic development and have been found to misexpress imprinted genes. Thus, DNA methylation is essential during development (Hendrich and Bird, 1998).

Entire gene clusters located on CpG islands can be silenced by the binding of MBDs (Fig 4A). Two mechanisms methylation dependent gene silencing have been proposed. In the direct mechanism (Fig 4B), DNA methylation prevents transcription by excluding transcription factors that contact cytosine residues or interfere with the binding

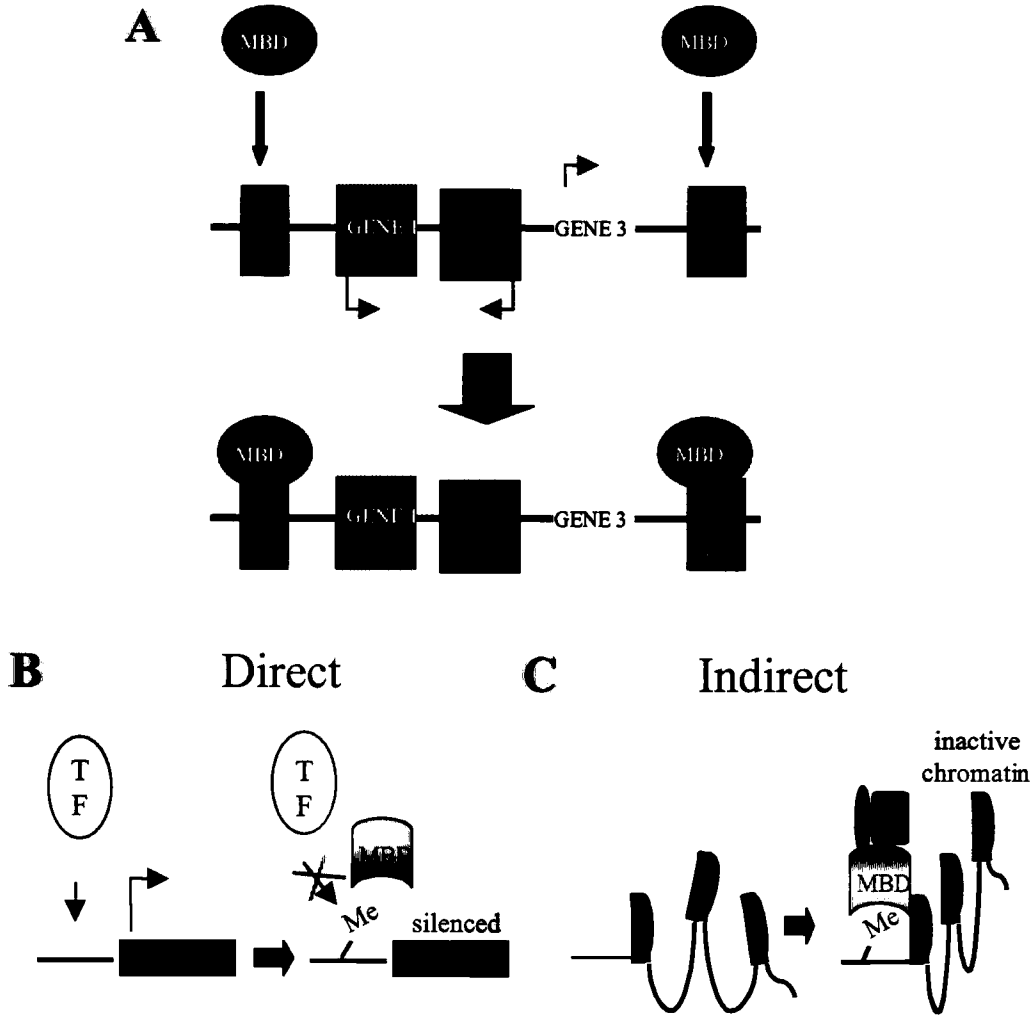

Figure 4: Mechanisms of methylation dependent silencing. (A) MBD mediated transcriptional silencing of genes clustered on CpG islands. Arrows indicate the direction of transcription. (B) Direct repression. Methylation of cytosine residues prevents the binding of transcription factors that require contact with cytosine residues. (C) Indirect repression. MBD transcriptional repressor complexes bind methylated DNA and alter chromatin structure, rendering chromatin transcriptionally inactive.

of transcriptional machinery to DNA. The majority of transcription factors require contact with cytosine residues; however, transcription factors are known that can bind to DNA independent of methylation status. In addition, it is known that densely methylated regions can be transcriptionally active in the absence of methyl-DNA binding proteins and/or chromatin modification proteins. Although methylation status may have a minor role in direct repression, an indirect mechanism involving alterations in chromatin structure, due to the binding of repressor complexes that include chromatin modification proteins, has also been proposed (Fig 4C). The observation that DNA methylation can act at a distance and that repression occurs after chromatin assembly supports this mechanism. There has been evidence supporting both the direct and indirect mechanisms of transcriptional repression; however, the identification of protein complexes capable of binding methylated DNA and that highly methylated DNA can be transcribed at near normal rates in the absence of these suggests that the indirect mechanism is more common.

Gene silencing by DNA methylation is thought to be mediated by the binding of repressor protein complexes. A family of five methyl-CpG binding domain (MBD) proteins: MeCP2, MBD1, MBD2, MBD3 and MBD4 have been identified that share the approximately 70 residue conserved MBD domain. All of the MBD proteins are expressed ubiquitously in somatic tissues; however, MeCP2, MBD1 and MBD2 are absent or expressed at very low levels in embryonic stem cells. MBDs have been found to associate with other MBD family members and chromatin modification proteins such as histone binding proteins, histone deacetylases (HDACs) and the co-repressor protein that recruits them, Sin3A. Thus, it appears that MBDs play an important role in

connecting DNA methylation and transcriptional repression through alterations in chromatin structure (Hendrich and Bird, 1998; Bird and Wolffe, 1999; Hendrich *et al.*, 1999; Wakefield *et al.*, 1999; Snape, 2000).

The founder member of the MBD protein family is MeCP2, which is expressed ubiquitously in somatic tissue and at very high levels in the brain. MeCP2 is a 52.4 kilodalton (kD) protein that contains both a MBD domain and a C-terminal transcriptional repression domain (TRD) and can bind to a single symmetrically methylated CpG in naked DNA and chromatin (Bird and Wolffe, 1999; Hendrich and Bird, 1999; Wakefield *et al.*, 1999; Free *et al.*, 2000). The MBD domain is necessary and sufficient to bind methylated DNA *in vitro* (Wakefield *et al.*, 1999; Free *et al.*, 2000); an internal deletion of the MBD domain abolishes methyl-DNA binding capability. This ability has been further confirmed using ES cells lacking functional DNMT. The absence of methylated DNA disrupts MeCP2 localization (Hendrich and Bird, 1999).

MeCP2 has been shown to repress transcription from methylated promoter gene constructs (Nan *et al.*, 1997). Nan *et al.* have identified the TRD as responsible for repression using deletion analysis and have found that MeCP2 is capable of long-range repression. Using a β-galactosidase reporter gene assay, it was found that MeCP2 can repress transcription up to 2kb away, although the strength of repression decreases with distance. Furthermore, deletion of the MBD domain prevents repression, thus linking the processes of binding methylated DNA and repression in MeCP2. The abundant distribution of MeCP2 suggests that it acts as a "global" transcriptional repressor (Hendrich and Bird, 1999; Wakefield *et al.*, 1999). Jones *et al.* (19998) have demonstrated that MeCP2 and methylated DNA recruit histone deacetylase to repress

transcription. Furthermore, immunoprecipitation experiments in mammalian and *Xenopus* cells have demonstrated that the TRD directly interacts with Sin3A and HDACs. Furthermore, experiments using the HDAC inhibitor trichostatin A have been shown to relieve repression (Hendrich and Bird, 1999).

Mutations in the MBD domain of MeCP2 have been found to be associated with the genetic disorder Rett syndrome. Rett syndrome (RTT) is a neurodevelopmental disorder that affects young females almost exclusively and occurs at a rate of 1 in 10,000. RTT patients appear to develop normally for the first 6-18 months upon which a sudden regression in development occurs with individuals losing purposeful hand use and speech. In addition, they also display characteristic hand-wringing movements, ataxia, seizures, autism, growth retardation and mental handicap. Following the initial regression event, RTT patients stabilize and survive into adulthood (Willard and Hendrich, 1999; Ballestar *et al.*, 2000).

Four mutations in the MBD domain have been have been identified in RTT patients. Three of these mutations have a severe effect on methyl-DNA binding ability, decreasing affinity by greater than 100-fold. This suggests that the inability to bind methylated DNA and repress transcription resulting in transcriptional noise due to the misexpression of genes contributes to RTT. However the fourth mutation only decreases methyl-DNA binding affinity by 2-fold; individuals with this mutation display the same disease phenotype. This suggests that developing neurons are highly sensitive to the MeCP2-methyl-DNA interaction or that the MBD domain may have other functions (Amir *et al.*, 1999). A MeCP2 knockout mouse has recently been generated that displays characteristics of RTT (Chen *et al.*, 2001; Guy *et al.*, 2001).

An additional methyl-DNA binding protein MeCP1, has been identified that has the ability to bind methylated DNA and repress transcription; however, MeCP1 does not share homology in the MBD domain. In contrast to MeCP2, its DNA binding ability is dependent on a threshold of methylation, requiring more than 10 methyl-CpGs to bind DNA. MeCP1 is a 75 kD protein that is a part of a large protein complex estimated to be 400-800 kD in size (Nan *et al.*, 1997; Hendrich and Bird, 1998). Three different MeCP1 bands referred to as complexes I, II and III, were identified in fibroblast cell lines (Hendrich *et al.*, 2001). It was initially thought that MBD1 was a part of this complex (Nan *et al.*, 1997; Hendrich and Bird, 1998); however, further studies have ruled out this possibility. Subsequent work by Ng *et al.* in HeLa cells has demonstrated that the MeCP1 repressor complex contains MBD2, HDAC1 and HDAC2 and the histone binding proteins RbAp46 and RbAp48. In this complex, MBD2 is capable of repressing transcription of reporter DNA if methylation patterns favor MeCP1 binding (Bird and Wolffe, 1999; Ng *et al.*, 1999). The requirements for binding DNA have led to the suggestion that MeCP1 may be involved in the repression of specific genes, as opposed to the global repression activity associated with MeCP2 (Nan *et al.*, 1997; Hendrich and Bird, 1998).

MBD1, originally called PCM1, was first identified by Cross *et al.* from a TBLASTN search of the dbEST database against the MBD domain of MeCP2. Sequence analysis showed that MBD1 also contains a TRD and two cysteine rich regions in human and three cysteine rich regions in mouse that share similarity to DNMTs. *In vitro* MBD1 selectively binds methylated DNA through its MBD domain and represses transcription. Further experiments have shown that MBD1 preferentially binds double-stranded,

symmetrically methylated DNA *in vitro* in a sequence independent manner, but can bind hemi-methylated DNA to a lesser extent.

MBD1 is an 80 kD protein that also generates a degradation product at 36 kD that is ubiquitously expressed in somatic tissue but absent in ES cells. Recombinant MBD1 alone can inhibit transcription *in vitro* (Cross *et al.*, 1997; Hendrich and Bird, 1999). Further characterization by Fujita *et al.*, demonstrated that at least five different splice variants exist that retain the MBD domain, suggesting that repression by different MBD1 splice variants may depend on differential methylation patterns (Fujita *et al.*, 1999; Fujita *et al.*, 2000).

Hendrich and Bird have identified three other MBD proteins by searching the EST database with the MBD domain: MBD2, MBD3 and MBD4. Recombinant forms of MBD2 and MBD4 are capable of binding methylated DNA probes *in vitro*, and binding complexes can be competed away by the addition of 100 times excess unlabeled methylated probe but not unmethylated probe. Both are localized to methylated DNA. Immunostaining for MBD2 and MBD4 localized the proteins to major satellite DNA, which is known to have a high proportion of methylated DNA. In contrast, recombinant MBD3 can bind methylated DNA but the binding complex cannot be competed away by addition of either unlabeled methylated probe or unmethylated probe; MBD3 does not localize to major satellite DNA. Using a variety of methylated DNA probes, it was found that MBD2, MBD3 and MBD4 preferentially bind double stranded, symmetrically methylated DNA. However like MBD1, MBD4 can also bind hemi-methylated DNA to a lesser degree (Hendrich and Bird, 1998).

MBD2 has two variants: one encoding a 43.5 kD protein referred to as MBD2 or MBD2a, and one encoding a 32.2 kD protein as a result of an internal ATG start codon, referred to as MBD2b. Sequence alignment with the MBD domain showed that MBD2 was most similar to MBD1 and MBD3 in primary sequence. Using Northern blot, Hendrich and Bird showed that MBD2 is expressed in a variety of somatic tissues including brain, heart, kidney, liver, skeletal muscle, spleen and testis as a doublet band suggesting differences in polyadenylation. The testis was found to have an alternatively spliced variant. MBD2 is lowly expressed in ES cells. MBD2 can bind methylated DNA *in vitro* and *in vivo*.

As previously discussed MBD2 is a part of the MeCP1 repressor complex. Transient overexpression of MBD2 in HeLa cells causes the repression of methylated reporter DNA if MeCP1 can recognize the methylation site and repression can be inhibited by the addition of HDAC inhibitor. Bhattacharya *et al.* showed that MBD2b is a DNA demethylase with the ability to remove methyl groups from methyl-cytosine bases and from methylated plasmid DNA transfected into HEK393 cells. This finding links methylation dependent silencing and active demethylation of DNA to bring about transcriptional activation; however, follow-up studies by Ng *et al.* and Wade *et al.* were not able to reproduce this demethylase activity. Removal of methyl groups from cytosine is energetically unlikely and other demethylase candidates are not known (Hendrich and Bird, 1998; Bhattacharya *et al.*, 1999; Ng *et al.*, 1999; Wade *et al.*, 1999; Snape *et al.*, 2000).

Hendrich *et al.* have generated MBD2-/- mice, which are viable, fertile and normal in gross appearance, by replacing exon 2 of the MBD2 gene with the promoter-

less βgeo cassette, which contains a transcription stop site that terminates transcription in the middle of the MBD domain. Since MBD2b has been reported as a DNA demethylase, Hendrich *et al.* looked at methylation levels in knockout animals. The absence of MBD2 does not affect global DNA methylation levels, contrary to what would be expected in the absence of a DNA demethylase. Molecular analysis showed that MeCP1 formation and activity is dependent on the presence of MBD2; in the absence of MBD2, complex I is also absent. Cell lines generated from wild-type, heterozygote and knockout mice showed that MBD2-/- deficient cells were also unable to repress transcription from a methylated reporter DNA construct. This lack of repression could be rescued by transfecting in MBD2. Behavioral analysis showed that MBD2-/- animals may display abnormalities in maternal behavior; pups born to an MBD2-/- mothers were smaller than in reciprocal crosses and postpartum MBD2-/- mothers were slower to retrieve their newborn pups to their nests than wild-type controls (Hendrich *et al.*, 2001).

In contrast to the other MBDs which only share homology in the MBD domain, MBD3 is highly similar to MBD2 with 71% overall amino acid identity; a noticeable difference is the acidic C terminus of MBD3 and absence of the N terminus. MBD3 is expressed widely in somatic tissue as well as in ES cells (Hendrich and Bird, 1998; Hendrich *et al.*, 2001). Wade *et al.* have shown that the NuRD/Mi-2 repressor complex contains MBD3. The NuRD/Mi-2 complex is a histone deacetylase transcriptional repressor and nucleosome remodeling complex that is a member of the SWI-SNF family of ATPases. The NuRD complex has been implicated in gene silencing in mammals, flies, nematodes and plants (Bird and Wolffe, 1999; Hendrich *et al.*, 2001). NuRD contain proteins that are associated with nucleosome remodeling and confer histone

deacetylase activity, in particular HDAC1, HDAC2, RbAp46, RbAp48, as seen in the MeCP1 repressor complex (Zhang *et al.*, 1999; Ahringer, 2000; Guschin *et al.*, 2000).

Although the methyl-DNA binding activity of MBD3 is not clear, studies in *Xenopus* have shown that it does preferentially bind methylated DNA. Furthermore, Zhang *et al.* have shown that the NuRD complex can interact with MBD2 *in vitro*. This has led to three possible roles for the MBD3/NuRD complex in transcriptional repression: 1) MBD2 may recruit the NuRD to methylated DNA, 2) although MBD3 may not have strong methyl-CpG binding activity, the NuRD complex can still act as a repressor complex alone, and 3) NuRD is not involved in transcriptional repression. The fact that NuRD is a SWI-SNF member supports the idea that active modification of histones within chromatin is a feature of the repression mechanism and occurs through its intrinsic ATP hydrolysis activity (Bird and Wolffe, 1999; Wade *et al.*, 1999; Zhang *et al.*, 1999).

Hendrich *et al.* have also generated a MBD3 knockout mouse. In contrast to MBD2-/- animals, MBD3-/- animals die early during embryogenesis, demonstrating that these two proteins are not functionally redundant although they do share significant homology. Following implantation, no normal MBD3-/- animals were observed and by E8.5 MBD3-/- embryos were retarded in growth. Intercrosses of MBD3+/- and MBD2-/- animals generated significantly less MBD3+/- when compared to crossing onto a MBD2+/+ background, suggesting that MBD3 viability is reduced when MBD2 is absent. This finding supports the idea that MBD2 and MBD3 physically interact. Hendrich *et al.* claim that their data supports the idea that MBD2 interacts with the MBD3/NuRD repressor complex and recruits the complex to methylated DNA (Hendrich *et al.*, 2001).

Based on MBD sequence alignment MBD4, a 62.6 kD protein, was found to share the highest homology with MeCP2 in primary sequence. Further searches with the MBD4 protein showed similarity to bacterial DNA repair enzymes, supporting the finding that MBD4 is a mismatch repair protein. RT-PCR showed that MBD4 is expressed widely in somatic tissue and ES cells (Hendrich and Bird, 1998; Hendrich and Wolffe, 1999; Hendrich *et al.*, 2001.

Transcriptional repression by MBD proteins and DNA methylation is a relatively new area and provides an interesting alternative to gene regulation, especially during development and in the nervous system. Understanding gene regulation events in olfactory neuronal development is important because it may provide clues into understanding gene regulation events in more complex neuronal subtypes. With respect to human diseases, disorders in olfaction are common indicators of disease. Olfactory dysfunctions are associated with schizophrenia, bipolar disorder and autism and are early indicators of Alzheimer's disease and potentially Huntington's disease.

***In vitro* olfactory neuronal models**-Although the OE is a simple model in which to study the processes of neuronal development, the generation of *in vitro* model systems will facilitate our understanding of these processes. The ability to manipulate culture conditions *in vitro* will allow us to address issues that are more difficult to address *in vivo*. These include turnover and differentiation of ORNs, and the role of OR expression and the physiological response to specific odorants in ORN function.

Several groups have generated olfactory neuronal cell lines from primary culture and immortalized cell lines. Even though primary cultures are truer representations of *in*

vivo developmental events, they are technically challenging to prepare and are limited by survival and their heterogeneous nature (Murrell and Hunter, 1999; Barber *et al.*, 2000; Illing *et al.*, 2001). Most recently two olfactory neuronal cell lines have been generated: the *Odora* cell line and the 3NA12 cell line.

Murrell and Hunter generated the *Odora* cell line by immortalizing cells from the OE of postnatal day 3 rats using a temperature sensitive transgene that would allow proliferation at the permissive temperature and differentiation at the non-permissive temperature. At the permissive temperature *Odora* cells proliferate and are epithelial in morphology. *Odora* cells express the globose basal cell marker GBC-1 and NCAM but not readily detectable levels of other neuronal markers such as GAP-43 and microtubule associated protein MAP-5, suggesting that they are dividing GBCs. At the non-permissive temperature *Odora* cells differentiate and acquire a bipolar morphology and rapidly cease to proliferate. They cease to express GBC-1, maintain NCAM expression, and acquire MAP-5, GAP-43, olfactory signal transduction proteins and OMP, suggesting that they differentiate into ORNs. *Odora* cells also express the three olfactory cyclic nucleotide gated channels, identified by RT-PCR. It is unclear whether or not they express endogenous ORs as they do not respond to six general odorant mixes; however cells transfected with ORs do respond to specific odorant stimuli with calcium influx (Murrell and Hunter, 1999).

Barber *et al.* generated immortalized cell lines from the OE of heterozygote H-$2k^b$-tsA58 mice of various ages. Mixed populations at the permissive temperature expressed Golf and ACIII. This expression was retained at the non-permissive temperature, in addition to OMP expression. Clonal cell lines were generated by FACS

sorting for NCAM-positive cells and one line, 3NA12, was further characterized. These cells were positive for olfactory neuronal markers and responded to odorant stimulation with calcium influx at a low level, suggesting some level of endogenous odorant receptor expression (Barber *et al.*, 2000).

Although both of these cell lines do possess a number of features that are characteristic of developing ORNs, only the 3NA12 line is clonal in nature. Neither have been demonstrated to definitively express endogenous ORs or exhibit electrophysiological activity typical of mORNs. One issue that these papers have not addressed is the role of retinoic acid (RA) in olfactory neuronal development. RA is a member of the steroid/thyroid superfamily of signalling molecules; it is involved in controlling gene expression and plays an important role in controlling vertebrate development, cellular differentiation and homeostasis. In particular, it is important in the ontogeny of the mammalian olfactory system.

RA is synthesized in target tissues from dietary vitamin A (retinol). The RA signal is mediated through nuclear retinoic receptors (RARs) that are RA-dependent transcriptional activators, which form heterodimers with retinoid X receptors (RXRs). Both RARs and RXRs have three isotypes (α, β, γ) that can each form different mRNA isoforms through the use of dual promoters and alternative splicing. RARs can cause changes in local chromatin structure at target genes containing RA responsive elements by recruiting multiprotein complexes that contain histone acetyl-transferase (HAT) and HDAC activity (Whitesides *et al.*, 1998; Zhang, 1999; Mollard *et al.*, 2000; Sirchia *et al.*, 2000).

Experimental evidence has suggested that RA has an effect on immature neurons and precursor cells *in* vitro and based on observations *in vivo*. Usmann *et al.* have shown that RA can induce the expression of neuron specific molecules associated with neurite outgrowth and axon guidance in embryonic carcinoma cell lines. Furthermore, RA promotes neurite outgrowth from spinal cord and dorsal root ganglion explants *in vitro* and has an effect on axon outgrowth and direction in optic nerve and hindbrain *in vivo*. It has been suggested that RA may contribute to the differentiation and neurite outgrowth of ORNs (Whitesides *et al.*, 1998).

Mouse knockouts of specific RAR isoforms have been generated. Individual knockouts did not produce detectable phenotypes, suggesting redundancy in RAR function; however, double knockouts of some RAR pairs have produced a variety of phenotypes that were embryonic or postnatal lethal. Knockout phenotypes include congenital malformations in the eye, skull, respiratory tract, heart, urogenital system (Lohnes *et al.*, 1994; Mendelsohn *et al.*, 1994; Luo *et al.*, 1996), hypoplastic lungs, ectopic thymus, testis defects (Luo *et al.*, 1996), abnormalities in the thyroid and parathyroid glands, diaphragm, lower digestive tract (Mendelsohn *et al.*, 1994). The variety of defects seen in RAR double knockouts clearly shows that RA signalling via RARs is essential in mouse development.

At least three RAR isoforms have been identified in the developing mouse OE: RARα1, RARα2 and RARβ2/4. Using *in situ* hybridization, Mollard *et al.* have looked at five embryonic time points and have found that amongst the three, RARβ2/4 is expressed most highly in the developing OE (Mollard *et al.*, 2000). Zhang has used RT-PCR and DNA sequence analysis to demonstrate that RARβ, RARα, RXRβ and RXRγ

are present in the OE of adult mice. *In vitro* studies have also shown that RA is actively synthesized in the OE (Zhang, 1999). The expression pattern of RARs in the developing and mature OE, along with the fact that RA is readily available in the OE, suggests that RA plays a major role in olfactory neuronal development.

Proposal Summary and Aims-Previously we identified MBD2 as a gene that is highly expressed in regenerating ORNs following bulbectomy in mouse. MBD2 is a methyl-DNA binding protein that is associated with transcriptional repression, suggesting that methylation dependant gene silencing via MBD2 is an important mechanism of gene regulation in olfactory neuronal development. This mechanism of transcriptional regulation has not yet been described in the olfactory system. Furthermore, the need for true *in vitro* models of mature olfactory neurons has led us to develop an immortalized embryonic mouse olfactory placodal cell line. To address these issues, MBD2 expression will be characterized during development, the primary olfactory neuraxis of MBD2-/- mice will be analyzed, and retinoic acid responsive embryonic mouse olfactory placodal cell lines will be further characterized to determine if they are appropriate models of ORN development and if they are appropriate models in which to study MBD2 function.

Chapter 2: Materials and Methods

Tissue Preparation-For fresh frozen sections, animals were anesthetized with xylaket (25 mg/ml ketmaine hydrochloride, 2.5 mg/ml xylazine, 14.2% ethanol, 0.0525 %sodium chloride) and perfused with ice cold phosphate buffered saline (PBS). The brain, OE and OB were dissected out, suctioned with warm OCT (Tissue-Tek) to fill the nasal cavities and embedded in OCT. For paraformaldehyde (PFA) fixed sections, animals were perfused with ice cold 4% PFA following PBS perfusion. The brain, OE and OB were dissected out and post-fixed with 4% PFA for 2 hours at 4°C before being put in 10% sucrose overnight at 4°C, followed by 30% sucrose at 4°C overnight before being suctioned and embedded in OCT. For fresh frozen embryonic sections, embryos were dissected out and embedded in OCT. For PFA fixed embryonic sections, embryos were dissected out, fixed with 4% PFA overnight at 4°C before being put in 10% sucrose overnight at 4°C, followed by 30% sucrose at 4°C overnight before being embedded in OCT. Eight to 20 μ thick tissue sections were cut on a cryostat (Zeiss). For protein samples, animals were anesthetized with xylaket, decapitated, tissue dissected out, immediately frozen on dry ice, and stored at –80°C until homogenization.

Probe Preparation and *In Situ* Hybridization-Anti-sense RNA probes for MBD2 and a control probe for OMP were generated from cDNAs ligated into pBluescript II SK+ and pGEMT, respectively. MBD2 and OMP plasmids transformed into XL1 Blue *E.* coli were grown in Luria Broth (LB) at 37°C with ampicillin selection. From this, template DNA was prepared using the Qiagen Mini-Prep kit (Qiagen) and linearized with the

following restriction enzymes: EcoRI for MBD2 and EagI for OMP, and then treated with 50 μg of Protease K (Gibco-BRL) for 30 min. at 37°C. The reaction was made up to a volume of 300 μL with Tris-EDTA (TE) buffer. The aqueous phase containing the DNA was extracted three times with buffer saturated phenol (Gibco-BRL), one time with 1:1 phenol:chloroform, and two times with chloroform. The DNA was precipitated out of the aqueous phase with 1/10 volume of 3M sodium acetate pH 5.2 and 95% ethanol for 30 min. at –20°C, pelleted for 5 min. at 13000 rpm, washed with ice cold 70% ethanol, and pelleted again. The DNA pellet was air dried on ice and re-suspended in TE at 1 μg/μL, assuming 85% yield. Digoxigenin-labeled probes were prepared according to the anti-digoxigenin RNA labeling mix (Roche). The anti-sense RNA probes were electrophoresed on a formaldehyde-agarose gel to determine probe integrity and yield. Probes were stored at –80°C.

For *in situ* hybridization, fresh frozen tissue sections were thawed on a slide warmer for 10 min., post-fixed in 4% PFA for 10 min, and washed three times 3 min. in PBS. Slides were acetylated for 10 min. in fresh acetylation mix (29.5 ml diethyl-pyrocarbonate treated H_2O, 400 μL triethanolamine (Sigma-Aldrich), 52.5 μL concentrated hydrochloric acid, 75 μL acetic anhydride). Tissue sections were circled with a Pap-Pen (Binding Site) and treated with hybridization buffer (50% formamide (Sigma-Aldrich), 5X SSC, 5X Denhardt's solution (Gibco-BRL), 250 μg/ml MRE 600 tRNA (Gibco-BRL), 500 μg/ml herring sperm DNA (Gibco-BRL)) for 2 hr. at room temperature or overnight at 4°C in hybridization chamber. Anti-sense DIG-labelled MBD2, MBD3 and OMP probes were diluted in hybridization buffer, denatured for 2 min. at 80°C and incubated with tissue sections and cover-slipped with silanized

coverslips. Slides were placed in a humidified hybridization chamber and incubated at 72°C overnight in a hybridization chamber. Slides were soaked in 5X SSC to removed the coverslips and washed extensively as follows: two times 10 min. with 0.2X SSC at 72°C, 5 min. with RNAse buffer (2 μg/ml RNAse H, 0.5M NaCl, 10 mM Tris buffer pH 7.5, 5 mM EDTA) pre-heated to 37°C, two times 20 min. with 0.2X SSC at 72°C, and 5 min. with B1 buffer (0.1 M Tris buffer pH 7.5, 0.15 M NaCl). Tissue sections were then incubated with B2 buffer (B1, 1% heat inactivated normal goat serum (Gibco-BRL)) for 1 hr. at room temperature before incubation with anti-digoxigenin antibody (1:5000) diluted in B2 for 2 hr. at room temperature or overnight at 4°C in a hybridization chamber. Slides were washed three times 5 min. with B1 buffer, equilibrated for 5 min. with B3 buffer (0.1M Tris pH 9.5, 0.1M NaCl, 50 mM $MgCl_2$) and developed in the dark with fresh B4 buffer (3.375 μL/ml NBT (Roche), 3.5 μL/ml BCIP (Roche), 0.24 mg/ml levamisole (Sigma-Aldrich), B3 buffer). The developing reaction was stopped by washing two time 10 min. in H_2O and cover-slipped with aquapolymount mounting media (Polysciences).

Immunohistochemistry-Sections were post-fixed in 4% PFA for 10 min., washed with PBS, permeabilized in 0.1% TritonX-100/PBS for 30 min., blocked 4% non-defined serum (NDS)/PBS for 20 min. and incubated in primary antibody at 4°C overnight in a humidified chamber. Sections were washed with PBS, incubated with biotinylated secondary antibody for 30 min. at room temperature and then washed with PBS, quenched with 0.5% hydrogen peroxide/PBS for 10 min. and washed with PBS. Signal was developed using the ABC Vectastain kit (Vector). The developing reaction was

stopped by washing two times for 10 min. in H_2O and cover-slipped with aquapolymount mounting media.

Immunofluorescence and Confocal Microscopy-Sections were post-fixed in 4% PFA for 10 min., washed with PBS, permeabilized in 0.1% TritonX-100/PBS for 30 min., washed with PBS, blocked with 4% NDS/0.1%TritionX-100/1% BSA/PBS for 1 hr. and incubated in primary antibody at 4°C in 2% NDS/0.05%TritionX-100/0.5% BSA/PBS overnight in a humidified chamber. Sections were washed with 0.1% TritonX-100/PBS, incubated with fluorescently conjugated secondary antibodies (Molecular Probes) in 2% NDS/PBS for 1 hr. at room temperature, washed with PBS, 0.1% TritonX-100/PBS and PBS and cover-slipped with Vectashield mounting media (Vector) and viewed under a confocal microscope.

Cell Culture-OP6 and OP27 were maintained at 33°C in DMEM media (Gibco-BRL) supplemented with 10% fetal bovine serum (FBS) (Gibco-BRL). For studies at the non-permissive temperature, cells were differentiated in DMEM/F12 media (Gibco-BRL) supplemented with 2% FBS, N-2 supplement (Gibco-BRL), 100 μM ascorbic acid (Sigma-Aldrich) and 10 μM all-trans retinoic acid (Sigma-Aldrich) at 33°C overnight prior being switched to 39°C. OP6 was differentiated at 85-95% confluencey and OP27 was differentiated at 50-60% confluencey. Media was supplemented with fresh retinoic acid to a final concentration of 10 μM every 2 days. For immunocytochemistry, glass slides were coated with laminin substrate (2 $\mu g/cm^2$) (Roche) overnight at 37°C. Cells

were plated onto the laminin-coated slides at a density of 8.3 x 10^3 cells/cm^2 and allowed to reach the desired density prior to differentiation.

Immunocytochemistry-Differentiated cells were washed with PBS, fixed with ice cold 4% PFA for 15 min., washed with PBS and stored in 0.1% sodium azide/PBS at 4°C. Cells were post-fixed in 4% PFA for 10 min., permeabilized in 0.1% TritonX-100/PBS for 30 min., blocked 4% NDS/PBS for 15 min. and incubated in primary antibody at 4°C overnight. Cells were washed with PBS, incubated with fluorescently conjugated secondary antibodies (Molecular Probes) for 1 hr. at room temperature and washed with PBS. Nuclei were stained with DAPI/PBS (1:15000) (Roche) for 3 min. at room temperature, washed with 0.1% TritonX-100/PBS and cover-slipped with Vectashield. For detection of MBD2 and MBD3, cells were treated as described above until the overnight primary antibody incubation. Following PBS washes, cells were incubated with biotinylated secondary antibody for 30 minutes, washed with PBS and developed according to the ABC Vectastain kit.

Protein Preparation-For preparation of tissue homogenates, harvested tissue was homogenized in homogenization buffer (50 mM Tris-HCl pH 8, 1% TritonX-100, 150 mM NaCl, 1 μg/ml apoprotin, 1 μg/ml leupeptin, 100 μg/ml PMSF) and stored at –80°C. For preparation of cell lysates, cells were grown in conditions as described above, washed with PBS, harvested by trypsinization, counted on a hemocytometer and pelleted by centrifugation. For SDS-PAGE, the cell pellet was lysed with 30μL cell lysis buffer (50 mM Tris-HCl pH 6.8, 1% NP-40, 150 mM NaCl, 5 mM EDTA pH 8, 1 μg/ml apoprotin

(Roche), 1 μg/ml leupeptin (Roche), 100 μg/ml PMSF (Roche)) per 10^5cells. For immunoprecipitations, the cell pellet was lysed for 1 hr. on ice with 30μL cell lysis buffer (50 mM Tris-HCl pH 8, 1% NP-40, 150 mM NaCl, 1 μg/ml apoprotin, 1 μg/ml leupeptin, 100 μg/ml PMSF) per 10^5cells. Cell debris was removed by centrifugation for 3 min. at 13000 rpm and the supernatant containing protein collected and stored at –20°C. Protein concentrations were determined with the BCA protein assay kit (Pierce).

SDS-PAGE and Western Blotting-Protein samples denatured for 3 min. at 90°C in SDS sample buffer (1:1) were electrophoresed on SDS-PAGE mini-gels (BioRad) at 100V, transferred on to Immobilon-P nitrocellulose membrane (Millipore). Membranes were blocked in 5% non-fat milk/TBS to prevent unspecific antibody binding and incubated in primary antibody in 2% milk/TBS at 4°C overnight. Membranes were washed with 0.05% Tween-20/TBS, incubated in horseradish peroxidase conjugated secondary antibody in 2% milk/TBS for 1 hr. at room temperature and washed with 0.05% Tween-20/TBS. Membranes were treated with ECL chemiluminescence substrate (Pierce) and signal detected on X-ray film.

Immunoprecipitation-All steps were performed on ice. A total of 100 μg of protein was made up to 500 μl with RIPA buffer (150 mM NaCl, 1% NP-40, 0.5% DOC, 0.1% SDS, 50 mM Tris pH 8.0) containing the protease inhibitors (1 μg/ml apoprotin, 1 μg/ml leupeptin, 100 μg/ml PMSF) and incubated with 2 μl of primary antibody at 4°C for 1 hour and then incubated with 50 μl of protein A or G sepharose beads at 4°C for 1 hour. The sepharose beads were pelleted by centrifugation and the supernatant was removed

and retained. The bead pellet was then washed 3 times with 1 ml of RIPA buffer by vortexing and re-pelleted by centrifugation. Following the final wash, the supernatant was aspirated off and the sepharose pellet was re-suspended in 50 µl SDS sample buffer.

HDAC Inhibition with Trichostatin A -Three different conditions were tested for initial HDAC inhibition experiments performed on OP27 at 33°C. For the first HDAC inhibition experiment, a TSA concentration of 25 nm was used. OP27 were grown until 70% confluent before the media was replaced with differentiation media or differentiation media containing TSA. OP27 were allowed to settle at 33°C overnight before being switched to 39°C. In the second experiment, OP27 were grown to 70% confluent before media was changed to differentiation media and left overnight at 33°C to settle. At the time of temperature shift, TSA was added at the reduced concentration of 10 nm. In the third experiment, OP27 were grown until 70% confluent and synchronized in metaphase with colcemid for 48 hours to prevent cell cycle arrest. Following synchronization, cells were released by replacing the media with differentiation media and cells were allowed to settle overnight at 33°C. At the time of temperature shift, TSA was added at a further reduced concentration of 2.5 nm.

MBD2-/- analysis and cell counting-PFA fixed sections of neonate (P5-P6) MBD2-/- and MBD2+/+ controls were prepared and stained using anti-NCAM and anti-OMP antibodies, as described above. Three MBD2-/- and three MBD2+/+ animals were examined. For each animal, sections were analyzed as follows: 1) the number of positively stained ORNs in three representative regions of OE were counted, 2) the

number of corresponding axon bundles beneath that region of OE was counted, 3) the maximum diameter of each axon bundle was measured, 4) for sections containing OB the number of glomeruli per OB were counted, and 5) the maximum diameter of a representative population of glomeruli were measured for six different measurements and. For OMP, regions of OE containing ORNs with high and low density staining were distinguished from each other. Values were analyzed and plotted with Microsoft Excel and student's t-tests were calculated. p-values<0.05 were scored with one asterisk and p-values<0.001 were scored with two asterisks.

Table 1. Sources and Dilutions of Antibodies Used.

Primary Antibodies	Species	Source	Dilution for Western Blot	Dilution for immunostaining
ACIII	Rabbit polyclonal	Santa Cruz Biotech	1:500	1:200
β-actin	Mouse monoclonal	Sigma	1:500	-
DAPI	-	Roche	-	1:15000
GAP-43	Mouse monoclonal	Boehringer Mannheim	1:5000	1:1000
Golf	Rabbit polyclonal	Santa Cruz	1:1000	1:1000
HDAC1	Rabbit polyclonal	Santa Cruz	1:500	-
HDAC2	Rabbit polyclonal	Santa Cruz	1:500	-
MBD2	Goat polyclonal	Santa Cruz	1:100	1:50
MBD3	Goat polyclonal	Santa Cruz	1:100	1:50
MBD3E	Rabbit polyclonal	Dr. James Eubanks, U of Toronto	-	1:50
MeCP2	Rabbit polyclonal	Upstate	1:500	-
mSin3A	Rabbit polyclonal	Santa Cruz	1:500	-
NST (β-III-NST)	Mouse monoclonal	BabCo	1:250	1:1000
NCAM	Rabbit polyclonal	Chemicon	-	1:500
OMP	Goat polyclonal	Dr. Frank	-	1:10000

		Margolis, U of Maryland		
P75	Rabbit polyclonal	Chemicon	1:1000	1:1000
Pax-6	Rabbit polyclonal	BabCo	1:200	-
PLC-γ2	Rabbit polyclonal	Santa Cruz	1:500	1:1500
TrkB	Rabbit polyclonal	Santa Cruz	1:200	1:500
TrkC	Rabbit polyclonal	Santa Cruz	1:200	1:500
Secondary Antibodies				
Anti-goat biotinylated	Rabbit IgG	Vector	-	1:200
Anti-rabbit biotinylated	Goat IgG	Vector	-	1:200
Anti-goat HRP	Rabbit IgG	Biorad	1:5000	-
Anti-Mouse HRP	Goat IgG	Biorad	1:5000	-
Anti-Rabbit HRP	Goat IgG	Biorad	1:5000	-
Alexa anti-goat A488, A594	Donkey IgG	Molecular Probes	-	1:50
Alexa anti-mouse A488, A546, A594	Goat IgG	Molecular Probes	-	1:50
Alexa anti-rabbit A488, A546, A594	Goat IgG	Molecular Probes	-	1:50
Amplex red reagent	-	Molecular Probes	-	1:400

Chapter 3: Results

3.1: *In vivo* Developmental Characterization of MBD2

Introduction-Previously we have identified MBD2 as a gene that is specifically up-regulated in ORNs following bulbectomy in the mouse using an *in vivo* subtraction/suppression reverse transcriptase polymerase chain reaction assay six and ten days post-bulbectomy to assess changes in gene expression (Jane Roskams, personal communication). The bulbectomy paradigm, which involves surgical removal of the OB, the target organ of ORNs, causes ORNs to undergo apoptosis after which they are replaced by ORN progenitors in the basal layer of the OE. The regeneration of these ORNs therefore recapitulates ORN developmental events; suggesting that MBD2 may be an important mechanism of transcriptional repression during development. To determine if MBD2 is important in development, *in situ* hybridization and immunohistochemistry were used to further examine when and where MBD2 is expressed during normal mouse development. Correlating the *in vivo* expression profile with known developmental events in olfactory neuronal development will provide insight into MBD2 function.

Results

MBD2 mRNA is developmentally expressed by ORNs in the OE-*In situ* hybridization was performed on tissue sections at embryonic day E13, E15, E17, postnatal day P1 and P5 using anti-sense RNA probes specific for MBD2 and the positive control OMP.

MBD2 mRNA is not noticeably expressed above background at E13 in the olfactory pit. Expression of MBD2 mRNA was first detected at E15 in proliferating ORN progenitor cells located in the basal OE (Fig 5A, arrowhead). As development proceeds to E17, MBD2 mRNA is expressed by immature receptor neurons (IRNs) in addition to mature ORNs (mORNs) (Fig 5B, arrowhead). At this developmental time point, ORN axons have made contact with the OB and are capable of odorant discrimination (Farbman, 1991). At E17, a subpopulation of ORNs in the VNO, an accessory olfactory organ responsible for detection of pheromones and social behaviour (Farbman, 1991; Farbman, 1992), also expresses MBD2 mRNA (Fig 5C). By P1 (Fig 5D, arrowhead) and P5 (Fig 5E), MBD2 mRNA is expressed by ORNs throughout the OE, with slightly higher expression seen in mORNs at P5. In the first few days following birth, ORN synapses with the OB are being strengthened and glomeruli are being formed. In adults, MBD2 mRNA is expressed by ORNs throughout the OE (Fig 5F).

At E17, the OMP positive control indicates the presence of mORNs demonstrating that the MBD2 and OMP anti-sense RNA probes are specific for two different cell populations in the OE (Fig 5G, arrowhead). The no probe negative controls demonstrate that there is minimal background and the signal is observed is specific (Fig 5H). Sense probes for MBD2 gave consistently high background, therefore probes specific for different cell populations were used as controls.

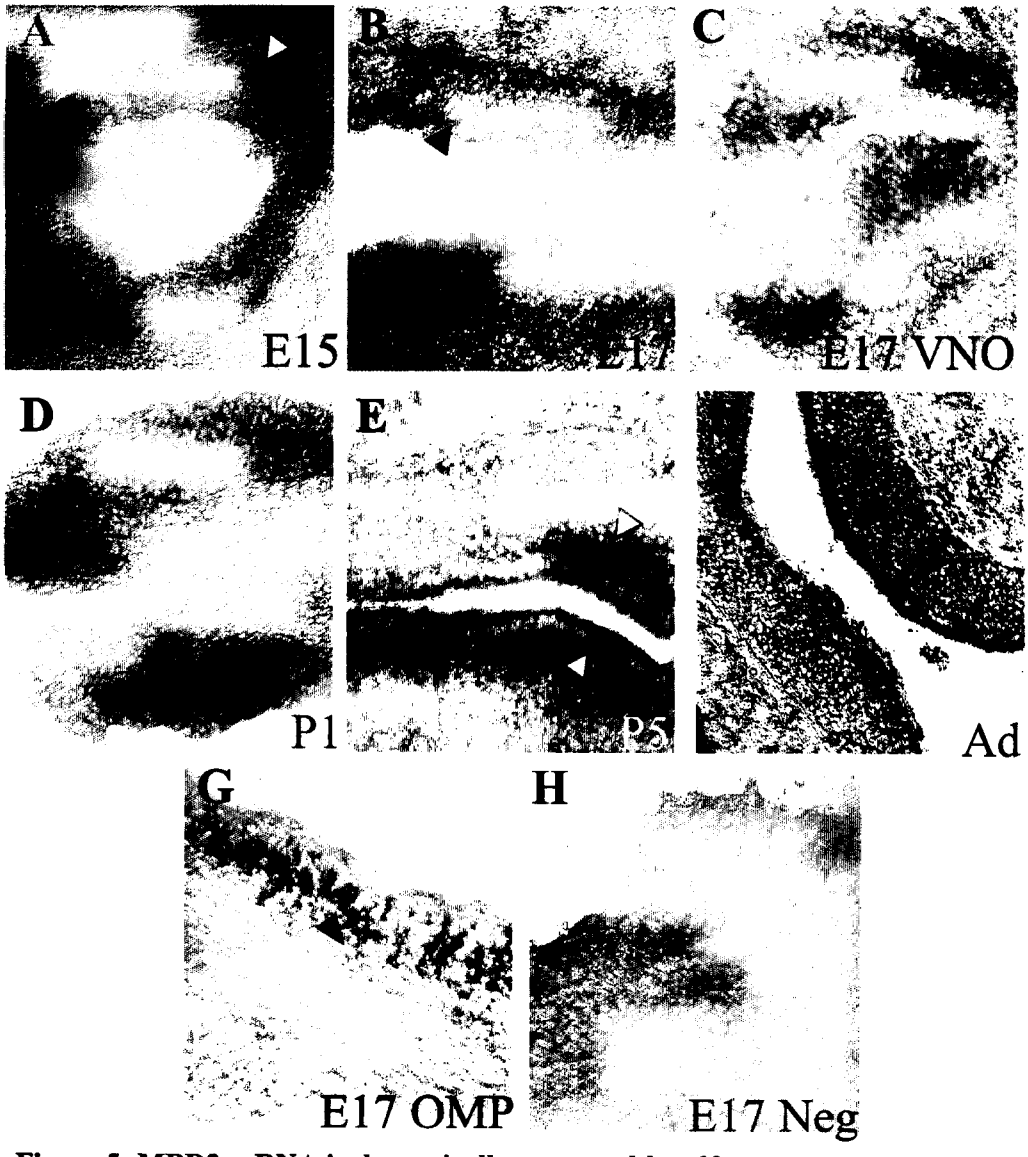

Figure 5: MBD2 mRNA is dynamically expressed by olfactory receptor neurons in the olfactory epithelium during development. (A) At E15 MBD2 mRNA is expressed in proliferating ORN progenitor cells (arrowhead). (B) At E17 MBD2 mRNA is expressed in mORNs (arrowhead), the same proliferating progenitor population and, (C) in a subpopulation of ORNs in the VNO. (D) At P1 and (E) P5, MBD2 mRNA is expressed by ORNs throughout the OE, with slightly higher expression seen in mORNs (arrowhead) at P5. (F) In the adult, MBD2 mRNA is expressed by ORNs throughout the OE. (G) E17 OMP positive control for mORNs (arrowhead), (H) E17 no probe negative control. Magnification 20x.

MBD2 protein is localized to the nucleus and dynamically expressed by ORNs in the OE-Immunohistochemistry was performed at corresponding developmental time points as above using MBD2 and MBD3 specific antibodies. Results similar to those obtained for the mRNA expression profile were observed at the protein level. To confirm that the commercially available MBD2 antibody (Santa Cruz) does not cross react with other MBD family members, liver homogenates from MBD2-/- and MBD2+/- mice were subjected to SDS-PAGE and western blotting with the anti-MBD2 primary antibody. Only the heterozygotes displayed the expected MBD2 band at 44 kD (data not shown). Loading controls were confirmed by western blotting for the housekeeping gene β-actin (data not shown).

MBD2 protein was not noticeably expressed at E13 or E15. At E17, expression is first detected in a sub-population of ORNs and is bilaterally symmetric (Fig 6A, arrowhead). At higher magnification (Fig 6B), MBD2 is localized to the nucleus of a subpopulation of IRNs (arrowhead) and mORNs (asterisk); however expression is zonal in nature. In the same coronal section, MBD2 is only expressed by sub-populations of ORNs within the dorsal-ventral axis of the OE and absent in other regions (arrow). Zonality is also observed in the anterior-posterior axis of the OE. Anterior coronal sections (Fig 6A and B) express MBD2 at noticeable levels, whereas a posterior coronal section from the same animal does not (Fig 6C). By P1 MBD2 is expressed by ORNs throughout the OE but predominantly in mORNs (Fig 6D, arrowhead). In the adult, MBD2 is expressed by ORNs throughout the OE (Fig 6E). Due to the zonal nature of

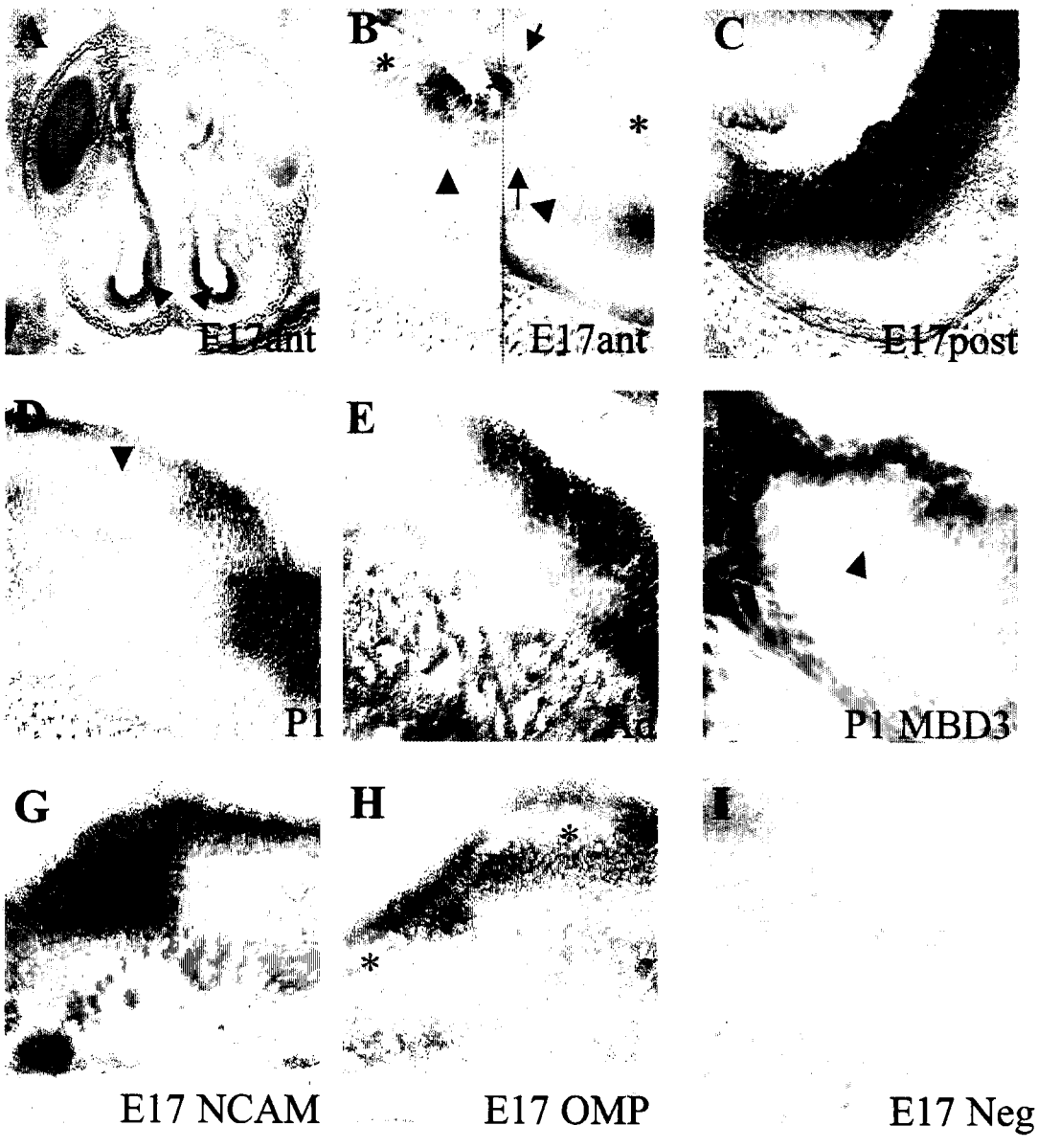

Figure 6: MBD2 and MBD3 are localized to the nucleus of olfactory receptor neurons. (A) MBD2 expression is first detected at E17 in a sub-population of ORNs (arrow) and is bilaterally symmetric. Magnification 2.5x. (B) In an anterior section at E17, MBD2 is localized to the nucleus of IRNs (arrowhead) and mORNs (*); however, expression is zonal in nature. An adjacent region of OE in the dorsal-ventral axis does not express MBD2 (arrow). In addition, a posterior section (C) does not appear to express MBD2 in a nuclear fashion. (D) At P1, MBD2 is expressed by ORNs throughout the OE, with slightly higher expression in mORNs (arrowhead). (E) In the adult, MBD2 is expressed by ORNs throughout the OE. (F) MBD3 expression is not seen until later in development at P1 in mORNS (arrowhead), where expression is seen to be limited. (G) E17 NCAM positive control staining all ORNs and axon bundles, (H) E17 OMP negative control staining mORNs (asterisk) and (I) E17 no probe negative controls. Magnification 20x.

MBD2 expression, it is possible that MBD2 is expressed at E15 in a very small population of ORNs in a particular coronal region of the OE.

The highly related protein MBD3 is also expressed by ORNs in the OE; however, expression is not seen until later in development. At P1 MBD3 is expressed by mORNS, where expression is seen to be limited (Fig 6F, arrowhead). Thus, a subpopulation of mORNs may co-express MBD2 and MBD3 later in development at P1. There is evidence to suggest that MBD2 and MBD3 may interact (Wolffe and Bird, 1998; Hendrich *et al.*, 2001). The NCAM positive control (Fig 6G), OMP negative control (Fig 6H) and secondary antibody only negative control (Fig 6I) demonstrate that the nuclear MBD2 signal is specific with minimal background.

Summary-The *in vivo* developmental characterization of MBD2 expression using *in situ* hybridization and immunohistochemistry shows similar expression profiles at both the mRNA and protein levels; with the exception that MBD2 protein is not detected until E17 as opposed to MBD2 mRNA, which is first detected at E15. MBD2 is dynamically expressed during development by ORNs in the OE. Early in development, MBD2 expression is limited to ORN progenitors but as development proceeds a shift in expression is seen, first to subpopulations of IRNs and mORNs and then to scattered populations of ORNs throughout the OE.

3.2: *In vivo* Characterization of MBD2-/- Neonate Mice

Introduction-The dynamic pattern of MBD2 expression in the developing mouse OE suggests that MBD2 may be involved in controlling gene expression during olfactory neuronal development. We have obtained MBD2-/- mice and studying their olfactory system will help to determine if and how MBD2 is involved in olfactory neuronal development.

As previously discussed, MBD2-/- mice are viable and fertile. In the absence of this gene, global DNA methylation levels appear normal when compared to controls; however, there are defects in the MeCP1 repressor complex and cell lines generated from MBD2-/- animals are unable to repress transcription from methylated reporter DNA construct, which can be rescued by transfecting in MBD2. Genetic crosses between MBD3+/- and MBD2-/- animals suggest that MBD3 viability is reduced when MBD2 is absent, supporting the idea that MBD2 and MBD3 physically interact. Behavioral analysis showed that MBD2-/- animals may display abnormalities in maternal behavior, as progeny born to MBD2-/- mothers were smaller than those born to MBD2+/+ or +/- mothers. In a cross-fostering experiment and newborn pup retrieval test, MBD2-/- mothers were shown to have abnormal maternal behavior (Hendrich *et al.*, 2001). The behavioral observations, which suggest olfactory defects in MBD2-/- animals, further support our results that MBD2-/- is involved in olfactory neuronal development. To determine if there are any morphological differences in the olfactory system of MBD2-/- mice, OMP and NCAM expression was evaluated in different regions of the primary olfactory neuraxis.

Results

MBD2-/- neonates display morphological differences in the olfactory system-All experiments were performed on MBD2-/- neonates at P5 or P6. PFA fixed coronal sections were stained for OMP and NCAM. OMP is a mature olfactory neuronal marker that only stains the cell bodies and axons of mORNs. A mORN is defined as an ORN that has synapsed with the OB. NCAM is a cell surface neuronal marker that stains all ORNs and their axons.

The anterior coronal MBD2-/- sections containing OE generally appeared normal for OMP and NCAM staining. In MBD2-/- neonates, the ORN staining appeared normal; however, for both animals there were regions of high and low density OMP staining of cell bodies, which was more pronounced in MBD2-/- neonates (Fig 7A, arrow high density, arrowhead low density). Upon closer examination, MBD2-/- neonates had extremely large and extremely small axon bundles (Fig 7B, arrowhead large, arrow small) when compared to MBD2+/+ controls. The large axon bundles observed in MBD2-/- animals were undefined and wispy in nature (Fig 7C, arrow) and in some cases, axons in the lamina propria of MBD2-/- neonates looked astray (Fig 7D, arrow). Based on these observations the following were quantified: 1) the number of immunoreactive cells per mm OE, 2) the number of axon bundles per mm OE, 3) axon bundle areas and 4) extreme axon bundle areas (the ten largest and smallest axon bundle areas were compared). Refer to pages 54-62.

The posterior coronal MBD2-/- sections containing OB contained obvious differences in OMP and NCAM staining when compared to MBD2+/+ neonates. MBD2-

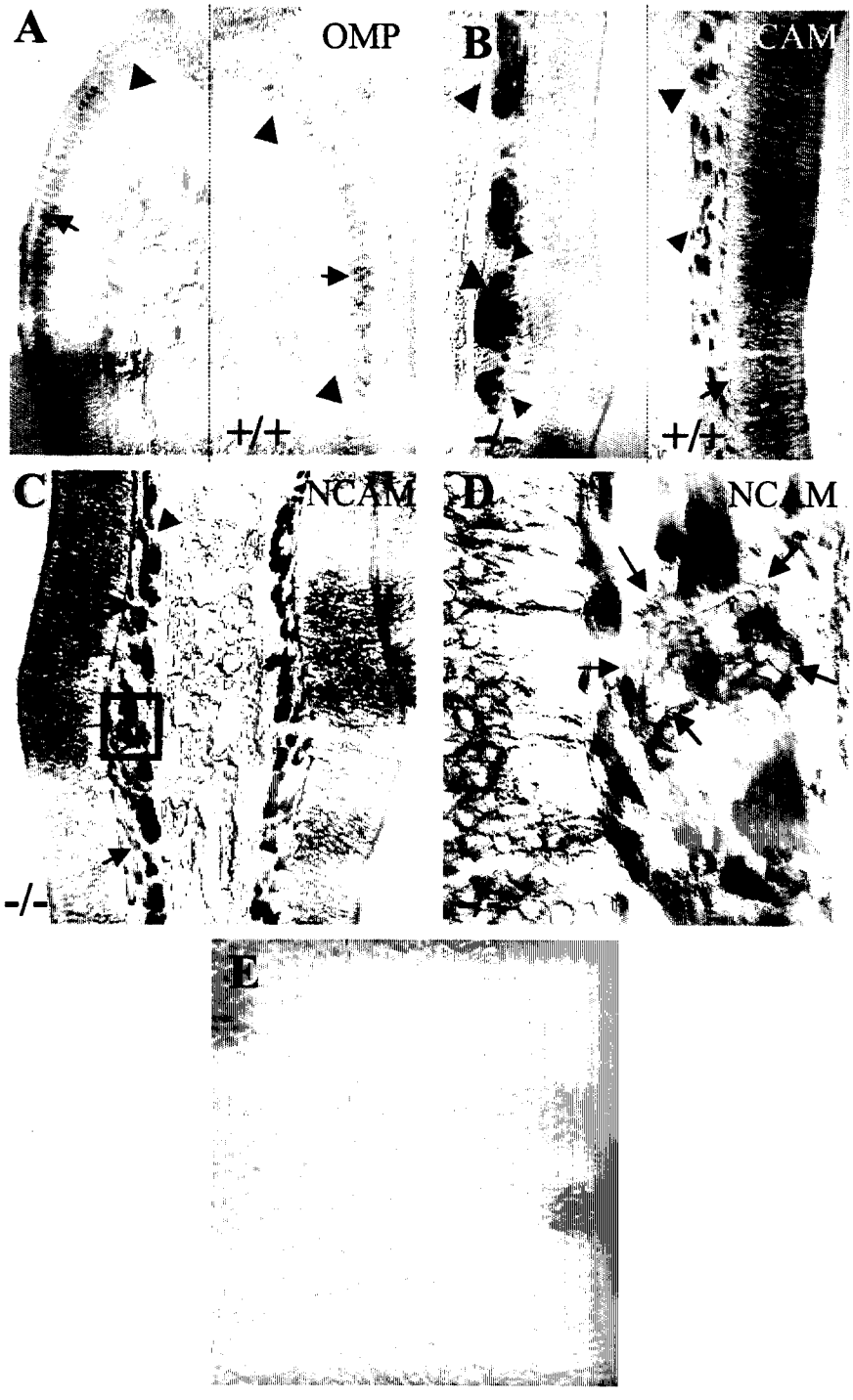

Figure 7: MBD2-/- neonates have morphological differences in the primary olfactory neuraxis. (A) High (arrow) and low density (arrowhead) OMP staining. Magnification 20x. (B) Large (arrowhead) and small axon bundles stained with NCAM. Magnification 20x. (C) NCAM staining of MBD2-/- septum showing wispy, undefined axon bundles (arrow). Magnification 20x. (D) 40x magnification of (C) showing stray axons in the laminia propria. (E) Secondary only negative control. Magnification 20x.

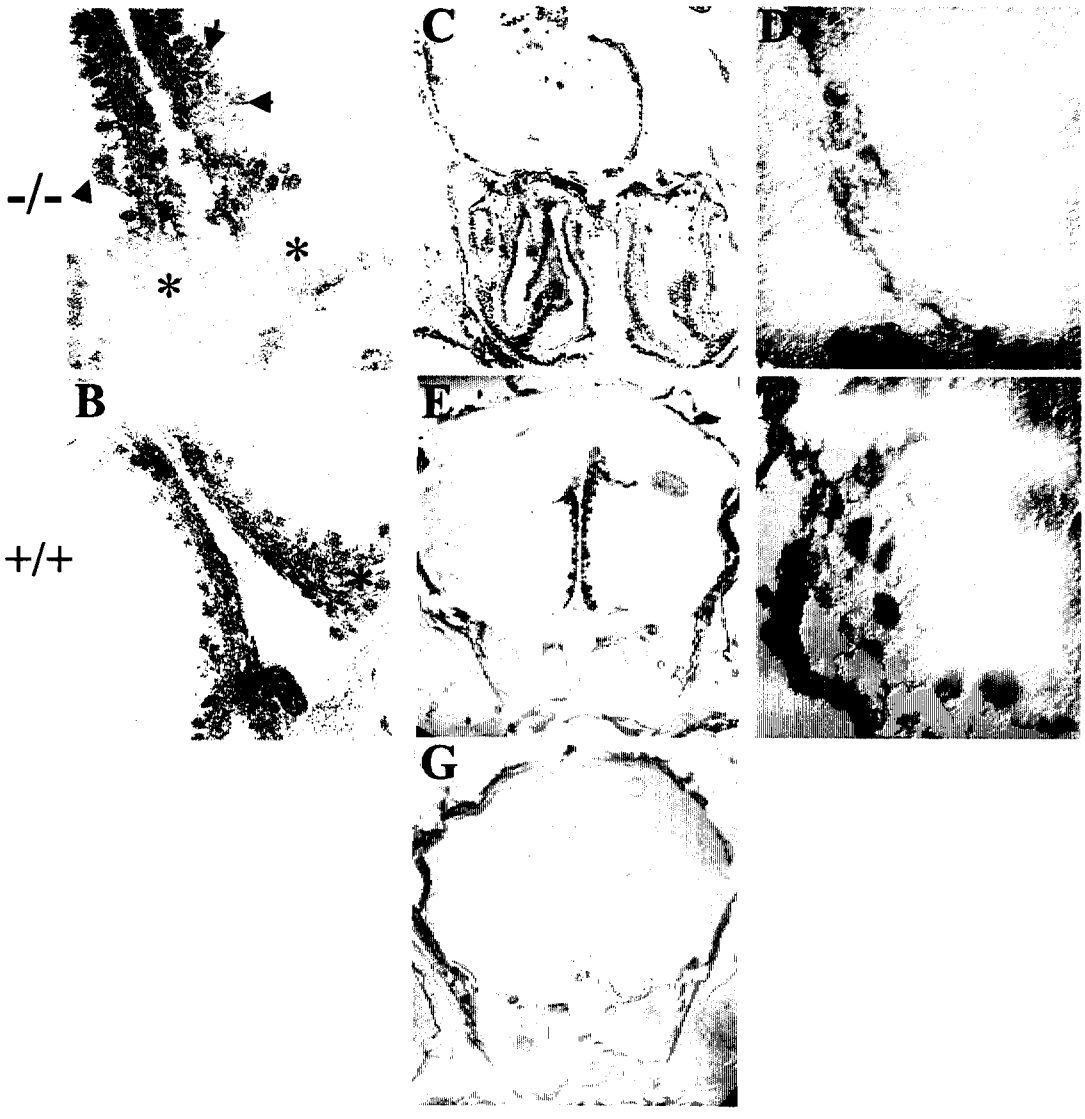

Figure 8: MBD2-/- neonates have changes in projection patterns to the olfactory bulb. (A) OMP staining of MBD2-/- olfactory bulb along the midline with large glomeruli (arrow) and thick olfactory nerve layer (asterisk). Magnification 10x. (B) OMP staining of MBD2+/+ olfactory bulb. Magnification 10x. (C) Posterior section of MBD2-/- do not have glomeruli in the olfactory bulb. Magnification 2.5x. (D) 20x magnification of (C). In contrast, posterior section of MBD2+/+ have glomeruli in the OB. Magnification 2.5x. (F) 20x magnification of (E). (G) Secondary only negative control. Magnification 10x.

/- neonates displayed a number of differences when compared to MBD2+/+ neonates, including: 1) a thicker olfactory nerve layer around the OB, 2) large glomeruli and 3) glomeruli at the rear of the OB (posterior) were absent. MBD2-/- neonates had larger glomeruli (Fig 8A, arrow) and thicker olfactory nerve layer (NFL) (Fig 8A, asterisk) than MBD2+/+ controls (Fig 8B). Although a olfactory nerve layer is present, glomeruli in posterior sections at the back of the OB were absent in MBD2-/- neonates (Fig 8C and D). In contrast, MBD2+/+ neonates have defined glomeruli in corresponding sections (Fig 8E and F). Based on these observations the following were quantified: 1) the number of glomeruli per mm OB, 2) glomeruli areas and 3) extreme glomeruli areas (the ten largest and smallest glomeruli were compared). Refer to pages 62-67.

MBD2-/- neonates possess quantitative differences in the primary olfactory neuraxis-The observations above were further strengthened through cell counts at three regions along the anterior-posterior axis of the olfactory system defined as middle of the OE (MOE) (Fig 9A), front of the OB (FOB) (Fig 9B) and middle of the OB (MOB) (Fig 9C). Sections representing these regions from three MBD2-/- and three MBD2+/+ neonates were stained for OMP and NCAM. Immunoreactive cells were counted as described in Materials and Methods.

Cell counts for ORNs were obtained from MOE, FOB and MOB regions. *In vivo* different regions of the OE undergo proliferation and maturation at different rates. Therefore regions of the OE with are thicker than others and the number or density of mORNs, as defined by OMP immunoreactivity, differs. In both MBD2-/- and +/+

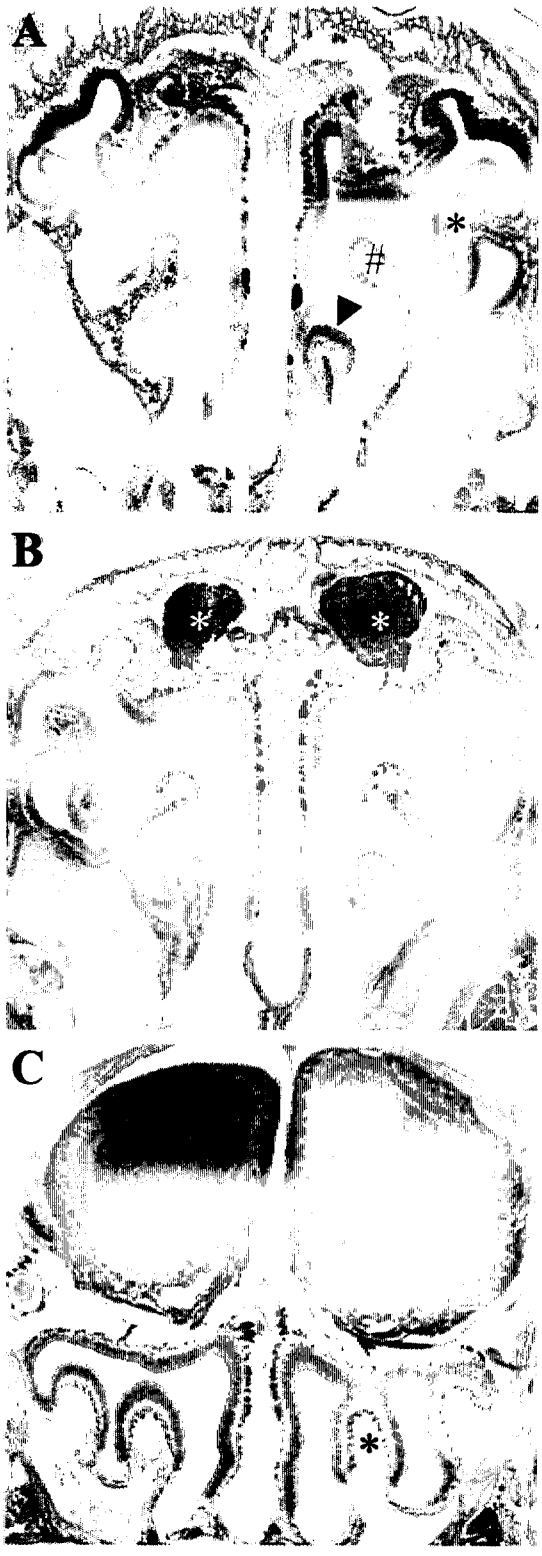

Figure 9: Cell count regions along the anterior-posterior axis of the olfactory system. (A) Middle OE (MOE) sections contain the three turbinates: superior (*), middle (#) and inferior (arrowhead). (B) Front OB (FOB) sections still contain the superior, middle and inferior turbinates as well as the front of the OB (*). (C) Middle OB (MOB) sections only contain the superior turbinate (*) but a large cross-section of OB. Sections are stained with NCAM. Magnification 2.5x.

neonates, regions of high and low density OMP positive ORN staining were present and were distinguished from each other in cell counts. For both low and high density OMP positive ORN staining, MBD2-/- neonates have a greater number of OMP positive ORNs per mm OE (Fig 10A). One exception is for high density OMP positive ORN staining at the FOB region and may be due to the small sample size. Although this observation is only significant for FOB low (student's t-test $p<0.05$) and high density ($p<0.05$) staining and MOB low density staining ($p<0.05$), there is an obvious trend towards more OMP positive ORNs per mm OE in MBD2-/- neonates, which is further substantiated by the total OMP positive ORNs per mm OE (Fig 10B). When total OMP positive ORNs per mm OE are counted, MBD2-/- neonates have greater numbers of OMP positive ORNs per mm OE at low ($p<0.05$) and high ($p>0.05$) density regions, when compared to MBD2+/+ neonates at low and high density regions. Values are summarized in Table 2. For NCAM staining similar results were obtained. At the MOE, FOB and MOB regions, MBD2-/- neonates also show a trend towards a greater numbers of NCAM positive ORNs per mm OE (Fig 10C), although these values are not significant ($p>0.05$) and may be due to small sample size. This is also reflected at significant levels for the total NCAM positive ORNs per mm OE ($p<0.05$; Fig 10D). Values are summarized in Table 3.

Axon bundles counts were obtained from MOE, FOB and MOB regions. Individual ORN axons join with other axons to form small axon fascicles in the lamina propria (Farbman, 1992). For OMP staining, MBD2-/- neonates have a greater number of OMP positive axon bundles per mm OE at all three regions (Fig 11A). Although this observation is only significant at MOE ($p<0.05$), it is apparent that MBD2-/- neonates have more OMP positive axon bundles per mm O E. The total OMP positive axon

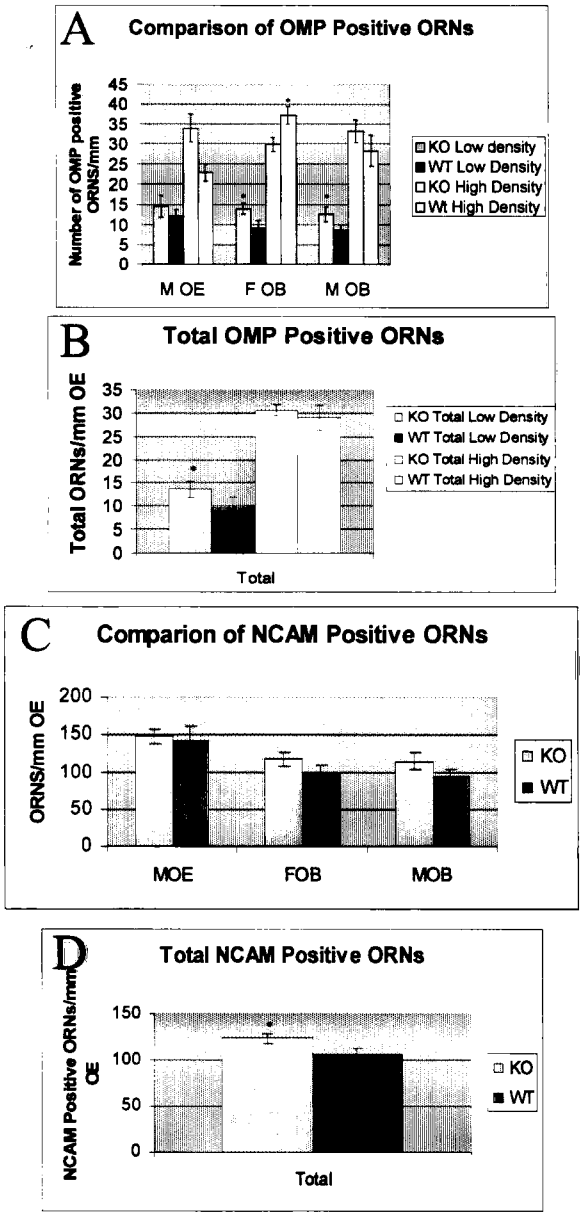

Figure 10: OMP and NCAM positive olfactory receptor neuron counts show that MBD2-/- neonates have more olfactory receptor neurons per mm of olfactory epithelium. (A) OMP positive ORNs per mm OE at MOE, FOB and MOB regions, distinguishing high and low OMP staining densities. FOB low density $p<0.05$, FOB high density $p<0.05$, MOB low density $p<0.05$. (B) Total OMP positive ORNs per mm OE, integrating MOE, FOB and MOB sections. Total low density $p<0.05$. (C) NCAM positive ORNs per mm OE. (D) Total NCAM positive ORNs per mm OE $p<0.05$. All plots show a general trend towards more OMP and NCAM positive ORNs per mm OE in MBD2-/- neonates.

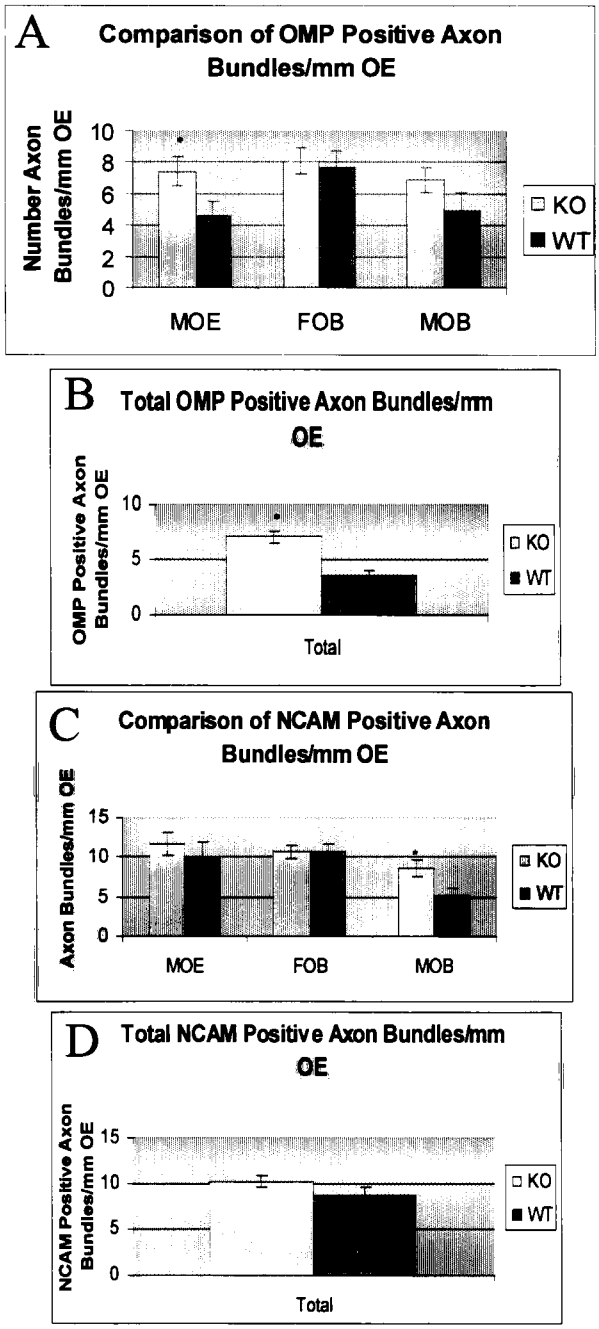

Figure 11: OMP and NCAM positive axon bundle counts show that MBD2-/- neonates have more axon bundles per mm of olfactory epithelium. (A) OMP positive axon bundles per mm OE at MOE, FOB and MOB regions. MOE $p<0.05$. (B) Total OMP positive axon bundles per mm OE $p<0.05$. (C) NCAM positive axon bundles per mm OE at the three regions. MOB $p<0.05$. (D) Total NCAM positive axon bundles per mm OE. All plots show that MBD2 -/- neonates have more axon bundles than MBD2 +/+ neonates.

bundles per mm OE further support this observation; overall MBD2-/- neonates have significantly more OMP positive axon bundles per mm OE ($p<0.05$; Fig 11B). For NCAM staining, equivalent results were obtained with MBD2-/- neonates having a greater number of NCAM positive axon bundles per mm OE at all three regions (Fig 11C) and for total NCAM positive axon bundles per mm OE in MBD2-/- (Fig 11D). Only the MOB regions was significantly different between the two animals ($p<0.05$). Values are summarized in Table 4.

In addition to the number of immunoreactive axon bundles per mm OE, their sizes were also considered. The maximum diameter of each axon bundle was measured and from this, areas were calculated. For OMP staining, the more anterior MOE ($p<0.001$) and FOB sections ($p<0.05$) had larger axon bundles as opposed to the posterior MOB region, which had smaller axon bundles ($p<0.05$; Fig 12A). Identical results were observed for NCAM staining (MOE: $p>0.05$; FOB, $p<0.05$; MOB, $p>0.05$; Fig 12B). Both extremely large and extremely small axon bundles were observed. To get a better comparison of these two extremes, the ten largest and ten smallest axon bundles were also compared. For both OMP (Fig 13A) and NCAM (Fig 13B) staining, MBD2-/- neonates had much larger axon bundles than MBD2+/+ (~3.8x). For OMP staining $p<0.05$ and for NCAM staining $p<0.001$. Out of the ten smallest axon bundles, both OMP (Fig 13B) and NCAM (Fig 13D) positive axon bundles for MBD2-/- were much smaller than MBD2+/+ (~1.6x). For NCAM staining $p<0.05$. Values are summarized in Table 5. In MBD2-/- neonates, the largest axon bundles were located in zone 1 (along the septum and roof) as opposed to the septum only of zone 1 for MBD2+/+ neonates. In

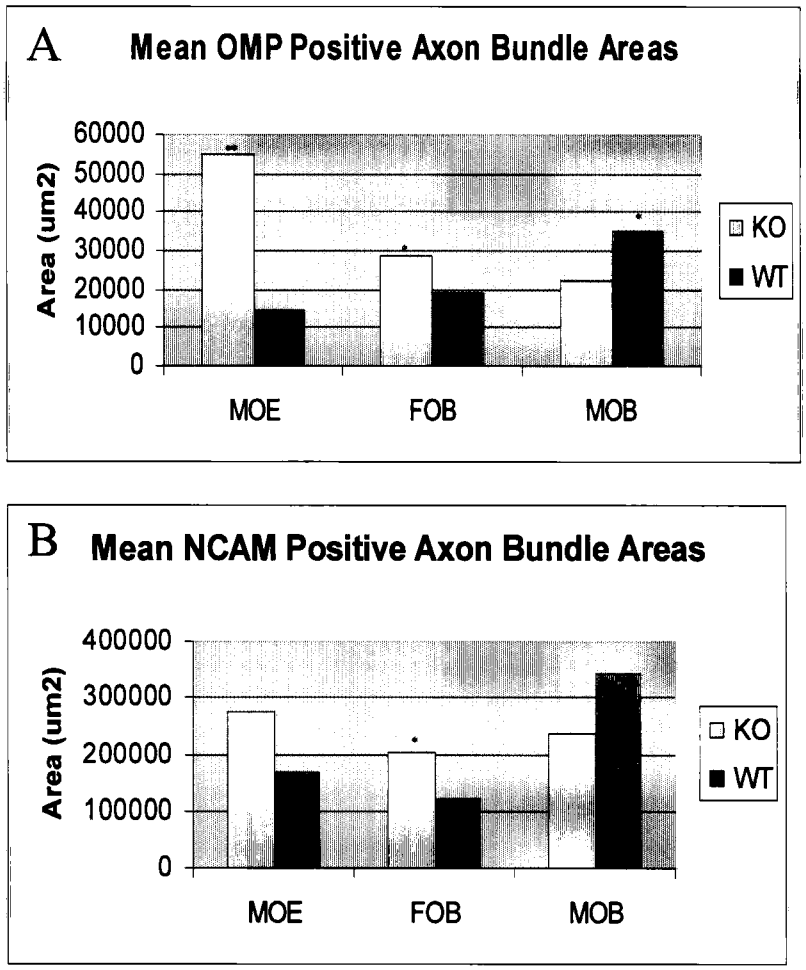

Figure 12: OMP and NCAM positive axon bundles areas show that MBD2-/- neonates have larger anterior axon bundles. (A) OMP positive axon bundle areas at MOE, FOB and MOB regions. MOE $p<0.001$ FOB $p<0.05$, MOB $p<0.05$. (B) NCAM positive axon bundle areas at the three regions. FOB $p<0.05$. For both OMP and NCAM staining, MBD2-/- neonates have larger anterior axon bundles.

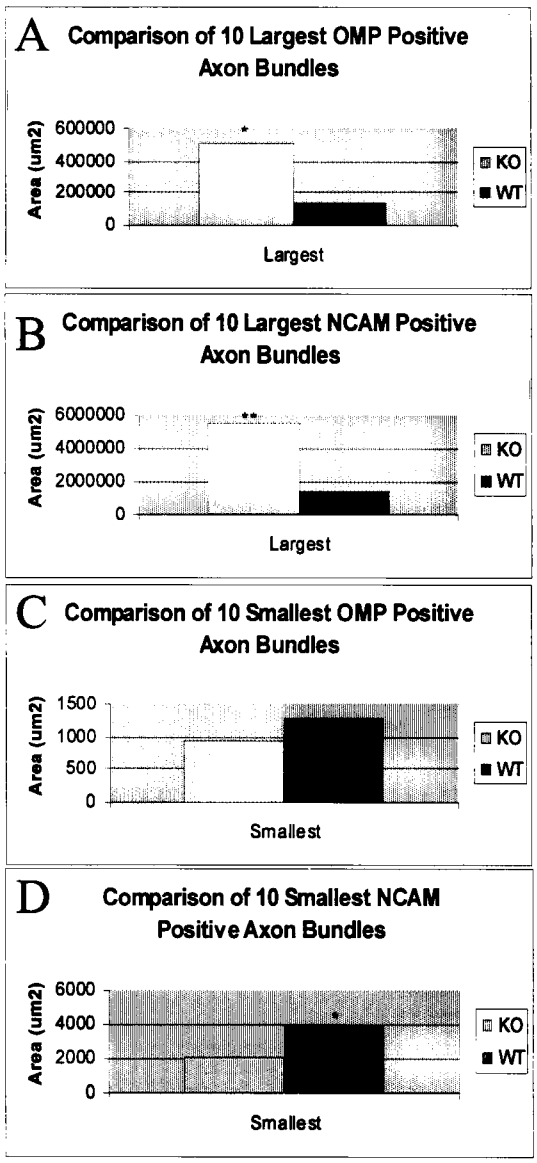

Figure 13: Extreme OMP and NCAM positive axon bundle areas. (A) OMP staining of the 10 largest axon bundles $p<0.05$. (B) NCAM staining of the ten largest axon bundles $p<0.001$. (C) OMP staining of the ten smallest axon bundles. (D) NCAM staining of the ten smallest axon bundles $p<0.05$. MBD2-/- neonates have significantly larger axon bundles (~3.8x) than the ten largest axon bundles in MBD2+/+ neonates and significantly smaller axon bundles (~1.6x) than the ten smallest axon bundles in MBD2+/+ neonates for NCAM staining.

MBD2-/- neonates, the smallest axon bundles were located in regions of both zones 2 and 3, whereas MBD2+/+ were located to regions of zone 2 only (Fig 13E).

To determine if these differences at the level of the OE in MBD2-/- neonates result in changes at the level of the OB, OMP and NCAM positive glomeruli were counted and measured at the FOB and MOB regions. MBD2-/- appear to have more glomeruli than MBD2+/+ for both OMP (Fig 14A) and NCAM staining (Fig 14B). These values are only significant for the MOB region (OMP: $p<0.05$; NCAM: $p<0.05$). A greater number of glomeruli was not observed at FOB regions, which may be due to the smaller size of the OB for these cross-sections or differences in glomeruli number may exist in the anterior-posterior axis.

There are also obvious differences in the sizes of glomeruli between the two animals. For OMP staining of MOB ($p<0.05$; Fig 15A) and NCAM staining of both FOB ($p<0.05$) and MOB ($p<0.05$) regions (Fig 15B), MBD2-/- have significantly larger glomeruli. As for axon bundle sizes, both extremely large and small glomeruli were seen in both MBD2-/- and MBD2+/+ neonates. To compare these two extremes, the ten largest and ten smallest glomeruli were compared. MBD2-/- neonates had significantly larger glomeruli (~2.6x) for both OMP ($p<0.001$; Fig 16A) and NCAM staining ($p<0.05$; Fig 16C). For OMP staining, the smallest glomeruli in MBD2-/- were slightly smaller (~1.05x) than MBD2+/+ ($p>0.05$; Fig 16B). In contrast for NCAM staining, the smallest glomeruli in MBD2-/- were still larger (~1.3x) than MBD2+/+ ($p<0.05$; Fig 16D). The differences observed for OMP and NCAM staining of the ten smallest glomeruli may be due to small sample size or may reflect differences in maturity of the smaller axon bundles. Values are summarized in Table 6. In the MBD2-/- neonates, the

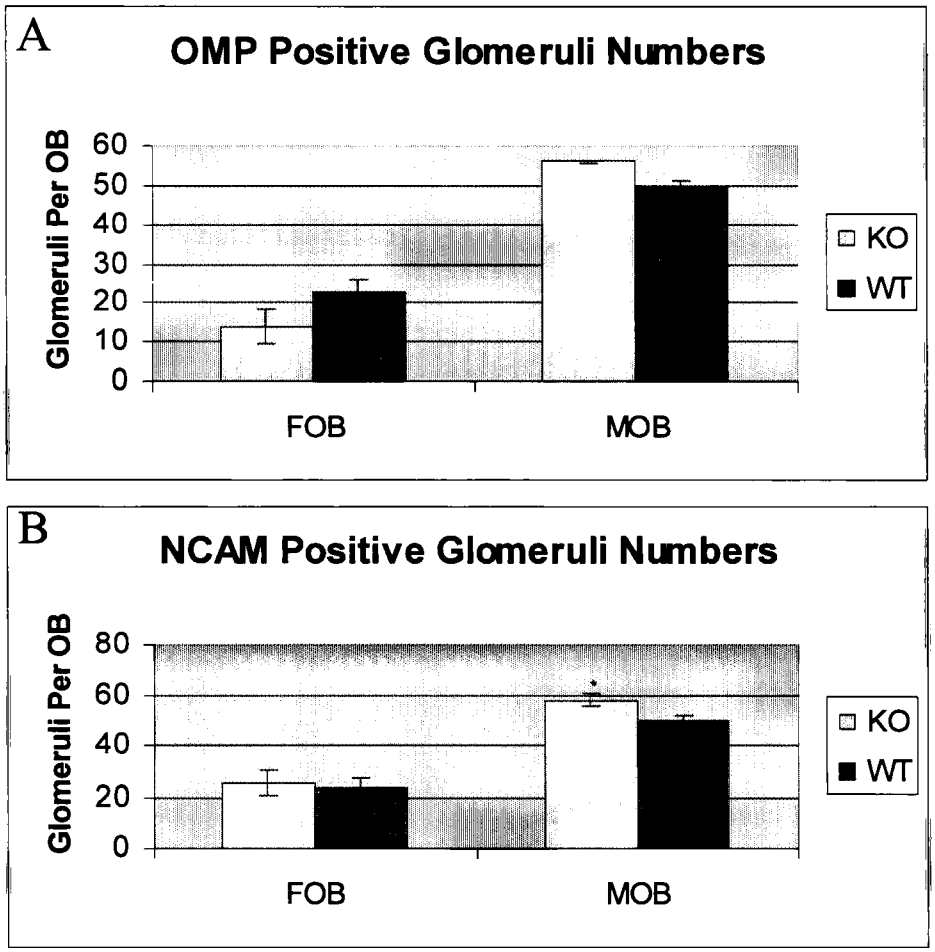

Figure 14: OMP and NCAM positive glomeruli counts show that MBD2-/- have more posterior glomeruli than MBD2+/+ neonates. (A) Number of OMP positive glomeruli per OB. MOB $p>0.05$. (B) Number of NCAM positive glomeruli per OB. MOB $p<0.05$.

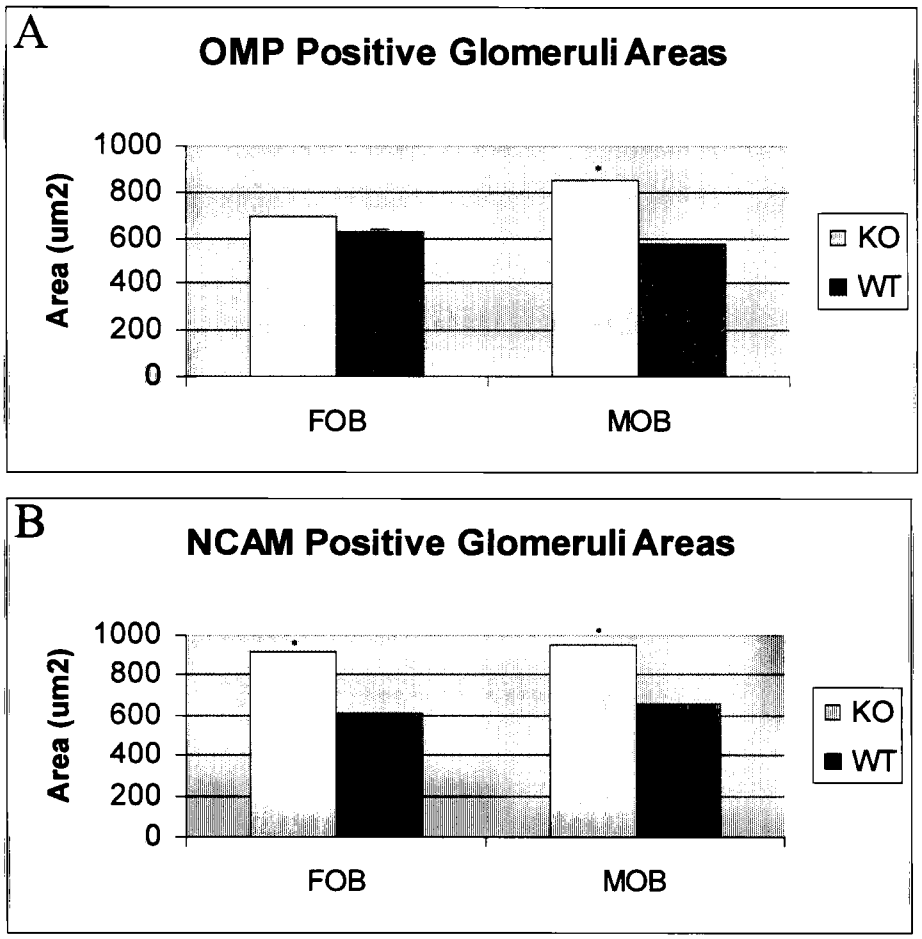

Figure 15: OMP and NCAM positive glomeruli areas show that MBD2-/- neonates have larger glomeruli. (A) Mean OMP positive glomeruli area at FOB and MOB regions. MOB $p<0.05$. (B) Mean NCAM positive glomeruli area at the two regions. FOB $p<0.05$; MOB $p<0.05$. MBD2-/- neonates have significantly larger glomeruli.

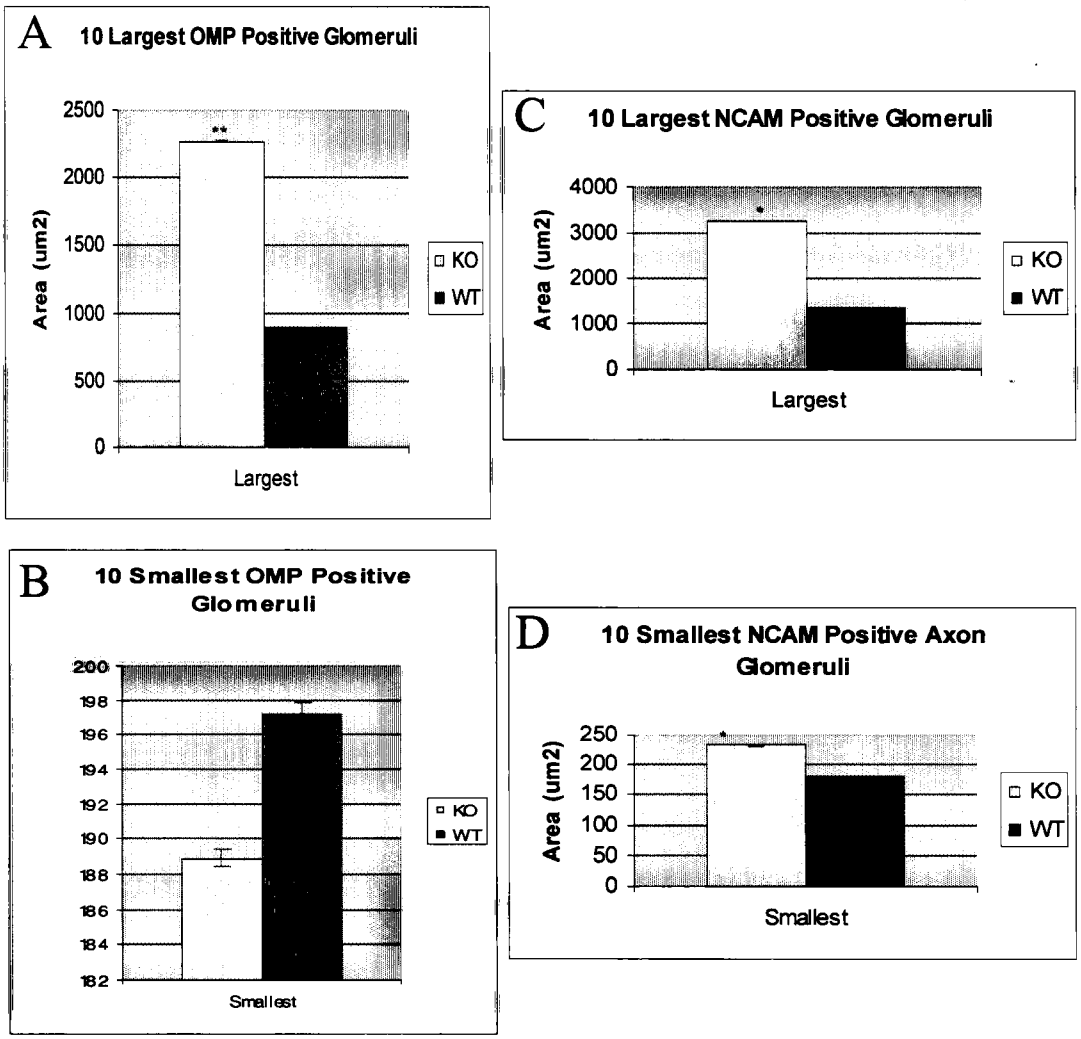

Figure 16: Extreme OMP and NCAM positive glomeruli areas. (A) OMP staining of the ten largest glomeruli $p<0.001$. (B) OMP staining of the ten smallest glomeruli $p>0.05$. (C) NCAM staining of the ten largest glomeruli $p<0.05$. (D) NCAM staining of the ten smallest glomeruli $p<0.05$. The ten largest glomeruli in MBD2-/- have significantly larger glomeruli (~2.6x) than the ten largest glomeruli in MBD2+/+ neonates for OMP and NCAM staining. However MBD2-/- neonates have slightly smaller OMP positive glomeruli (~1.05x) than the ten smallest glomeruli in MBD2+/+ neonates. In contrast, NCAM positive glomeruli are still significantly larger (~1.3x) in MBD2-/- neonates for the ten smallest glomeruli.

Table 2: Total OMP positive ORNs per mm of olfactory epithelium.

MBD2 -/- Low Density ORNs per mm OE	MBD2 +/+ Low Density ORNs per mm OE	MBD2 -/- High Density ORNs per mm OE	MBD2 +/+ High Density ORNs per mm OE
13.6 ± 1.2	9.7 ± 1.0	30.7 ± 1.2	29.0 ± 2.7
p=0.049		p=0.13	

Table 3: Total NCAM positive ORNs per mm of olfactory epithelium.

MBD2 -/- ORNs per mm OE	MBD2 +/+ ORNs per mm OE
123.5 ± 6.1	105.9 ± 7.7
p=0.040	

Table 4: Total axon bundles per mm of olfactory epithelium.

	OMP positive axon bundles per mm OE	NCAM positive axon bundles per mm OE
MBD2 -/-	7.1 ± 0.6	10.2 ± 0.6
MBD2 +/+	3.5 ± 0.6	8.7 ± 0.8
p=0.017		p=0.080

Table 5: Extreme axon bundle areas.

Mean Areas:	10 largest OMP positive axon bundles (μm^2)	10 largest NCAM positive axon bundles (μm^2)	10 smallest OMP positive axon bundles (μm^2)	10 smallest NCAM positive axon bundles (μm^2)
MBD2 -/-	512 451 ± 35	5,541,476 ± 78	936 ± 1	3,985 ± 2
MBD2 +/+	134,910 ± 14	1,395,940 ± 67	1284 ± 2	2,117 ± 3

Table 6: Extreme glomeruli areas.

Mean Areas:	10 largest OMP positive glomeruli (μm^2)	10 largest NCAM positive glomeruli (μm^2)	10 smallest OMP positive glomeruli (μm^2)	10 smallest NCAM positive glomeruli (μm^2)
MBD2 -/-	2,273 ± 1	3,243 ± 3	188.9 ± 0.5	232.0 ± 0.3
MBD2 +/+	885 ± 1	1,332.4 ± 0.9	197.2 ± 0.7	179.8 ± 0.5
	p=0.005	$p=2.8x10^{-6}$	p=0.055	P=0.030

largest glomeruli were located on the lateral sides, midline and ventral regions of the OB and the smallest were located on the dorsolateral region of the OB. In contrast, in MBD2+/+ neonates, the largest glomeruli were located on the lateral sides, ventral and ventrolateral regions of the OB and the smallest were located along the midline and ventral region of the OB.

Immunofluorescence-To directly compare the relationship between mature and immature ORNs, MBD2-/- and MBD+/+ neonates were stained with the mature ORN marker OMP, general neuronal marker NCAM and immature neuronal marker GAP-43. Sections were either co-stained with NCAM and OMP or GAP-43 and OMP.

As previously discussed at the level of the OE, both animals have large axon bundles; however, extremely large axon bundles are abundant in MBD2-/- neonates (Fig 17B, open arrowhead) as compared to some large axon bundles in MBD2+/+ neonates (Fig 17C, open arrowhead). In addition, the large axon bundles in MBD2-/- neonates appear to be taking over the smaller, adjacent axon bundles (Fig 17D, arrow). Both animals appear to have similar NCAM staining patterns in ORNs in the OE and in axon bundles in the lamina propria; however, the OMP staining appears different. Unlike MBD2+/+ (Fig 17C, open arrowhead), MBD2-/- staining of mORNs does not appear as a uniform row of cells along the most apical side of the OE, rather it is staggered (Fig 17B, open arrowhead). Also the majority of axon bundles in MBD2-/- do not co-localize NCAM and OMP expression, instead most axon bundles do not appear to express OMP and are only NCAM positive (Fig 17B, arrow). In contrast, the majority of axon bundles in MBD2+/+ co-localize NCAM and OMP expression (Fig 17C, arrow).

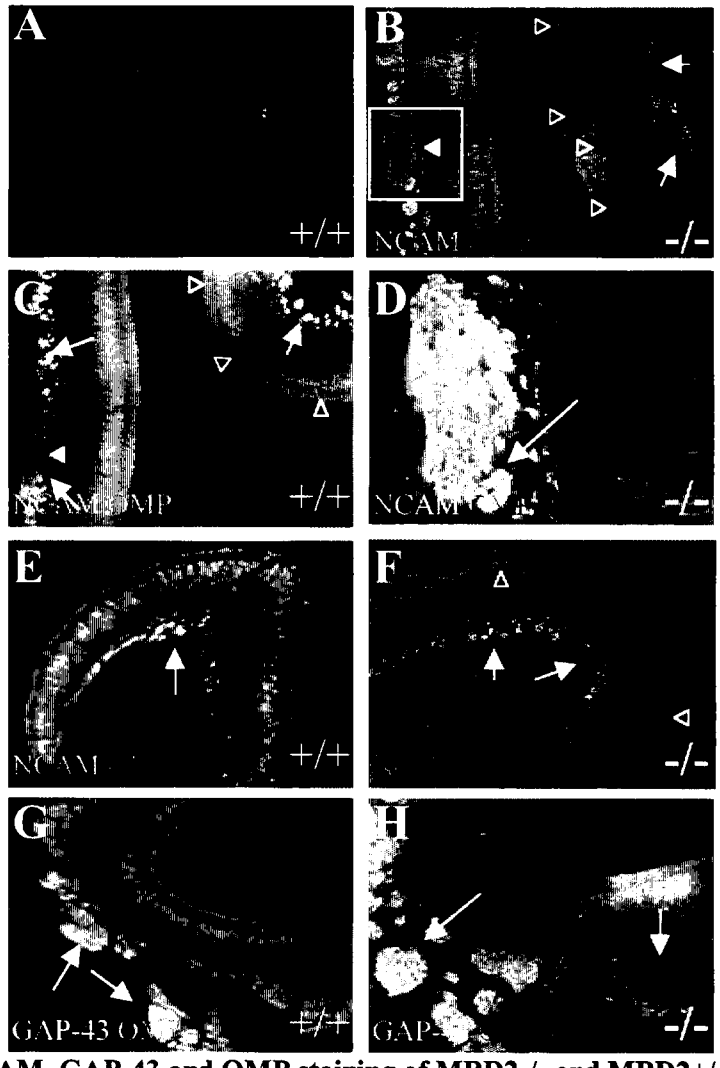

Figure 17: NCAM, GAP-43 and OMP staining of MBD2-/- and MBD2+/+ olfactory epithelium. (A) Secondary only negative control. (B-D) NCAM (red), OMP (green), co-localization (yellow). (B) MBD2-/- neonates have extremely large axon bundles (closed arrowhead), non-uniform OMP staining (open arrowhead) and only NCAM positive axon bundles (arrow). Magnification 20x. In comparison, MBD2+/+ neonates (C) have some large axon bundles (closed arrowhead), uniform OMP staining (open arrowhead) and co-localize NCAM and OMP in axon bundles (arrow). Magnification 20x. (D) The extremely large axon bundles in MBD2-/- appear to be taking over smaller, adjacent axon bundles (arrow). Magnification 63x. (E) MBD2+/+ show co-localization of NCAM and OMP (arrow) whereas (F) MBD2-/- do not. Axon bundles appear to only express NCAM (arrow); however mORNs do express OMP but expression is non-uniform (arrowhead). Both animals have similarly sized axon bundles. Magnification 20x. (G-H) GAP-43 (red), OMP (green), co-localization (yellow). Both MBD2-/- and MBD2+/+ neonates have similar ORN staining pattern for GAP-43 and OMP. (G) MBD2+/+ shows predominantly OMP positive glomeruli (arrow). Magnification 20x. In contrast, MBD2-/- (H) do not appear to express equivalent levels of OMP in axon bundles and predominantly show GAP-43 immunoreactivity (arrow). Magnification 20x.

Previously it was found that the extremely large axon bundles in MBD2-/- are observed in the more anterior MOE and FOB sections. The posterior MOB sections, which only contain the superior turbinate, have similarly sized axon bundles between MBD2+/+ (Fig 17E) and MBD2-/- neonates (Fig 17F). However as seen above, MBD2+/+ co-localize NCAM and OMP expression in axon bundles (Fig 17G, arrow) but MBD2-/- do not appear to express OMP and the axon bundles are only NCAM positive (Fig 17H, arrow). In addition, the OMP staining in MBD2-/- is not uniform (Fig 17H, arrowhead).

For GAP-43 and OMP staining patterns for ORNs in MBD2-/- and MBD2+/+ appeared similar with GAP-43 labeling IRNs and OMP labeling the ORNs. However the staining pattern in the axon bundles also appeared different. The majority of axon bundles in MBD2+/+ are OMP positive (Fig 17G, arrow). In contrast, the majority of axon bundles in MBD2-/- do not appear to equivalent levels of OMP and only predominantly express GAP-43 (Fig 17H, arrow).

At the level of the OB, differences in the staining pattern are also apparent and highlighted in Figure 18. A schematic of the locations of the largest (red) and smallest (purple) glomeruli are shown in Fig 18B and C for MBD2+/+ and MBD2-/-, respectively. The regions of the OB, subsequently shown in higher magnification, are shown in Fig 18D and E for MBD2+/+ and MBD2-/-, respectively. The NFL surrounding the OB in both animals was found to co-localize NCAM and OMP (Fig 18F and G), although the ONL in MBD2-/- appeared to express higher levels of NCAM when compared to OMP. In contrast to MBD2+/+ which co-localized NCAM and OMP expression in glomeruli

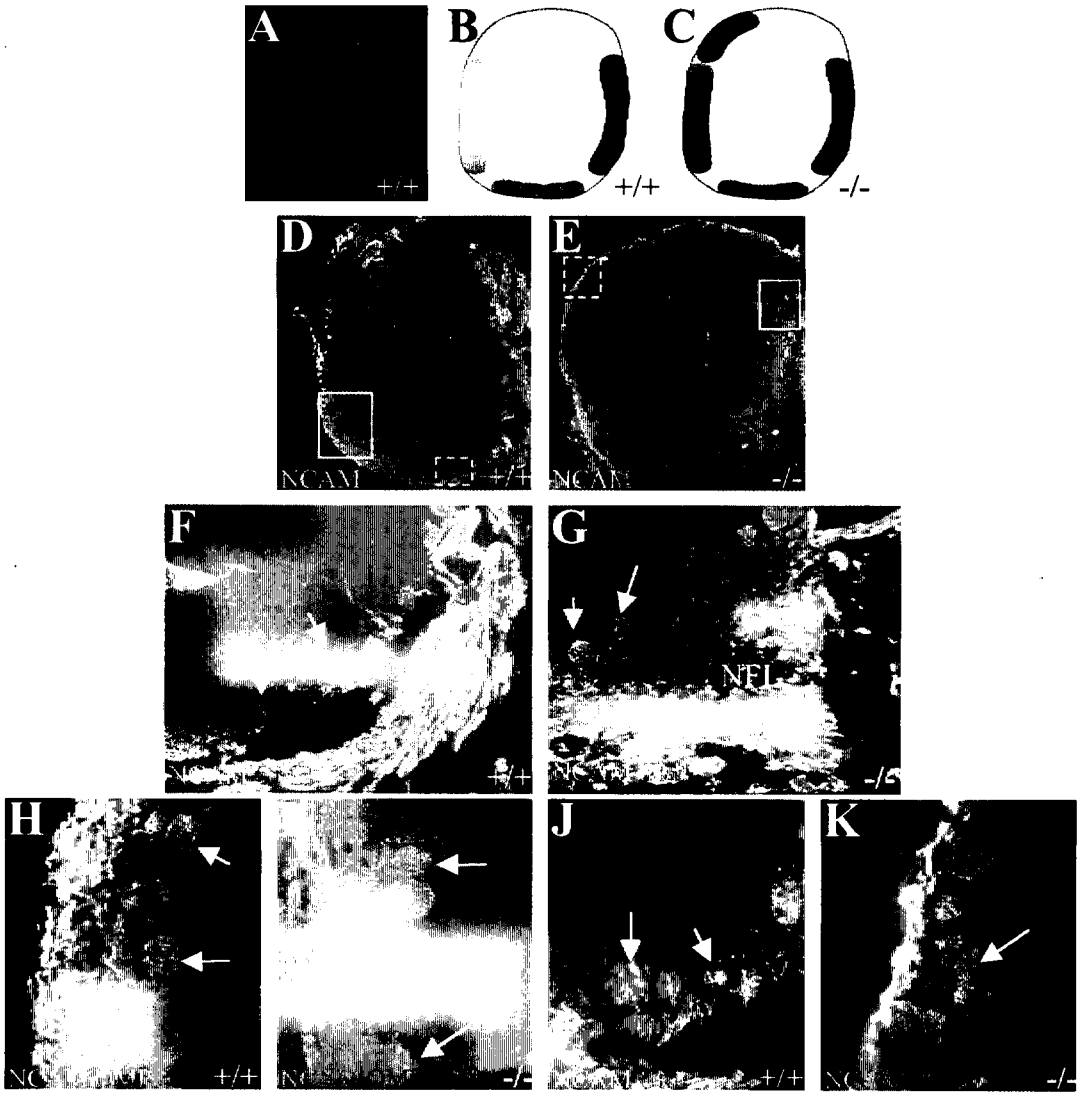

Figure 18: NCAM and OMP staining of MBD2-/- and MBD2+/+ olfactory bulb. (A) Secondary only negative control. (B-E) Dorsal is top, ventral is bottom, medial is right and lateral is left. (D-K) NCAM (red), OMP (green), co-localization (yellow). Location of largest (red) and smallest (purple) glomeruli in (B) MBD2+/+ and (C) MBD2-/- neonates. Coronal section of (D) MBD2+/+ and (E) MBD2-/- OBs. Magnification 2.5x. (F) Medio-ventral OB showing the NFL surrounding the OB and glomeruli (arrow). Magnification 10x. (G) In contrast, MBD2-/- neonates have a thicker NFL and larger glomeruli (arrow). Magnification 10x. (H) The largest glomeruli in MBD2+/+ from the ventro-lateral (closed box in D) side show co-localization of NCAM and OMP (arrow), whereas (I) the largest glomeruli (closed box in E) in MBD2-/- from the midline only express OMP (arrow); although the NFL shows co-localization. Magnification 20x. (J) The smallest glomeruli in MBD2+/+ (dashed box in D) from the ventral side also show co-localization of NCAM and OMP (arrow), whereas (K) the smallest glomeruli in MBD2-/- (dashed box in E) from the dorso-lateral side only express OMP (arrow); although the NFL shows co-localization. Magnification 20x.

(Fig 18F, arrowhead), the glomeruli in MBD2-/- appear to only express OMP (Fig 18G, arrowhead). This observation was consistent in glomeruli throughout the OB.

The differences in glomeruli sizes are highlighted in Figures 18H-K. The largest glomeruli in MBD2+/+ are commonly located on the lateral and ventral sides of the OB; the smallest glomeruli are commonly located along the midline and ventral sides of the OB (Fig 18B). Both the largest glomeruli from the ventro-lateral side of the OB (Fig 18H) and the smallest glomeruli from the ventral side of the OB (Fig 18J) co-localize NCAM and OMP expression. In contrast, the large glomeruli in MBD2-/- are commonly located on the midline and lateral and ventral sides of the OB; the smallest glomeruli are commonly located in the dorso-lateral side of the OB (Fig 18C). Both the largest glomeruli from the midline (Fig 18I) and the smallest glomeruli from the ventral side of the OB (Fig 18K) appear to only express OMP.

Summary-MBD2-/- neonates display a number of phenotypic differences in the olfactory system at the morphological and cellular level for ORN markers. In the OE, MBD2-/- neonates had more ORNs that were randomly distributed in high and low density regions for OMP staining, more axon bundles and extremely large anterior axon bundles. The axon bundles did not co-localize OMP and NCAM, as observed in MBD2+/+, and appeared not to express OMP at equivalent levels. In the OB, MBD2-/- had a thick ONL and extremely large glomeruli, which were absent at the back of the OB. Although the ONL co-localized OMP and NCAM staining, the majority of glomeruli in MBD2-/- appeared to only express OMP.

3.3: Characterization of OP6 and OP27, Conditionally Immortalized Cell Lines from the Embryonic Mouse Olfactory Placode

Introduction-As previously discussed, the generation of accurate *in vitro* models of olfactory neuronal development will help us to understand a number of issues including ORN turnover and differentiation, acquisition of OR expression and the physiological response to specific odorants in ORN function. The manipulation of culture conditions will allow us to address such issues, which are more difficult to address *in vivo*. Several groups have attempted to generate olfactory neuronal cultures using a variety of approaches. Although a number of these cell lines do possess ORN characteristics, they do not express endogenous OR or electrophysiological activity typical of mature ORNs. An additional issue that has not been considered is the role of retinoic acid (RA) in olfactory neuronal development. RA has been implicated in the control of gene expression and vertebrate development, cellular differentiation and homeostasis (Whitesides *et al.*, 1998).

Boolay (1998) generated sixty clonal olfactory placodal (OP) cell lines from E10.5 olfactory placode primary culture. Forty-eight of these survived clonal isolation and expansion. These cell lines proliferate at the permissive temperature of 33°C and differentiate at the non-permissive temperature of 39°C when the immortalizing U19 tsA58 SV40 large T antigen is inactive. Boolay performed an initial screen of four cell lines for transcription factors known to be expressed in early olfactory neuronal development. Based on morphology and the expression of neuronal markers, two of

these cell lines: OP6 and OP27 were judged to be neuronal in nature and chosen for further characterization (Boolay, 1998).

At the permissive temperature, OP6 divides at once every 99 hours and appears as immature process bearing ORNs, with triangular cell bodies. At the non-permissive temperature in differentiation conditions containing retinoic acid (RA), OP6 ceases to divide, differentiates and acquires an elongated, bipolar phenotype (6-8 DIV). In contrast, at the permissive temperature OP27 divides once every 52 hours and grows in cell clusters. At the non-permissive temperature in differentiation conditions containing retinoic acid (RA), OP27 undergoes an additional round of division before differentiating and first appears as a network of cells with triangular cell bodies (2-5 DIV) before acquiring an elongated, bipolar phenotype similar to OP6. RA was shown to enhance the expression of transcription factors and odorant receptors by RT-PCR (Boolay, 1998).

Upon differentiation, both OP6 and OP27 expressed BF-1, a marker of proliferating neuronal progenitors and post-mitotic neurons and O/E-1, an ORN transcription factor, OTX-2, a neuronal precursor marker and ORs. Highly differentiated OP6s (8 DIV) lose BF-1 expression. OP27 was also found to express Pax-6 at the non-permissive temperature. *In vivo*, Pax-6 is expressed by different sub-populations of cells in the embryonic OE (Boolay, 1998).

Both lines also express endogenous ORs. OP6 was found to express two different ORs. Sequence analysis showed that OR6a is identical to the mouse F12 OR and OR6b is homologous to the F12 OR. The two ORs expressed by OP6 are highly related in terms of sequence, phylogenicity and gene clustering within the genome. In contrast

OP27 was found to express only one OR that is identical to the M65 OR (Boolay, 1998; Illing *et al.*, 2001). These ORs are located on mouse chromosome 11.

OP6 and OP27 were further characterized for markers of the olfactory neuronal development, mature olfactory neurons and neurotrophin signal transduction molecules, using a combination of western blotting and immunohistochemistry. Confirming that OP6 and OP27 are true *in vitro* models of developing ORNs will allow the study of various ORN developmental events and in particular, MBD2 function.

Boolay's data suggests that OP6 and OP27 are *in vitro* models of developing olfactory neurons. To strengthen this data, OP6 and OP27 were further characterized with neuronal, mature olfactory neuronal and neurotrophin signal transduction markers, using a combination of western blotting and immunohistochemistry. These experiments to confirm that OP6 and OP27 are true *in vitro* models of developing ORNs will allow the study of various ORN developmental events and in particular, MBD2 function.

Results

OP6 and OP27 express neuronal markers-To determine where OP6 and OP27 lie in the olfactory lineage, the expression of general neuronal markers was examined by western blotting and immunocytochemistry. The expression of the neuronal markers Growth Associated Protein-43 (GAP-43), β-III neuron specific tubulin (NST) and NCAM were studied. The more immature neuronal marker GAP-43 is expressed by OP27 before and after differentiation; however, expression is lost as OP6 differentiates and acquires a mature neuronal phenotype, characterized by an elongated, bipolar morphology (Fig 19A). NST is expressed by both OP6 and OP27 before and after differentiation but

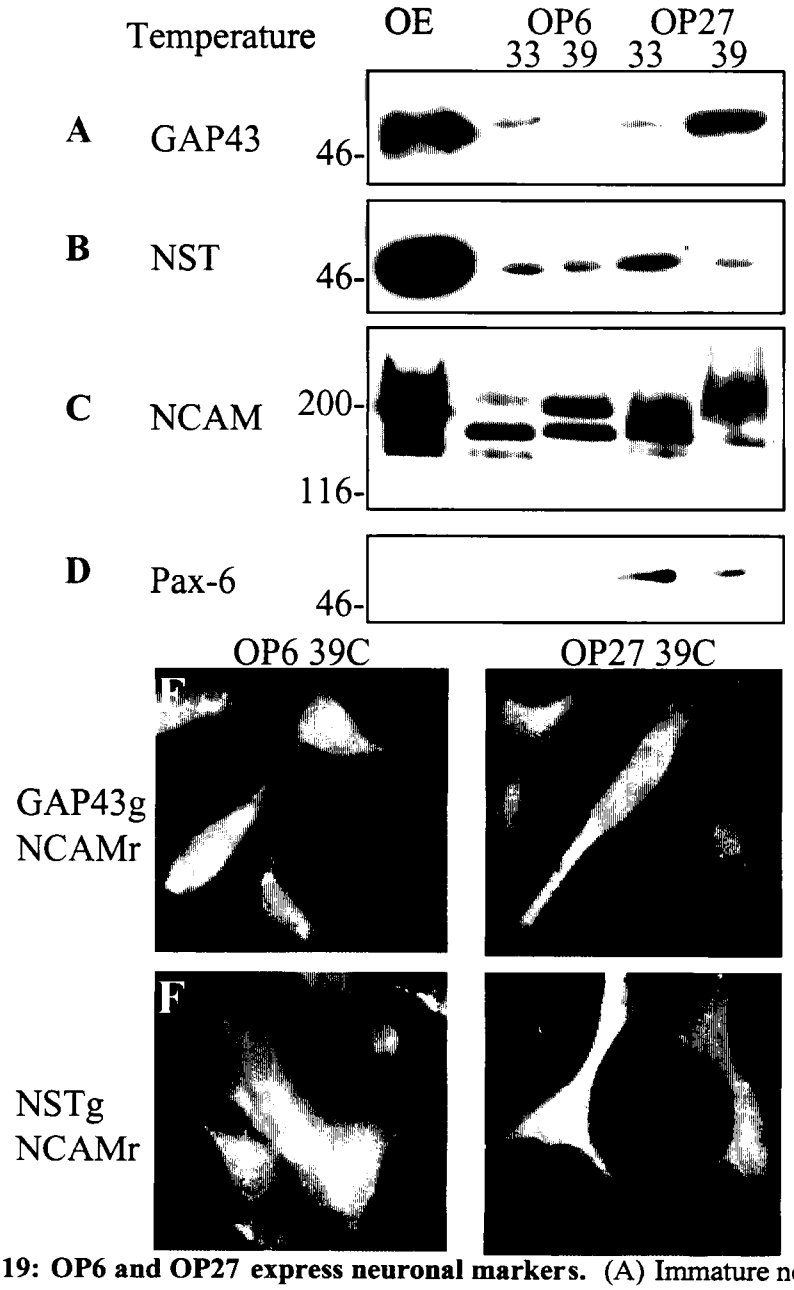

Figure 19: OP6 and OP27 express neuronal markers. (A) Immature neuronal marker GAP-43 is expressed by OP27 before and after differentiation but OP6 loses expression upon differentiation. (B) NST is expressed by both OP6 and OP27 before and after differentiation, with a decrease in expression upon differentiation. (C) NCAM is expressed in OP6 and OP27 before and after differentiation, upon differentiation NCAM undergoes alternate splicing to form a mature processed, non-polysialated form. (D) Pax-6 is only expressed in OP27 and expression decreases upon differentiation. (E) GAP-43 is most concentrated at the axon hillock and seen occasionally in the neurites of the less mature OP27 line. (F) NST is concentrated in the axon hillock and neurites. NCAM is evenly distributed on the cell surface of OP6 and OP27. Magnifcation 40x.

expression appears to decrease upon differentiation (Fig 19B). This is in accordance with observations that NST significantly decreases with ORN maturation (Roskams *et al.*, 1998). Different forms of NCAM are expressed in both OP6 and OP27 before and after differentiation (Fig 19C). Upon differentiation, NCAM undergoes alternate splicing to form a mature processed, non-polysialated form. Pax-6 is only expressed in OP27 and expression decreases upon differentiation (Fig 19D). From immunocytochemistry, GAP-43 is most concentrated at the axon hillock and seen occasionally in the neurites of the less mature OP27 line (Fig 19E), NST appears to be concentrated in the axon hillock and neurites (Fig 19F) and NCAM is evenly distributed on the cell surface of OP6 and OP27 (Fig 19E and F).

OP6 and OP27 express mature olfactory neuronal markers-To determine if differentiated OP6 and OP27 are capable of functioning as mature ORNs, the expression of mature ORN markers belonging to the olfactory signal transduction cascade was examined by western blotting and immunocytochemistry. These include the olfactory G protein (Golf), adenylate cyclase III (ACIII) and OMP.

Both OP6 and OP27 express Golf and ACIII before and after differentiation (Fig 20A). Although levels of expression are not being quantified, an unexpected decrease in ACIII expression is observed following differentiation. Intuitively, one would expect ACIII levels to remain the same or to increase following maturation; however, genes are known to be highly expressed during development and down-regulated following maturation (Jane Roskams, personal communication). This may be due to protein quality. From immunocytochemistry, Golf (Fig 20B) and ACIII (Fig 20C) are localized

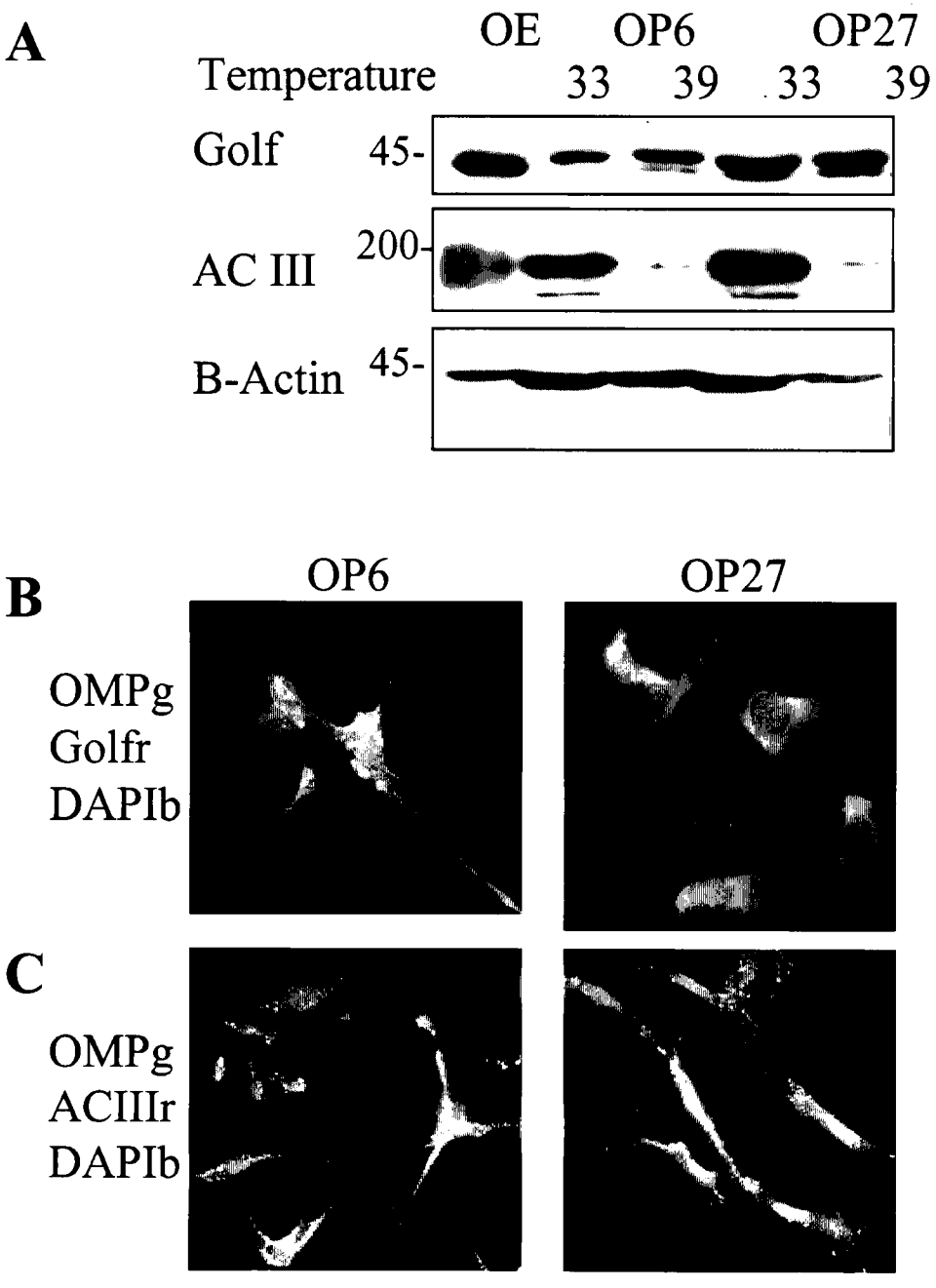

Figure 20: OP6 and OP27 express mature olfactory neuronal markers. (A) OP6 and OP27 express Golf and ACIII before and after differentiation. β-actin loading control. (B) Golf and (C) ACIII are localized to outgrowing neurites and mature processes. The Golf and ACIII signal significantly overlap with the mature olfactory neuronal marker OMP. Magnifcation 20x.

to outgrowing neurites and mature processes, and significantly overlap with the mature olfactory neuronal marker OMP (Fig 20B and C). Boolay have also detected the olfactory cyclic nucleotide gated channel subunit OCNC1 by RT-PCR. By electrophysiology OP6 and OP27 are electrophysiologically competent, displaying calcium and inwardly-rectifying potassium channel activity. Only once they acquire a mature, fully differentiated phenotype do they demonstrate voltage-gated sodium channel activity similar to what is seen in ORN primary culture (Mary Lucero, personal communication).

OP6 and OP27 express and regulate neurotrophin signal transduction systems in a differentiation dependant fashion-BDNF and NT-3 are known to influence the differentiation and survival of ORN primary cultures (Roskams *et al.*, 1996). When OP6 and OP27 are treated with BDNF and NT-3, enhanced expression of NST and OMP was observed, in addition to cell survival following differentiation. To determine which pathways capable of transducing differentiation signals are present in OP6 and O27, we examined the expression of the neurotrophin receptors TrkA, TrkB, TrkC and p75, and their cytoplasmic transduction components PLC-γ2 by western blotting and immunocytochemistry.

The high affinity nerve growth factor (NGF) receptor TrkA could not be detected in OP6 or OP27. TrkB is expressed in its kinase active 140 kD full-length form and its kinase inactive 80 kD truncated form in OP6 and OP27 before differentiation (Fig 21A). Upon differentiation, the predominant form of TrkB is the truncated form, consistent with what is seen *in vivo* in the OE. TrkC is also expressed in both full-length and truncated

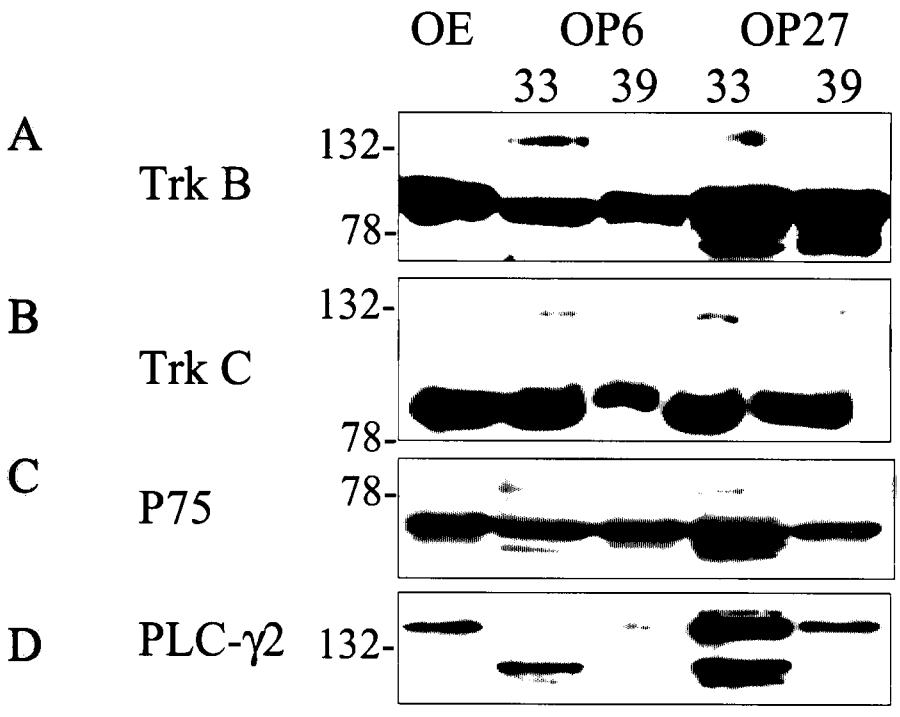

Figure 21: OP6 and OP27 express neurotrophin receptors. (A) TrkB is expressed in its kinase active 140 kD full-length form and its kinase inactive 80 kD truncated form in OP6 and OP27 before differentiation. Upon differentiation, the predominant form of TrkB is the truncated form, consistent with what in seen *in vivo* in the. (B) TrkC is also expressed in both full-length and truncated form in both OP6 before differentiation and OP27 before and after differentiation. Only the truncated form is present in the mature differentiated OP6. (C) p75 is expressed in OP6 and OP27 before and after differentiation. Expression levels do not appear to change. (D) PLC-γ2, which transduces TrkB and TrkC signals intracellularly, is expressed both before and after differentiation in OP6 and OP27. The high affinity nerve growth factor (NGF) receptor TrkA could not be detected in OP6 or OP27.

forms in both OP6 before differentiation and OP27 before and after differentiation. Only the truncated form is present in the most mature differentiated OP6 (Fig 21B). The low affinity NGF receptor p75 is expressed in OP6 and OP27 before and after differentiation. Expression levels do not appear to change (Fig 21C). PLC-γ2, which transduces TrkB and TrkC signals intracellularly, is expressed both before and after differentiation in OP6 and OP27 (Fig 21D). By immunocytochemistry, TrkB (Fig 22A), TrkC (Fig 22B) and p75 (Fig 22C) are expressed on the surface of the cell body and processes of OP6 and OP27. PLC-γ2 is localized to the processes of OP6 and OP27 (Fig 22D).

Summary-In order to better understand olfactory neuronal development, two conditionally immortalized cell lines, OP6 and OP27, were further characterized. The expression of neuronal, mature olfactory neuronal and neurotrophin signal transduction markers were assessed by western blotting and immunocytochemistry to determine where OP6 and OP27 lie in the olfactory lineage and if they are capable of functioning as mature ORNs. OP27 expresses more immature neuronal markers, even after differentiation, suggesting that they are less mature than OP6 in the ORN lineage (Fig 23). OP27 can be placed at the transition from transit amplifier to immediate neuronal precursor whereas OP6 can be placed at the IRN stage. Upon differentiation, OP6 and OP27 express the mature olfactory neuronal marker OMP. OP6 and OP27 are electrophysiologically competent and display channel activity similar to ORN primary culture once they acquire a mature, fully differentiated phenotype.

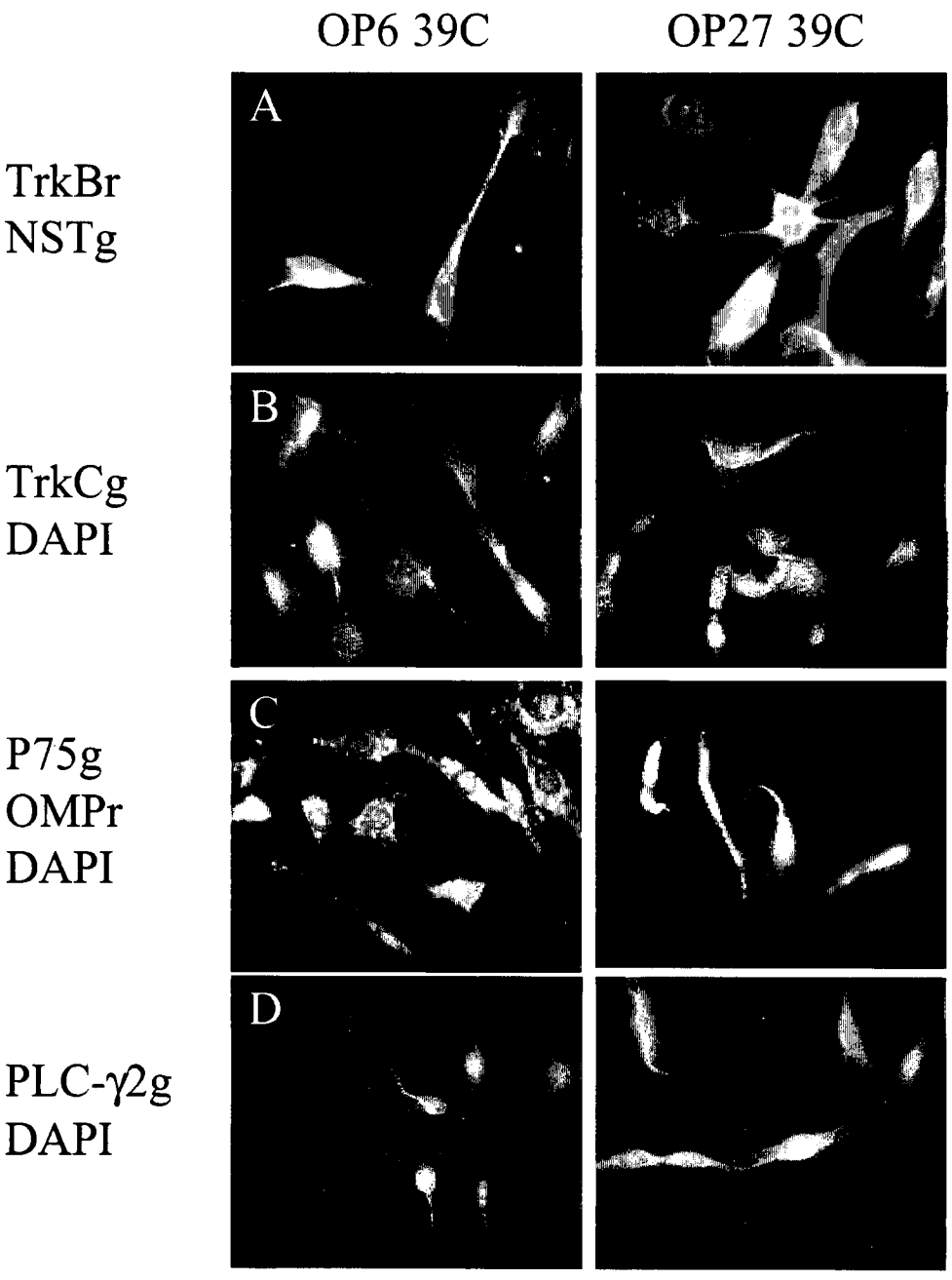

Figure 22: Immunocytochemical localization of neurotrophin receptors. (A) TrkB, (B) TrkC and (C) p75 are expressed on the surface of the cell body and processes of OP6 and OP27. (D) PLC-γ is localized to the processes of OP6 and OP27. Magnifcation 20x.

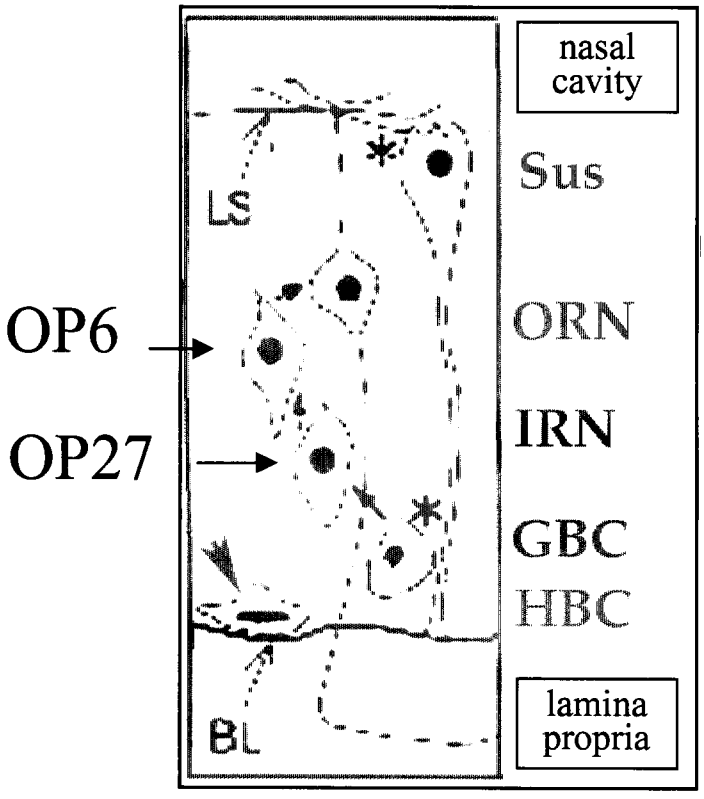

Figure 23: OP6 and OP27 are staggered in the olfactory lineage. Based on expression profile, morphology and behavior *in vitro*, OP6 and OP27 can be placed at slightly staggered but successive stages in the ORN lineage.

3.4: *In vitro* characterization of MBD2 and MBD3 in OP6 and OP27

Introduction-Together, the *in vivo* MBD2 expression profile and the *in vivo* MBD2-/- neonate and MBD2 expression data suggest a role for MBD2 in controlling gene expression events during olfactory neuronal development. Based on expression profile and morphology, OP6 and OP27 have been demonstrated to be olfactory neuron-like in nature, with slightly staggered stages of maturation. OP27 appears to be slightly less mature than OP6 in the ORN lineage. It is difficult to determine gene function *in vivo* in the presence of extraneous noise. The use of simple *in vitro* models, such as OP6 and OP27, will allow the study of developmental events and in particular MBD2 function. The manipulation of culture conditions and use of MBD2 complex inhibitors such as the HDAC inhibitor trichostatin A (TSA) or DNA methylation inhibitor 5-AZA-2'-deoxcytidine (5'AZA-CdR) will provide insight into MBD2 function. TSA, produced by *Streptomyces*, is a potent reversible inhibitor of HDACs that causes histone hyperacetylation, thereby regulating gene transcription. Depending on dose, TSA affects induction of differentiation, cell cycle arrest at G0/G1 and G2 phases and at concentrations in the μm range, apoptotic cell death (Jones *et al.*, 1998; Salminen *et al.*, 1998; Inokoshi *et al.*, 1999). 5-AZA-CdR is a potent and specific demethylating agent that has been shown to reactivate the expression of genes silenced by methylation (Bovenzi *et al.*, 2000). In order to utilize OP6 and OP27 as *in vitro* models for MBD2 function, it is necessary to demonstrate that OP6 and OP27 express MBD2 in a manner similar to what is observed *in vivo*.

Results

OP6 and OP27 express MBD2 and MBD3-Using western blotting, OP6 and OP27 express MBD2 (Fig 24A) and MBD3 (Fig 25A) before and after differentiation. The OE positive control lane for both blots shows low levels of MBD2 and MBD3 expression as compared to OP6 and OP27. This is likely due to the relatively small proportion of cells that express MBD2 and MBD3 in the heterogeneous population of cells in the OE protein homogenate, which includes sustentacular cells, olfactory ensheathing glia and the different cell types found in the lamina propria, in addition to ORNs at various stages of maturation.

Using immunocytochemistry, both MBD2 and MBD3 have been localized to the nucleus of OP6 and OP27. For MBD2, there is low expression in the nucleus of a very small sub-population of the least mature OP27 line before differentiation (Fig 24B). For OP27 after (Fig 24C) and OP6 before differentiation (Fig 24D), a sub-population of cells express MBD2 in the nucleus; at this point both are at a similar stage in the ORN lineage. Nuclear expression appears to be up-regulated in highly differentiated OP6, which are the most mature in phenotype (Fig 24E). Similar to what has been seen *in vivo*, MBD2 appears to be expressed in the nucleus of a sub-population of immature ORNs and is up-regulated in more mature ORNs (Fig 5A-D).

For MBD3, there is also low expression in the nucleus of a very small sub-population of cells for OP27 before (Fig 25B) and after differentiation (Fig 25C) and OP6 before differentiation (Fig 25D). Noticeable levels of nuclear MBD3 expression are seen

in differentiated OP6 (Fig 25E). Similar to what has been seen *in vivo*, MBD3 appears not to be expressed or expressed at very low levels in the nucleus of immature ORNs and

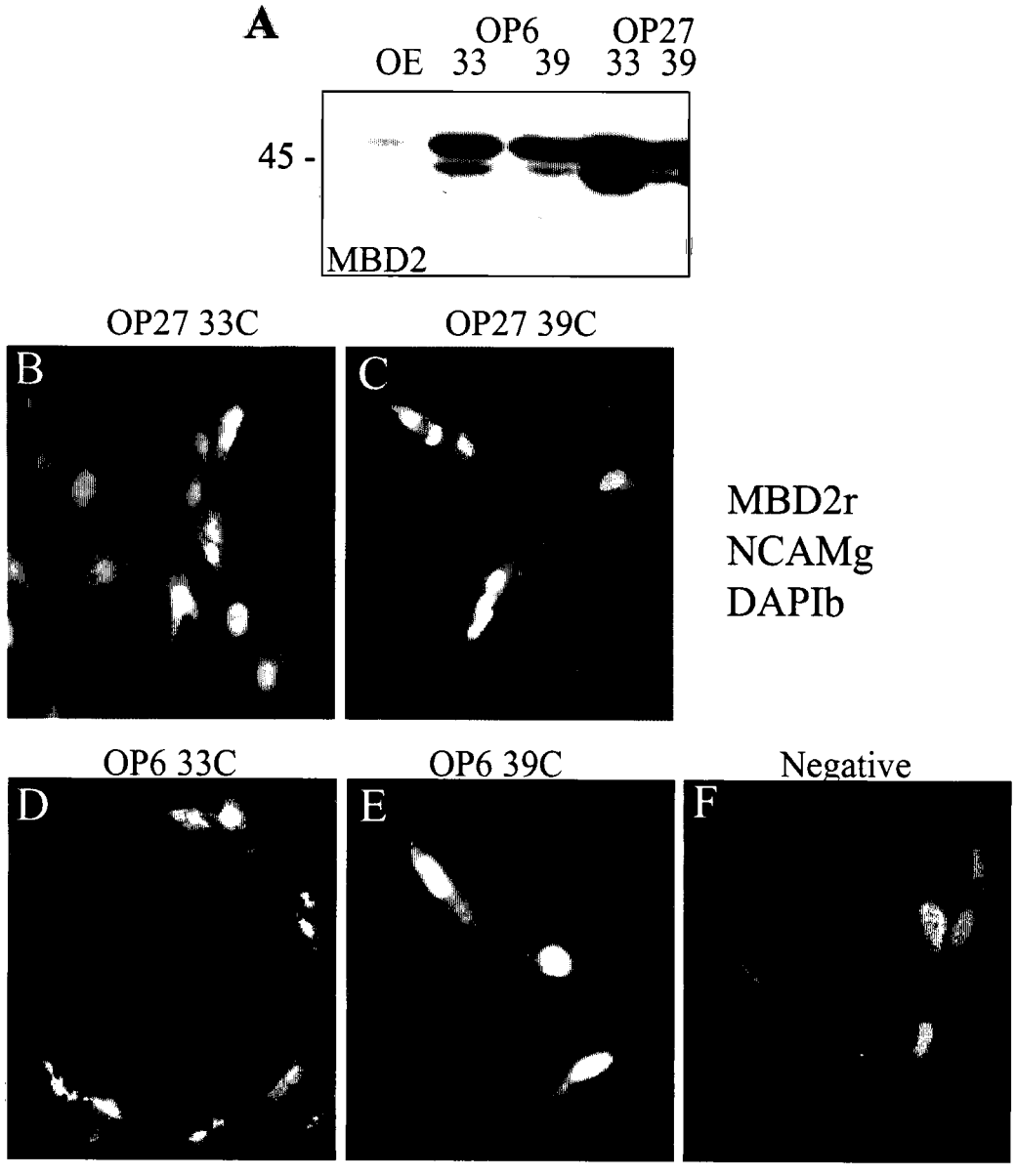

Figure 24: OP6 and OP27 express MBD2 in the nucleus. (A) MBD2 western blot. The OE positive control lane shows low levels of MBD2 and is likely due to the small proportion of cells that express MBD2 and MBD3 in the heterogeneous population of cells in the OE protein homogenate. (B) The least mature OP27 line before differentiation expresses MBD2 at low levels in a very small sub-population of cells. (C) A sub-population of OP27 after differentiation and (D) OP6 before differentiation express MBD2 in the nucleus. (E) The most mature differentiated OP6 up-regulates MBD2 in the nucleus. (F) Secondary only negative control. Consistent with observations *in vivo*, MBD2 is expressed in the nucleus of a sub-population of immature ORNs and is up-regulated in more mature ORNs. Magnification 20x.

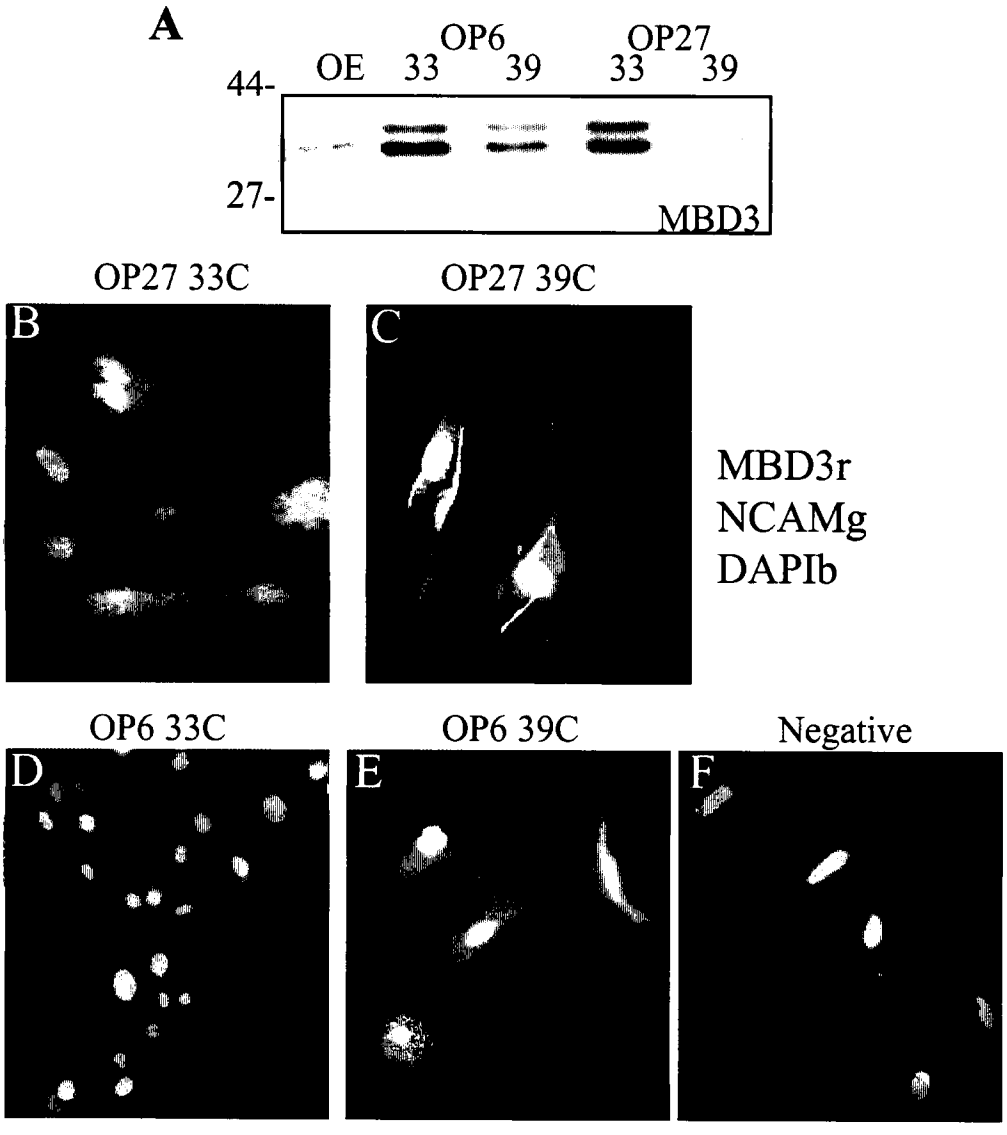

Figure 25: Sub-populations of OP6 and OP27 express MBD3 in the nucleus. (A) MBD3 western blot. The OE positive control lane shows low levels of MBD3 and is likely due to the small proportion of cells that express MBD2 and MBD3 in the heterogeneous population of cells in the OE protein homogenate. (B) MBD3 is expressed at a low level in the nucleus of a very small sub-population of OP27 before, (C) after differentiation and (D) OP6 before differentiation. (E) Differentiated OP6 express a noticeable level of MBD3. (F) Secondary only negative control. Consistent with observations *in vivo*, MBD3 appears not to be expressed or expressed at very low levels in the nucleus of immature ORNs and readily detectable levels of MBD3 are not seen until after differentiation in more mature ORNs. Magnification 20x.

readily detectable levels of MBD3 are not seen until after differentiation in more mature ORNs (Fig 5F). Thus, OP6 and OP27 appear to express both MBD2 and MBD3 in a differentiation dependent manner consistent with observations *in vivo*.

OP6 and OP27 express and interact with chromatin modification proteins-As previously discussed, MBDs have been found to associate with other MBD family members and chromatin modification proteins such as histone binding proteins, histone deacetylases (HDACs) and the co-repressor protein that recruits them, Sin3A. MBD2 belongs to the MeCP1 repressor complex that includes HDAC1, HDAC2, RbAp46 and RbAp48 in HeLa extracts (Hendrich and Bird, 1998; Bird and Wolffe, 1999; Hendrich et al., 1999; Ng *et al.*, 1999; Wade *et al.*, 1999; Snape *et al.*, 2000).

OP6 and OP27 have already been shown to express MBD3, a potential MBD2 protein interactor. Using western blotting, OP6 and OP27 also express MeCP2, HDAC1, HDAC2 and mSin3A. OP6 and OP27 before and after differentiation appear to express uniform levels of MeCP2 (Fig 26A), HDAC1 (Fig 26B) and HDAC2 (Fig 26C). The expected 140 kD mSin3A band is present in both lines except in differentiated OP27 (Fig 26D). An additional three smaller bands are seen at approximately 120 kD, 75 kD and 70 kD. The three additional bands are expressed in the same pattern as the 140 kD band. The 70 kD band is also expressed in OP27 after differentiation. In the literature, the predominant mSin3A band is the 140 kD band; however, both the 120 kD and 70 kD bands are expressed at low levels. The β-actin loading control is shown in Fig 26E. OP27 at 39°C (Fig 26E, Lane 5) appears slightly under-loaded when compared to the other lanes; however expression is being assessed and not being quantitated. Pilot

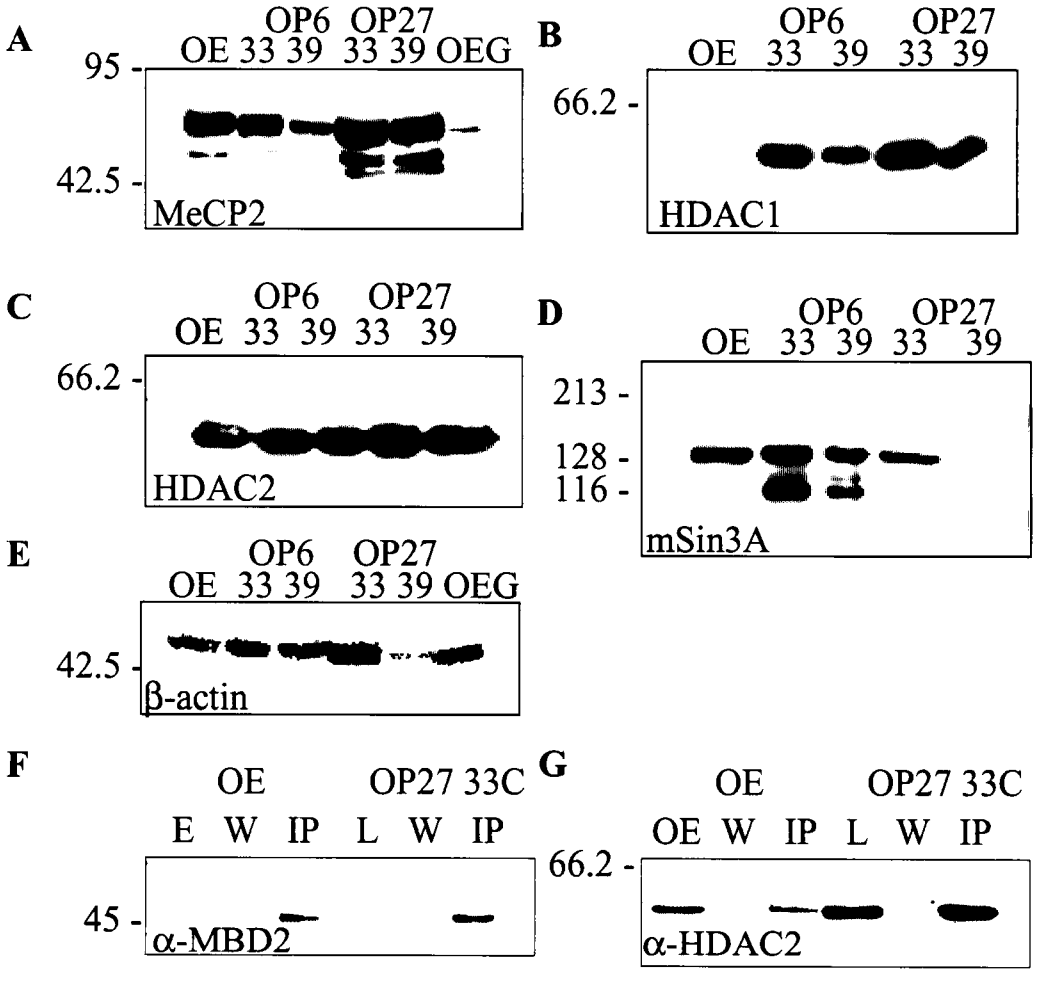

Figure 26: OP6 and OP27 express MBDs and chromatin modification proteins. (A) MeCP2 western blot, (B) HDAC1 western blot, (C) HDAC2 western blot. OP6 and OP27 appears to express uniform levels of MeCP2, HDAC1 and HDAC2. (D) Sin3A western blot. The 140 kD Sin3A band is absent in OP27 after differentiation. Three additional smaller bands are present at approximately 120 kD, 75 kD (not shown) and 70 kD (not shown) and are expressed in the same pattern as the 140 kD band. The 70 kD band is also expressed in OP27 after differentiation. (E) β-actin loading control. OP27 39C appears under-loaded, however we are trying to assess protein expression and not relative levels of expression. (F) Immunoprecipitation with MBD2 in OP27 (33°C) enriches for MBD2 and (G) MBD2 interacts with HDAC2. E=OE protein homogenate, L=lysate; W=IP wash; IP=IP product.

immunoprecipitation experiments have demonstrated that MBD2 can interact with chromatin modification proteins. Preliminary experiments were performed in OP27 at 39°C using MBD2 antibody. As a positive control, western blots for MBD2 demonstrates that MBD2 is enriched in the final immunoprecipitation product (Fig 26F, Lanes 3 and 6). Western blots for HDAC2 demonstrates that HDAC2 is expressed in the OE protein homogenate and OP27 39°C cell lysate before immunoprecipitation (Fig 26G, Lanes 1 and 4) and that MBD2 interacts with HDAC2 in the final immunoprecipitation product (Fig 26G, Lanes 3 and 6).

HDACs are essential to OP27 survival-Initial HDAC inhibition experiments were carried out on OP27 at 33°C. Various groups have successfully used TSA to inhibit HDACs in the range of 3-30 nm. At 3 nm, Jones *et al.* demonstrated an 80% inhibition as opposed to 100% at 30 nm (Jones *et al.*, 1998); TSA concentrations in the μm range are known to cause apoptosis (Salminen *et al.*, 1998). For the initial HDAC inhibition experiment, a TSA concentration of 25 nm was used. OP27 were grown at 33°C until 70% confluencey before being the media was replaced with differentiation media or differentiation media containing TSA. OP27 were allowed to settle at 33°C overnight before being switched to 39°C. During this overnight incubation, approximately 50% of OP27 treated with TSA died in contrast to nearly no cells for minus TSA conditions. After 5 days of differentiation, the normal time course of differentiation for OP27, all of the cells treated with TSA died.

Many of the HDAC inhibition experiments do not use neuronal cell lines. Neuronal cell lines are often more sensitive to culture conditions as opposed to other mammalian cell lines (Jane Roskams, personal communication), so in an attempt to decrease cell death the TSA concentration was decreased to 10 nm. In addition, TSA was added immediately prior to cells being switched to 39°C. After 6 hours *in vitro*, OP27 did not appear to be adversely affected. After 24 hours, the majority of OP27 (~85%) treated with TSA died but the remaining cells looked very neuronal in nature, with long bipolar processes. This morphology is not normally achieved until 5 days *in vitro* (DIV). However by 5 DIV, all of the cells treated with TSA died.

TSA also causes cell cycle arrest (Salminen *et al.*, 1998; Inokoshi *et al.*, 1999). To eliminate this factor as a contributor to cell death, OP27 were synchronized in metaphase with colcemid for 48 hours. TSA concentration was also decreased to 2.5 nm. Following colcemid treatment, colcemid containing media was replaced with differentiation media and allowed to settle at 33°C before being switched to 39°C; TSA was added at this time. As previously observed, the majority of cells treated with TSA died but appeared to be dying at a slower rate. By 2 DIV, ~85% of cells treated with TSA died. After 4 DIV the cells that remained were large and flat in morphology, reminiscent of progenitor-like cells (Fig 27A) and did not appear neuronal at all, in contrast to cells that were not treated with TSA (Fig 27B), which appeared bipolar in morphology with processes.

Based on these initial HDAC inhibition experiments, it appears that TSA affects the survival and possibly differentiation of OP27. For future experiments a paradigm to test is to differentiate OP6 and OP27 under normal differentiation conditions for various

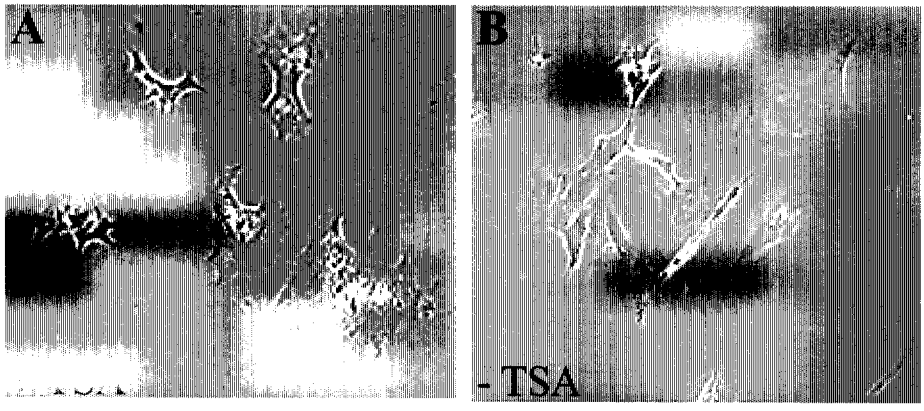

Figure 27: Trichostatin A treatment of differentiating OP27. OP27 were arrested at 33°C in metaphase with colcemid treatment. Cells were released from metaphase under differentiation conditions in the (A) presence or (B) absence of 2.5 nm TSA. OP27 were differentiated for 4 DIV. Cells treated with TSA had a progenitor-like morphology of large, flattened cells with no processes. In contrast cells that were not treated with TSA differentiated into process-bearing cells that were neuronal in morphology. Magnification 20x.

timepoints before TSA treatment, and shortening the length of TSA treatment to determine if there is a balance between time and length of TSA treatment, cell survival and differentiation before harvesting cells for further analysis.

Summary-OP6 and OP27 are appropriate *in vitro* models in which to study MBD2 function. Both lines express MBD2 and MBD3 before and after differentiation by western blotting. Using immunocytochemistry, both MBD2 and MBD3 have been localized to the nucleus of OP6 and OP27 and are expressed in a differentiation dependent manner consistent with observations *in vivo*. Both OP6 and OP27 express other MBD family members and chromatin modification proteins including MBD3, MeCP2, HDAC1, HDAC2 and mSin3A. Pilot immunoprecipitation experiments have shown that MBD2 interacts with HDAC2. Initial HDAC inhibition experiments show that TSA affects the survival and possibly differentiation of OP27.

Chapter 4: Discussion

The *in situ* hybridization and immunohistochemistry together demonstrate that MBD2 is dynamically expressed in the mouse OE during development. Although MBD2 mRNA is expressed in proliferating ORN progenitors at E15, there is a brief lag period before MBD2 protein is expressed at E17 in the nucleus of IRNs and sub-populations of mORNs in a bilaterally symmetrical manner. At P1, MBD2 mRNA is expressed by ORNs throughout the OE. The protein distribution is similar, with slightly higher MBD2 expression in mORNs. In the adult, MBD2 is expressed in subpopulations of ORNs throughout the OE. MBD3 is also expressed by ORNs in the OE but expression is not seen until later in development at P1 in mORNS, where expression appears to be maintained.

Although MBD2 is expressed from E17 onwards the expression pattern is not uniform, rather it is zonal in nature. Briefly, at E17 sub-populations of IRNs and mORNs express MBD2 in the OE in the anterior-posterior and dorsal-ventral axes of the primary olfactory neuraxis. Anterior coronal sections express MBD2 at detectable levels in regions of the OE, whereas posterior coronal sections from the same animal do not appear to express nuclear MBD2. This zonal expression pattern is also observed at P1; only sub-populations of mORNs appear to up-regulate MBD2 expression. Due to the zonal nature of MBD2 expression and the fact that it is only expressed in a sub-population of ORNs embryonically, it is possible that at E15 a very small sub-population of ORNs express MBD2 in a particular coronal section of the OE. The NCAM positive control, which stains the surface of ORN cell bodies and axons, and OMP, which stains mORN cell

bodies and axons, and the secondary-alone negative controls show that the MBD2 nuclear signal is specific with minimal background staining.

Early in olfactory neuronal development, ORNs are capable of generating action potentials in response to odorant ligands. Single cell patch clamp experiments have shown that at E16 in rat (equivalent to E13 in mouse), ORNs can respond to all classes of odorant ligands. The appearance of MBD2 mRNA at E15 and subsequently, protein in the nucleus of ORNs at E17 roughly coincides with selective odorant discrimination *in vivo*, which is thought to occur at approximately E18 to E19 (equivalent to E16 in mouse). At E17, ORN axons have made contact with the OB and are capable of odorant discrimination (Farbman, 1991).

ORNs have the ability to distinguish between odorant ligands due to the diversity of OR genes, estimated to be 500-1000 in number. The OR gene family is the largest in the genome and is organized into gene clusters. ORs are expressed in 4 distinct spatial zones along the anterior-posterior and dorsal-ventral axes of the primary olfactory neuraxis; it is thought that the distribution of ORs in the anterior-posterior axis acts as an initial sorting of olfactory information. The mechanism controlling selective OR expression and expression within a given zone is not known. It is has been speculated that clustering of OR genes may be important in how they are regulated (Chess *et al.*, 1994; Sullivan *et al.*, 1996; Malnic *et al.*, 1999; Mombaerts, 1999; Strotmann *et al.*, 1999; Buck, 2000).

The developmental timepoint at which MBD2 expression first appears, its zonal and bilaterally symmetrical expression pattern, the clustering of OR genes in the genome and presence of CpG di-nucleotides adjacent to OR genes or gene clusters as potential

methylation sites raise the possibility that MBD2 mediated transcriptional repression may be involved in silencing OR clusters. It has been previously suggested that when an ORN chooses to express an OR, its choice is initially limited to a single OR gene cluster and that selection from that cluster is stochastic in nature (Malnic *et al.*, 1999). It is possible that early in olfactory neuronal development in the absence of MBD2, ORNs have the ability to express all ORs and can therefore respond to all odorant ligand classes, as observed in single cell patch clamp experiments in rat (Farbman, 1991). As ORNs differentiate and mature in the OE, tissue specific signals that are regional in nature may influence gene expression and acquisition of a mature ORN phenotype. Thus, ORNs in different regions of the OE and at slightly different stages of maturation would receive slightly different signals. These signals, together with the appearance of MBD2 expression in ORNs, may serve to turn off entire OR gene clusters. Therefore, ORNs are limited to stochastically choose an OR to express from a single or limited number of OR gene clusters. ORNs in different regions of the OE that have different signals would be limited to choose from different OR gene clusters.

The dynamic pattern of MBD2 expression in the developing mouse olfactory system suggests that MBD2 is involved in controlling an aspect of gene expression during olfactory neuronal development. To further determine the role of MBD2 in the olfactory system, we have studied the olfactory system of MBD2-/- mice. Hendrich *et al.* have generated MBD2-/- animals, which are viable and fertile. Intercrosses between MBD3+/- and MBD2-/- animals support the hypothesis that MBD2 and MBD3 are protein interactors. Crossing these animals produced significantly less MBD3+/- pups as compared to crossing onto a MBD2+/+ background, suggesting that MBD3 viability is

reduced when MBD2 is absent. Behavioral analysis shows that MBD2-/- animals may display abnormalities in maternal behaviour; pups born to MBD2-/- mothers were smaller than in reciprocal crosses and postpartum MBD2-/- mothers were slower to retrieve their newborn pups to their nests than wild-type controls (Hendrich *et al.*, 2001). These behavioral observations showing olfactory defects in MBD2-/- animals further support our results that MBD2-/- is involved in olfactory neuronal development.

MBD2-/- neonates display a number of quantitative differences in the primary olfactory neuraxis when compared to MBD2+/+ neonates for OMP and NCAM staining. MBD2-/- neonates have more total ORNs per mm OE for NCAM staining ($p<0.05$), low density OMP staining ($p<0.05$) and high density OMP staining, although the latter values are not statistically significant ($p>0.05$). There is also a trend towards a greater number of axon bundles in MBD2-/- neonates, which is statistically significant at the MOE region ($p<0.05$) for OMP staining and MOB region ($p<0.05$) for NCAM staining. Axon bundle sizes were significantly different between the animals; both extremely large and extremely small axon bundles were observed. To get a better comparison of these two extremes, the ten largest and ten smallest axon bundles were also compared. MBD2-/- neonates had on significantly larger axon bundles for OMP ($p<0.05$) and NCAM staining ($p<0.001$) that were undefined and wispy in nature, but significantly smaller axon bundles for NCAM staining ($p<0.05$), as well. In some instances, axons in the lamina propria of MBD2-/- neonates looked astray.

To compare the IRN and mORN populations, double immunofluorescence was used to directly compare the relationship between IRNs and mORNs. The expression patterns for NCAM and GAP-43 in the epithelium appeared normal in MBD2-/-;

however, differences in OMP staining were apparent. The OMP staining of ORN cell bodies was not uniform in the epithelium, instead OMP positive neurons were staggered along the apical surface of the OE. In addition, axon bundles in MBD2-/- did not appear to express OMP at a level comparable to control animals; with the majority of axon bundles only expressing the general neuronal marker NCAM and the immature neuronal marker GAP-43. This observation is consistent along the anterior-posterior axis of the OE.

Quantitative and qualitative differences were also found in the OB. MBD2-/- neonates had a greater number of posterior glomeruli for both OMP ($p<0.05$) and NCAM staining ($p<0.05$). This may be due to the larger cross-section of OB on posterior MOB sections as compared to FOB sections. MBD2-/- neonates also had extremely large and extremely small glomeruli; the ten largest and ten smallest glomeruli were compared between the two animals. MBD2-/- glomeruli were larger in size when compared to MBD2+/+ glomeruli but only reached statistically significant values for NCAM staining ($p<0.05$). However differences for the smallest glomeruli were observed between OMP and NCAM staining. MBD2-/- neonates had slightly smaller OMP positive glomeruli but significantly larger NCAM positive glomeruli than MBD2+/+ neonates ($p<0.05$). MBD2-/- neonates appeared to have a thicker ONL around the OB; however this was not quantified because of limited tissue and because ONL measurements will be highly sensitive to skewed sections. Immunofluorescence showed that the ONL in MBD2-/- co-localized NCAM and OMP expression, in contrast to the lack of co-localization seen in axon bundles. However, the ONL of MBD2-/- neonates appeared to express NCAM at a

much higher level than OMP. In addition, their glomeruli in the OB appeared to only express OMP.

The immunofluorescence data comparing the relationship between IRNs and mORNs suggests that ORNs may be failing to make proper synapses at the OB in MBD2-/-, or that this process is developmentally delayed. Although the role of OMP is not currently known, it is widely accepted that acquisition of OMP expression depends on a number of events, which include: 1) OR expression, 2) electrophysiological competence, 3) physical contact with the OB in the form of a synapse and 4) a retrograde signal from the OB to ORN cell body to direct OMP expression. The observation that the majority of axon bundles in MBD2-/- neonates are OMP negative and the majority of glomeruli in the OB are OMP positive initially seems counterintuitive. The lack of OMP positive axon bundles, which predominantly express NCAM and GAP-43, suggests that the majority of ORNs in the OE have not made synapses with the OB. However, the fact that there are OMP positive ORNs and that small parts of some axon bundles express OMP demonstrate that these ORNs have contacted the OB. It is likely that these OMP positive ORNs have formed the observed OMP positive glomeruli. Many of the glomeruli in MBD2-/- neonates are large and undefined in appearance possibly because many ORNs have not yet synapsed with the OB. The greater number of ORNs observed in MBD2-/- may be due to increased cellular differentiation because the correct synapses are not being made and therefore, there are less OMP positive mORNs to negatively regulate differentiation of progenitor cells in the basal OE. The majority of excess ORNs in MBD2-/- may be immature and therefore expressing NCAM and GAP-43, which may dilute out the OMP signal of the mORNs, as observed for immunofluorescence. The

ORNs that have made weak synapses with the OB may be waiting for other ORNs expressing similar ORs to synapse with the OB, before synapses in the glomeruli are strengthened and pruned back. Lastly, since the role of OMP *in vivo* is not known, it is not yet possible to determine if the abnormal OMP staining observed in MBD2-/- neonates is a direct result of functional abnormalities in ORN maturation as opposed to abnormal acquisition of OMP expression or distribution.

The expression of ORs in the OE is zonal in nature; ORs are only expressed in one of four zones in the OE. These zones lie in the anterior-posterior and dorsal-ventral axes of the olfactory system. The location of the phenotypic differences observed in the MBD2-/- neonates can be correlated with these zones. As mentioned, regions of extremely high and low density OMP staining were observed in both MBD2-/- and MBD2+/+; the high density OMP staining was mainly localized to regions of zone 1 and 2 for MBD2-/- and MBD2+/+ but low density OMP staining did not appear to be localized to regions of any OR expression zones. In both the MBD2-/- and MBD2+/+ neonates, large axon bundles are located in zone 1, which includes the septum and roof; however the large axon bundles in MBD2+/+ neonates are limited to the septum only. In contrast the small axon bundles in MBD2-/- neonates can be matched to regions of both zones 2 and 3, whereas MBD2+/+ neonates are located in regions of zone 2 only. There did not appear to be any relationship between high/low density OMP staining and the size of axon bundles.

The OR expression zones can also be correlated with the main projections made to the OB. ORNs within each zone project their axons to glomeruli in defined regions of the OB; this is referred to as the zone-to-zone principle. OR expression zone 1 is located

in the dorso-medial region of the OE and ORNs within this zone project their axons to the corresponding dorso-medial region of the OB. Likewise ORNs in OR expression zone 4, which is the most ventro-lateral, project their axons to the ventro-lateral region of the OB (Yoshihara and Mori, 1997). Further work with specific ORs expressed in zone 1 and zone 4 has demonstrated that ORNs project their axons to glomeruli in the dorsal region and medial and lateral regions of the OB, respectively (Ressler *et al.*, 1994; Vassar *et al.*, 1994; Tsuboi *et al.*, 1999). The projections from zone 2 and 3 to the OB have yet to be clearly defined.

In MBD2-/- neonates, the largest glomeruli were located on the lateral sides, midline and ventral regions of the OB and the smallest were located on the dorso-lateral region of the OB; these correspond to projections from zone 4 and parts of zone 1, respectively. In MBD2+/+ neonates, the largest glomeruli were located on the lateral sides, ventral and ventro-lateral regions of the OB and the smallest were located along the midline and ventral region of the OB, which corresponds to zones 4.

Based on this zonal analysis there currently does not appear to be any correlation between the zonal location of the smallest and largest axon bundles and the zonal location of the smallest and largest glomeruli in the OB. Further experiments using OR *in situ* hybridization in MBD2-/- neonates with OR RNA probes expressed in different zones of the OE will clarify a number of issues regarding MBD2 function including: 1) whether ORs are expressed in the correct zones of the OE, 2) if ORNs are making the correct projections to glomeruli in the OB, 3) if the zone-to-zone principle is maintained and 4) if there is a correlation between the zonal location of the smallest/largest axon bundles and smallest/largest glomeruli.

The MBD2 -/- phenotype corresponds with a phenotype expected in the absence of a transcriptional repressor gene, in that more genes may be expressed. This is likely due to a more relaxed chromatin structure in the absence of the MBD2 repressor complex that is more conducive to transcription. The additional misexpressed genes would lead to the abnormal production of more protein and potentially an increase in cell size. This may be direct, through the expression of structural proteins, or indirect through the expression of proteins that contribute to the balance between cell death and survival or cell proliferation and differentiation. Further experiments need to be done to identify the genes that are being silenced by MBD and are contributing to the knockout phenotype.

A number of plausible scenarios can explain the knockout phenotype observed and are discussed as follows. In the first scenario, MBD2 may be involved in silencing OR clusters as previously discussed. This would initially lead to the misexpression of ORs by ORNs during development and could then result in incorrect development of the primary olfactory neuraxis and improper formation of OR expression zones. In such a scenario it is possible that ORNs, which are MBD2-dependent, that are expressing incorrect ORs in particular zones of the OE would be continuously produced as they are trying to find the proper connections in the OB. A subset of ORNs may be MBD2-independent and would account for the OMP positive ORNs and glomeruli observed in the MBD2-/- neonates. This MBD2-independent population would likely undergo differentiation and maturation earlier in development, prior to MBD2-dependent developmental events in neighboring ORNs. The increased number of ORNs would be OMP negative since they have not synapsed with the OB and would therefore produce more and/or larger axon bundles. This would also support the observation of wispy,

undefined axon bundles and glomeruli and the presence of stray axons in the lamina propria of MBD2 -/- neonates, as axons are having difficulties coalescing together into axon bundles and synapsing with the OB. The MBD2-independent population that have made weak synapses with the OB in the form of undefined, OMP positive glomeruli may be awaiting similar ORs to synapse with the OB before the glomeruli are strengthened and pruned back. A thicker olfactory nerve layer and more glomeruli in the OB could also be a consequence of an increased number of ORNs.

In the second scenario, MBD2 may control the expression of genes required by mORNs. MBD2 may control the expression of axon guidance factors, which may be required in a population of developing ORNs. In the absence of the correct guidance cues, MBD2-dependent ORNs would not be able to form proper axon bundles in the lamina propria or project their axons up to the OB to form glomeruli. Likewise, MBD2 may control the expression of factors such as adhesion molecules that promote axon-axon interactions or axon-glial interactions, both of which would promote the formation of axon bundles and/or glomeruli. Both of these scenarios can account for the stray axons and wispy, undefined axon bundles observed in the lamina propria of MBD2-/- neonates.

In the third scenario, MBD2 may control the expression of genes that are important in controlling developmental switches in the ORN lineage. This could potentially occur at two different stages in the ORN lineage: 1) as progenitor cells in the basal OE are making the decision to proliferate or differentiate, or 2) as IRNs are differentiating into mORNs. Abnormal regulation of either of these switches can account for some of the observed differences in MBD2-/- neonates such as an increased number of ORNs, the absence of OMP expression in the majority of axon bundles, and

predominantly NCAM and GAP-43 positive axon bundles. These events may occur at different times in different regions of the OE, as sub-populations of ORNs are known to proliferate and differentiate at different times during development *in vivo*, and could also result in incorrect timing of differentiation or maturation events between neighboring ORN populations. Again sub-populations of ORNs that undergo differentiation and maturation earlier in development may be MBD2-independent.

In an attempt to address issues regarding ORN development and in particular MBD2 function in ORN development two cell lines, OP27 and OP6, were generated from the embryonic mouse olfactory placode that represent two distinct and slightly staggered stages of olfactory neuron development. At the permissive temperature at which the cells divide OP6 and OP27 differ in morphology; however after differentiation both cells achieve the same morphology and antigenic profile.

Retinoic acid has been demonstrated to play a role in olfactory neuronal differentiation *in vitro* in OP6 and OP27. There has been evidence to suggest that RA has an effect on immature neurons and precursor cells *in vitro* and based on observations *in vivo*. Usmann *et al.* have shown in embryonic carcinoma cell lines that RA induces the expression of neuron specific molecules associated with neurite outgrowth and axon guidance. In spinal cord and dorsal root ganglion explants, RA has been shown to promote neurite outgrowth and has an effect on axon outgrowth and direction in optic nerve and hindbrain *in vivo*. It has been suggested that RA may contribute to the differentiation and neurite outgrowth of ORNs (Whitesides *et al.*, 1998). Both OP6 and OP27 require RA to enhance differentiation and to establish a mature ORN phenotype.

Based on expression profile, OP27 can be placed at the transition from transit amplifier to immediate neuronal precursor. OP27 expresses immature neuronal markers such as Pax-6 while dividing at the permissive temperature and undergoes at least an additional round of cell division following inactivation of the immortalizing transgene at the non-permissive temperature. During differentiation in the presence of retinoic acid, OP27 first differentiates into cells that resemble immature olfactory receptor neurons (3-5 DIV), similar in morphology to OP6 at the permissive temperature, before achieving a mature, bipolar ORN phenotype (7-10 DIV). In contrast, at the permissive temperature OP6 resembles an IRN and when placed under differentiation conditions at the non-permissive temperature, they do not undergo an additional round of cell division. Instead, OP6 immediately differentiates in the presence of retinoic acid into cells resembling mature, bipolar ORNs.

Both cell lines express GAP-43, NST, NCAM and PLC-γ2; however, OP27 expresses GAP-43 and NST at higher levels in comparison to OP6. GAP-43 and NST expression are both down-regulated in mature ORNs *in vivo* (Farbman, 1992; Roskams *et al.*, 1996). Based on expression profile, behavior and morphology OP27 is at a stage of development earlier than OP6 in the ORN lineage. As OP6 and OP27 differentiate and become fully mature ORNs, they acquire OMP expression. Both OP6 and OP27 express the olfactory signal transduction molecules, Golf and ACIII. Upon odorant binding, ORs are activated and a signal transduction cascade is initiated, which is tranduced by Golf to ACIII. The expression of Golf and ACIII in OP6 and OP27 demonstrate that both lines contain the necessary molecules to transduce the odorant signal and regulate olfactory cyclic nucleotide gated channels. This suggests that these cells are functionally

active and capable of generating action potentials to the OB in response to odorant binding.

In vivo, neurotrophin signaling plays an important role in the balance between proliferation and differentiation of ORN progenitors (Roskams *et al.*, 1996). OP6 and OP27 express TrkB, TrkC, p75 and the neuronal marker NCAM in a differentiation dependent manner. As ORNs differentiate, there is a shift from the full-length kinase active form to the truncated inactive form in Trk B and Trk C. The full-length form promotes differentiation as opposed to the truncated form, which promotes survival.

OP6 and OP27 are valid *in vitro* models that represent two successive stages in the olfactory neuronal lineage. They are valuable models in which to study a number of events in olfactory neuronal development and in particular, MBD2 function. OP6 and OP27 display nuclear expression of MBD2 and MBD3. MBD2 is detected at low levels in a very small proportion of OP27 cells at the permissive temperature. At this stage, OP27 is the least mature in the ORN lineage. As OP27 differentiate into IRN-like cells, resembling OP6 at the permissive temperature, MBD2 is expressed in both lines in a sub-population of cells at detectable levels. As OP6 differentiates into mature ORN-like cells, MBD2 is up-regulated in the nucleus. As seen *in vivo*, MBD2 is expressed in IRNs and is up-regulated in more mature ORNs. In contrast, MBD3 is expressed at very low levels in OP27 at the permissive temperature, following differentiation and in OP6 at the permissive temperature. MBD3 is not detected until OP6 differentiates into mature, ORN-like cells. MBD3 is expressed at a high level, as seen *in vivo*, in the most mature, bipolar ORN-like cells. Thus, OP27 and OP6 express MBD2 and MBD3 in a manner similar to what has been observed *in vivo*.

Two mechanisms of transcriptional repression as a result of DNA methylation have been proposed and there has been evidence to support both mechanisms. In the direct mechanism, DNA methylation prevents transcription by excluding transcription factors, the majority of which require contact with cytosine residues. In the indirect mechanism, MBDs link DNA methylation with transcriptional repression by interacting with chromatin modification proteins, thus altering chromatin structure.

In support of the direct mechanism, the majority of transcription factors are known to require contact with cytosine residues. These interactions are prevented by methylation; however, much of the current data suggests that the indirect mechanism may be more common. Transcription factors have been identified that have the capability of binding to methylated DNA. Furthermore, densely methylated regions can be transcriptionally active in the absence of MBDs and/or chromatin modification proteins suggesting that methylation status alone has a minor role in direct repression. This and the observation that DNA methylation can act at a distance and repression occurs after chromatin assembly support an indirect mechanism. Protein complexes have been identified that include MBDs and chromatin modification proteins that are capable of binding methylated DNA. The observation that highly methylated DNA can be transcribed at near normal rates in the absence of these complexes suggests that the indirect mechanism is more common (Hendrich and Bird, 1998; Bird and Wolffe, 1999; Hendrich *et al.*, 1999; Wakefield *et al.*, 1999; Snape, 2000).

In HeLa extracts, MBD2 has been found to belong to the MeCP1 repressor complex that includes HDAC1, HDAC2, RbAp46 and RbAp48 (Ng *et al.*, 1999). OP6 and OP27 have been demonstrated to express the chromatin modification proteins

HDAC1 and HDAC2 at the permissive temperature and following differentiation; mSin3A is also expressed by OP6 in both conditions. In contrast, mSin3A is only expressed in OP27 at the permissive temperature; it is not expressed in OP27 following differentiation.

It has been suggested that MBD2 interacts with MBD3 and recruits the MBD3/NuRD repressor complex to methylated DNA. Experiments by Hendrich *et al.* further support this. Intercrosses of MBD3+/- and MBD2-/- animals produce less MBD3 +/- offspring, when compared to crossing onto a MBD2+/+ background and suggests that MBD3 viability is reduced in the absence of MBD2 (Wolffe and Bird, 1999; Hendrich *et al.*, 2001). OP6 and OP27 also express the MBD protein family members MBD3 and MeCP2.

The expression of chromatin modification proteins and other MBD family members, both of which are potential protein interactors implicates an indirect mechanism of MBD2 mediated transcriptional repression *in vitro* in OP6 and OP27 and *in vivo* in the ORN lineage. Further work is currently being done to determine the extent of protein interactions in an attempt to clarify the mechanism of MBD2 mediated silencing. Previous work to identify MBD protein interactors have utilized pull down assays in which recombinant proteins have been transfected in to cell lines. OP6 and OP27 express these proteins endogenously. Using immunoprecipitation in these lines will permit the identification of endogenous protein interactors and potentially novel protein interactors.

Preliminary experiments to determine MBD2 function *in vitro* using the HDAC inhibitor TSA have been performed on the OP27 cell line at 33°C. TSA has been

successfully used to inhibit HDACs in the concentration range of 3-30 nm (Jones *et al.*, 1998); concentrations in the μm range are known to cause apoptosis (Salminen *et al.*, 1998). Based on the initial HDAC inhibition experiments, it appears the TSA affects cell survival and differentiation. TSA causes OP27 cells to die on a much faster time scale than for the normal differentiation paradigm. The cells that remain following the normal time course of differentiation (3-5 DIV) do not achieve a neuronal morphology; instead cells were large and flat, reminiscent of immature progenitor-like cells.

These initial HDAC inhibition experiments demonstrate a role for HDACs in the survival and differentiation of OP27. In conjunction with the idea that MBD2 silences genes not required to achieve a mature ORN phenotype, perhaps in silencing OR clusters, inhibiting the indirect mechanism of transcriptional repression which acts through HDACs will affect survival and differentiation. Preventing OP27 cells from differentiating and achieving a mature ORN phenotype and expression of mature ORN genes with TSA causes the cells die. Similar events occur in the normal developing nervous system; cells that fail to achieve the proper cell fate at the correct time and place die. Whether the HDAC inhibition observations are directly due to inhibition of MBD2 mediated gene silencing as opposed to general HDAC function in other cellular processes will have to be determined.

In this thesis I have demonstrated that MBD2 is dynamically expressed by ORNs in the OE and that it is essential for the proper formation of the primary olfactory neuraxis. In the absence of MBD2 a number of abnormalities are present in the primary olfactory neuraxis. Two conditionally immortalized temperature sensitive cell lines generated from the embryonic mouse olfactory placode, OP6 and OP27, were shown to

be olfactory neuron-like in nature and appropriate *in vitro* models of ORN development, based on antigenic profile, morphology and behavior *in vitro*. Both also express MBD2 and MBD3 in a pattern consistent with observations *in vivo*. Thus, OP6 and OP27 are appropriate *in vitro* models in which to study MBD2 function. Together, the *in vivo* and *in vitro* data in this thesis demonstrate that MBD2 is important in regulating gene expression during olfactory neuronal development.

Conclusions

Previously, we have found that MBD2 is highly up-regulated in ORNs following bulbectomy in the mouse. Using *in situ* hybridization and immunohistochemistry, MBD2 was been shown to be dynamically expressed in a zonal fashion in the anterior-posterior and dorsal-ventral axes of the OE during development. The highly homologous protein MBD3 is also expressed by ORNs in the OE; however, expression is not seen until later in development at P1 in mORNs. Consistent with the idea that MBD2 is an important mechanism of transcriptional repression in olfactory neuronal development, MBD2-/- neonates display a number of qualitative and quantitative differences in the primary olfactory neuraxis including: 1) a greater number of ORNs per mm OE, 2) a trend towards a greater number of axon bundles per mm OE, 3) larger anterior axon bundles, 4) extreme axon bundle areas, 5) a greater number of posterior glomeruli per OB, 6) a thicker olfactory nerve layer and 6) larger glomeruli.

Two cell lines generated from the embryonic mouse olfactory placode, OP27 and OP6 were demonstrated to be olfactory neuron-like in nature based on antigenic profile, morphology and behavior *in vitro* and are appropriate models of ORN development. OP27 can be placed at the transition from transit amplifier to immediate neuronal precursor whereas OP6 can be placed at the IRN stage. OP6 and OP27 express MBD2 and MBD3 in a differentiation dependent manner consistent with observations *in vivo*. Both lines also endogenously express MeCP2 and the chromatin modification proteins HDAC1, HDAC2 and mSin3A, all potential protein interactors of MBD2.

The mechanism controlling selective OR expression and expression within a given zone of the OE is currently not known. The *in vivo* and *in vitro* results, and in particular the clustering and potential methylation sites of OR genes and the developmental timepoint at which MBD2 expression first appears raises the interesting possibility that MBD2 mediated transcriptional repression may be involved in silencing OR clusters. It has been previously suggested that when an ORN chooses to express an OR, its choice is initially limited to a single or limited number of OR gene clusters and that selection from that cluster is stochastic in nature (Malnic *et al.*, 1999). It is possible that early in olfactory neuronal development before MBD2 is expressed, ORNs have the ability to express all ORs and can therefore respond to all odorant ligand classes. As ORNs differentiate and mature in the OE, tissue specific signals that are regional in nature may influence gene expression and acquisition of a mature ORN phenotype. Thus, ORNs in different regions of the OE and at slightly different stages of maturation would receive slightly different signals. These signals, together with the appearance of MBD2 expression in ORNs, may serve to turn off entire OR gene clusters. Therefore, ORNs are limited to stochastically choose an OR to express from a single or limited number of OR gene clusters. ORNs in different regions of the OE would be limited to choose from different OR gene clusters. Further experiments are currently being done to: 1) determine MBD2 biochemistry, 2) inhibit MBD2 repression with TSA and 5'AZA-CdR in order to understand the mechanism of MBD2 mediated silencing, 3) to identify the genes that are being silenced by MBD2 and 4) to determine if ORs are expressed in the correct zones.

References

Ahringer J (2000) NuRD and SIN3 histone deacetylase complexes in development. Trends in Genetics 16(8): 351-356.

Amir RE, Van den Veyver V, Wan M, Tran CQ, Francke U, Zoghbi HY (1999) Rett syndrome is caused by mutations in X-linked MECP2, encoding methyl-CpG binding protein 2. Nature Genetics 23: 185-188.

Ashraf SI, Ip YT (1998) Transcriptional control: Repression by local chromatin modification. Current Biology 8: R683-R686.

Astic L, Peller-Monnin V, Godinot F (1998) Spatio-temporal patterns of ensheathing cell differentiation in the rat olfactory system, during development. Neuroscience 84(1): 295-307.

Ballestar E, Yusufzai TM, Wolffe A (2000) Effects of Rett syndrome mutations of the methyl CpG binding domain of the transcriptional repressor MeCP2 on selectivity for association with methylated DNA. Biochemistry 29: 7100-7106.

Barber RD, Jaworsky DE, Yau KW, Ronnett GV (2000) Isolation of *in vitro* differentiation of conditionally immortalized murine olfactory receptor neurons. Journal of Neuroscience 20(10): 3695-3704.

Beatus P, Lendahl U (1998) Notch and neurogenesis. Journal of Neuroscience Research 54: 125-136.

Begley CG, Lipkowitz S, Gobel V, Mahon KA, Bertness V, Green AR, Gough NM, Kirsch IR (1992) Molecular characterization of NSCL, a gene encoding a helix loop-helix protein expressed in the developing nervous system. Proceedings of the National Academy Sciences 89: 38-42.

Bhattacharya SK, Ramchandani S, Cervoni NC, Szyf M (1999) A mammalian protein with specific demethylase activity for mCpG DNA. Nature 397: 579-583.

Bird AP, Wolffe AP (1999) Methylation-induced repression-belts, braces, and chromatin. Cell 99: 451-454.

Boolay S (1998) Immortalisation, characterisation and differentiation of temperature sensitive cell lines from the olfactory neuroepithelium.

Bovenzi V, Momparler RL (2000) Quantitation of inhibition of DNA methylation of the retinoic acid receptor β gene by 5-Aza-2'-deoxycytidine in tumor cells using a single-nucleotide primer extension assay. Analytical Biochemistry 281: 55-61.

Brock GJR, Charlton J, Bird A (1999) Densely methylated sequences that are preferentially localized at telomere-proximal regions of human chromosomes. Gene 240: 269-277.

Brunjes PC, Borror MJ (1983) Unilateral odor deprivation: differential effects due to time of treatment. Brain Research Bulletins 11(5):501-3.

Buck L, Axel R (1991) A novel multigene family may encode odorant receptors: a molecular basis for odorant recognition. Cell 65(1): 175-187.

Buck L (2000) The molecular architecture of odor and pheromone sensing in mammals. Cell 100: 611-618.

Calof AL, Chikaraishi DM (1989) Analysis of neurogenesis in a mammalian neuroepithelium: Proliferation and differentiation of an olfactory neuron precursor in vitro. Neuron 3: 115-127.

Calof AL, Mumm JS, Rim PC, Shou J (1998) The neuronal stem cell of the olfactory epithelium. Journal of Neurobiology 36(2): 190-205.

Cau E, Gradwohl G, Fode C, Guillemot F (1997) Mash1 activates a cascade of bHLH regulators in olfactory neuron progenitors. Development 124: 1611-1621.

Chess A, Simon I, Cedar H, Axel R (1994) Allelic inactivation regulates olfactory receptor gene expression. Cell 78: 823-834.

Chen RZ, Akbarian S, Tudor M, Jaenisch R (2001) Deficiency of methyl-CpG binding protein 2 in CNS neurons results in a Rett-like phenotype in mice. Nature Genetics 27(3): 327-331.

Cross SH, Meehan RR, Nan X, Bird A (1997) A component of the transcriptional repressor MeCP1 shares a motif with DNA methyltransferase and HRX proteins. Nature Genetics 16: 256-259.

Dattani MT, Martinez-Barbera JP, Thomas PQ, Brickman JM, Gupta R, Martensson IL, Toresson H, Fox M, Wales JKH, Hindmarsh PC, Krauss S, Beddington RSP, Robinson, ICAF (1998) Mutations in the homeobox gene HESX1/Hesx1 associated with septo-optic dysplasia in human and mouse. Nature Genetics 19: 125-133.

Dattani MT, Martinez-Barbera JP, Thomas PQ, Brickman JM, Gupta R, Wales JKH, Hindmarsh PC, Beddington RSP, Robinson, ICAF (1999) HESX1: a novel gene implicated in a familial form of septo-optic dysplasia. Acta Paediatricia. Supplement 88: 49-54.

Davis JA, Reed RR (1996) Role of Olf-1 and Pax-6 transcription factors in

neurodevelopment. Journal of Neuroscience 16(16): 5082-5094.

Doucette R (1990) Glial influences on axonal growth in the primary olfactory system. Glia 3(6):433-49.

Doucette R (1991) PNS-CNS transitional zone of the first cranial nerve. Journal of Comparative Neurology 312(3):451-66.

Ebrahimi FAW, Chess A (1998) Olfactory G proteins: Simple and complex signal transduction. Current Biology 8: R431-R433.

Farbman AI, Margolis FL (1980) Olfactory marker protein ontogeny: Immunohistochemical localization. Developmental Biology 74: 205-215.

Farbman AI (1991) Developmental neurobiology of the olfactory system. Smell and Taste in Health and Disease. Raven Press.

Farbman AI (1992) Cell biology of olfaction. Cambridge University Press.

Fujita N, Takebayashi S, Okumura K, Kudo S, Chiba T, Saya H, Nakao M (1999) Methylation mediated transcriptional silencing in euchromatin by methyl-CpG binding protein MBD1 isoforms. Molecular and Cellular Biology 19(9): 6415 6426.

Fujita N, Shimotake N, Ohki I, Chiba T, Saya H, Shirakawa M, Nakao M (2000) Mechanism of transcriptional regulation by methyl-CpG binding protein MBD1. Molecular and Cellular Biology 20(14): 5107-5118.

Free A, Wakefield RID, Smith BO, Dryden DTF, Barlow PN, Bird AP (2001) DNA recognition by the methyl-CpG binding domain of MeCP2. Journal of Biological Chemistry 276: 3353-3360.

Gradwohl G, Fode C, Guillemot F (1996) Restricted expression of a novel murine atonal related bHLH protein in undifferentiated neural precursors. Developmental Biology 180: 227-241.

Graziadei PPC (1973) Cell dynamics in the olfactory mucosa. Tissue Cell 5: 113-131.

Graziadei PPC, Monti-Graziadei GA (1978) The olfactory system: a model for the study of neurogenesis and axon regeneration in mammals. In: CW Cotman (Ed.), Neuronal Plasticity.

Guillemot F, Lo LC, Johnson JE, Auerbach A, Anderson DJ, Joyner AL (1993) Mammalian achaete-scute homolog 1 is required for the early development of olfactory and autonomic neurons. Cell 75: 463-476.

Guillemot F (1995) Analysis of the role of basic helix-loop-helix transcription factors in the development of neural lineages in the mouse. Biology of the Cell 84(1-2): 3-6.

Guschin D, Wade PA, Kikyo N, Wolffe AP (2000) ATP-Dependent histone octamer mobilization and histone deacetylation mediated by the Mi-2 chromatin remodelling complex. Biochemistry 39: 5238-5245.

Guy J, Hendrich B, Holmes M, Martin JE, Bird AP (2001) A mouse MeCP2-null mutation causes neurological symptoms that mimic Rett syndrome. Nature Genetics 27(3): 322-326.

Hanel ML, Wevrick R (2001) Establishment and maintenance of DNA methylation patterns in mouse Ndn: implications for maintenance of imprinting genes in target genes of the imprinting center. Molecular and Cellular Biology 21(7): 2384-2392.

Hempstead JL, Morgan JI (1983) Monoclonal antibodies to the rat olfactory sustentacular cell. Brain Research 288: 289-295.

Hendrich B, Bird A (1998) Identification and characterization of a family of mammalian methyl-CpG binding proteins. Molecular and Cellular Biology 18(11): 6538-6547.

Hendrich B, Abbott C, McQueen H, Chambers D, Cross S, Bird A (1999) Genomic structure and chromosomal mapping of the murine and human *Mbd1, Mbd2, Mbd3* and *Mbd4* genes. Mammalian Genome 10: 906-912.

Hendrich B, Guy J, Ramsahoye B, Wilson VA, Bird A (2001) Closely related proteins MBD2 and MBD3 play distinctive but interacting roles in mouse development. Genes and Development 15 (6): 710-723.

Hinds JW, Hinds PL (1976) Synapse formation in the mouse olfactory bulb. Journal of Comparative Neurology 169: 15-62.

Huard JM, Youngentob SL, Goldstein BJ, Luskin MB, Schwob JE (1998) Adult olfactory epithelium contains multipotent progenitors that give rise to neurons and non neural cells. Journal Comparative Neurolology 400(4):469-86.

Illing N, Boolay S, Cheng JS, Casper D, Roskams AJ (2001) OP6 and 27 are conditionally immortalized clonal cell lines from the olfactory placode which differentiate into olfactory neurons. Journal of Neuroscience (Re-submitted).

Inokoshi J, Katagiri M, Arima S, Tanaka H, Hayashi M, Kim YB, Furumai R, Yoshida M, Horinouchi S, Omura S (1999) Neuronal differentiation of Neuro 2a cells by inhibitors of cell cycle progression, trichostatin A and butyrolactone I.

Biochemical and Biophysical Research Communications 256: 372-376.

Jan YN, Jan LY (1990) Genes required for specifying cell fates in Drosophila embryonic sensory nervous system. Trends in Neuroscience 13(12): 493-497.

Jan YN, Jan LY (1993) HLH proteins, fly neurogenesis, and vertebrate myogenesis. Cell 75: 827-830.

Jan YN, Jan LY (1994) Genetic control of cell fate specification in Drosophila peripheral nervous system. Annual Reviews in Genetics 28: 373-393.

Jones PL, Veenstra GJC, Wade PA, Vermaak D, Kass SU, Landsberger N, Strouboulis J, Wolffe AP (1998) Methylated DNA and MeCP2 recruit histone deacetylase to repress transcription. Nature Genetics 19: 187-191.

Kageyama R, Sasai Y, Akazawa C, Ishibashi M, Takebayahi K, Shimizu, C, Tomita K, Nakanishi S (1995) Regulation of mammalian neural development by helix-loop helix transcription factors. Critical Reviews in Neurobiology 9(2&3): 177-188.

Kageyama R, Ishibashi M, Takebayahi K, Tomita K (1997) bHLH transcription factors and mammalian neuronal differentiation. International Journal of Biochemistry and Cell Biology 29(12): 1389-1399.

Klambt C, Knust E, Tietze K, Campos-Ortega JA (1989) Closely related transcripts encoded by the neurogenic gene complex Enhancer of split of Drosophila melanogaster. EMBO Journal 8(1): 203-210.

Lee JE (1997) Basic helix-loop-helix genes in neural development. Current Opinion in Neurobiology 7(1): 13-20.

Lewis J (1996) Neurogenic genes and vertebrate neurogenesis. Current Opinion in Neurobiology 6: 3-10.

Lohnnes D, Mark M, Mendelsohn C, Dolle P, Dierich A, Gorry P Gansmuller A, Chambon P (1994) Function of the retinoic acid receptors (RARs) during development I. Craniofacial and skeletal abnormalities in RAR double mutants. Development 120: 2723-2748.

Lucero M (2000) Personal communication.

Luo J, Sucov HM, Bader JA, Evans RM, Giguere V (1996) Compound mutants for retinoic acid receptors (RAR) beta and RAR alpha 1 reveal developmental functions for multiple RAR beta isoforms. Mechanisms in Development 55: 33-44.

Ma Q, Chen Z, del Barco Barrantes I, Anderson DJ (1998) Neurogenin1 is essential for the determination of neuronal precursors for proximal cranial sensory ganglia. Neuron 20:469-482.

Malnic B, Hirono J, Sato T, Buck LB (1999) Combinatorial receptor codes for odors. Cell 96: 713-723.

Margolis FL, Verhaagen J, Biffo S, Huang FL, Grillo M (1991) Regulation of gene expression in the olfactory neuroepithelium: a neurogenic matrix. Progress in Brain Research 89: 97-121.

Mendelsohn C, Lohnnes D, Decimo D, Lufkin T, LeMeur M, Chambon P, Mark M (1994) Function of the retinoic acid receptors (RARs) during development II. Multiple abnormalities at various stages of organogenesis in RAR double mutants. Development 120: 2742749-2742771.

Mollard R, Viville S, Ward SJ, Decimo D, Chambon P, Dolle P (2000) Tissue-specific expression of retinoic acid receptor isoform transcripts in the mouse embryo. Mechanisms of Development 94: 223-232.

Mombaerts P (1999) Odorant receptor genes in humans. Current Opinion in Genetics and Development 9: 315-320.

Murray RC, Calof AL (1999) Neuronal regeneration: Lessons from the olfactory system. Cell and Developmental Biology 10: 421-431.

Murrell JR, Hunter DD (1999) An olfactory sensory neuron line, *Odora*, properly targets olfactory proteins and responds to odorants. Journal of Neuroscience 19(19): 8260-8270.

Nan X, Compoy FJ, Bird A (1997) MeCP2 is a transcriptional repressor with abundant binding sites in genomic chromatin. Cell 88: 471-481.

Nan X, Ng HH, Johnson CA, Laherty CD, Turner BM, Eisenman RN, Bird A (1998) Transcriptional repression by the methyl-CpG-binding protein MeCP2 involves a histone deacetylase complex. Nature 393: 386-389.

Ng HH, Zhang Y, Hendrich B, Johnson CA, Turner BM, Erdjument-Bromage H, Tempst P, Reinberg D, Bird A (1999) MBD2 is a transcriptional repressor belonging to the MeCP1 histone deacetylase complex. Nature Genetics 23: 58-66.

Nibu K, Li G, Zhang X, Rawson NE, Restrepo D, Kaga K, Lowry LD, Keane WM, Rothstein JL (1999) Olfactory neuron-specific expression of NeuroD in mouse and human nasal mucosa. Cell and Tissue Research 298: 4-5-414.

Ressler KJ, Sullivan SL, Buck LB (1994) Information coding in the olfactory system:

Evidence for a stereotyped and highly organized epitope map in the olfactory bulb. Cell 79: 1245-1255.

Roskams AJ (2001) Personal communication.

Roskams AJ, Bethel MA, Hurt KJ, Ronnett GV (1998) Sequential expression of Trks A, B and C in the regenerating olfactory neuroepithelium. Journal of Neuroscience 10(4): 1294-1307.

Roskams AJ, Cai X, Ronnett GV (1996) Expression of neuron-specific beta-III tubulin during olfactory neurogenesis in embryonic and adult rat. Neuroscience 83(1): 191-200.

Salminen A, Tapiola T, Korhonen P, Suuronen T (1998) Neuronal apoptosis induced by histone deacetylase inhibitors. Molecular Brain Research 61: 203-206.

Schwob JE, Szumowski KE, Stasky AA (1992) Olfactory sensory neurons are trophically dependant on the olfactory bulb for their prolonged survival. Journal of Neuroscience 12: 3896-3919.

Sirchia SM, Ferguson AT, Sironi E, Subramanyan S, Orlandi R, Sukumar S, Sacchi N (2000) Evidence of epigenetic changes affecting the chromatin state of the retinoic acid receptor β2 promoter in breast cancer cells. Oncogene 19: 1556-1563.

Snape A (2000) MBDs mediate methylation, deacteylation and transcriptional repression. Trends in Genetics 16(1): 20.

Strotmann J, Wanner I, Helfrich T, Beck A, Meinken C, Kubick S, Breer H (1994) Olfactory neurones expressing distinct odorant receptor subtypes are spatially segregated in the nasal neuroepithelium. Cell and Tissue Research 276: 429-438.

Strotmann J, Hoppe R, Conzelmann S, Feinstein P, Mombaerts P, Breer H (1999) Small subfamily of olfactory receptor genes: structural features, expression pattern and genomic organization. Gene 236: 281-291.

Sosinsky A, Glusman G, Lancet D (2000) The genomic structure of human olfactory receptor genes. Genomics 70(1):49-61.

Sullivan SL, Adamson MC, Ressler KJ, Kozak CA, Buck LB (1996) The chromosomal distribution of mouse odorant receptor genes. Proceedings of the National Academy of Sciences 93: 884-888.

Tsuboi A, Yoshihara S, Yamazaki N, Kasai H, Asai-Tsuboi H, Komatsu M, Serizawa S, Ishii T, Matsuda Y, Nagawa F, Sakano H (1999) Olfactory neurons expressing closely linked and homologous odorant receptor genes tend to project their

axons to neighboring glomeruli on the olfactory bulb. Journal of Neuroscience 19(19): 8409-8418.

Vassar R, Chao SK, Sitcheran R, Nunez JM, Vosshall LB, Axel R (1994) Topographic organization of sensory projections in the olfactory bulb. Cell 79: 981-991.

Verhaagen J, Oestreicher AB, Gispen WH, Margolis FL (1989) The expression of the growth associated protein B50/GAP42 in the olfactory system of neonatal and adult rats. Journal of Neuroscience 9: 683-691.

Wade PA, Gegonne A, Jones PL, Ballestar E, Aubrey F, Wolffe AP (1999) Mi-2 complex couples DNA methylation to chromatin remodelling and histone deacetylation. Nature Genetics 23: 62-66.

Wang F, Nemes A, Mendelsohn M, Axel R (1999) Odorant receptors govern the formation of a precise topographic map. Cell 93(1):47-60.

Wang SS, Tsai RYL, Reed RR (1997) The characterization of the Olf-1/EBF-like HLH transcription factor family: Implications in olfactory gene regulation and neuronal development. Journal of Neuroscience 17(11): 4149-4158.

Wakefield RID, Smith BO, Nan X, Free A, Soteriou A, Uhrin D, Bird AP, Barlow PN (1999) The solution structure of the domain from MeCP2 that binds to methylated DNA. Journal of Molecular Biology 291: 1055-1065.

Weinmaster G (1997) The ins and outs of Notch signaling. Molecular and Cellular Neuroscience 9: 91-102.

Weinmaster G (1998) Notch signaling: direct or what? Current Opinion in Genetics and Development 8: 436-442.

Willard HF, Hendrich BD (1999) Breaking the silence in Rett syndrome. Nature Genetics 23: 127-128.

Whitesides J, Hall M, Anchan R, LaMantia AS (1998) Retinoid signaling distinguishes a subpopulation of olfactory receptor neurons in the developing and adult mouse. Journal of Comparative Neurology 394: 445-461.

Xu F, Greer CA, Shepherd GM (2000) Odor maps in the olfactory bulb. Journal of Comparative Neurology 422(4):489-95.

Yoshibara Y, Mori K (1997) Basic principle and molecular mechanisms of olfactory axon pathfinding. Cell and Tissue Research 290: 457-463.

Zhang QY (1999) Retinoic acid biosynthetic activity and retinoid receptors in the olfactory mucosa of adult mice. Biochemical and Biophysical Research

Communications 256: 346-351.